A Relation Between Select Hydraulic Properties and Sediment Transport Volume Through Experimental Culvert Configurations and Techniques for Measuring Sediment Transport Volumes

by

Jeremy D. Dixon

A Thesis

In

Civil Engineering

Department of Civil and Environmental Engineering

Submitted to the Graduate Faculty
of Texas Tech University in
Partial Fulfillment of
the Requirements for
the Degree of

Masters of Science

Approved

Theodore G. Cleveland, Ph.D., P.E.
Chair of Committee

William H. Asquith, Ph.D., Ph.D., P.G.

Peggy Gordon Miller
Dean of the Graduate School

December, 2011

Acknowledgments

I am especially grateful to the many people who have helped me directly and indirectly in the completion of this thesis.

To my advisor and committee chair, Dr. Theodore G. Cleveland: Thank you for your assistance and encouragement in my attempts to learn two new programming languages: LaTeX, R.

To the other member of my committee, Dr. William H. Asquith: Thank you for your initial instruction in operating the total station that made this project possible, for your guidance in coding, and for your insights into this project.

To my fiancée Kari: Thank you for your patience and constant support in the completion of this task. I know you of all people have been waiting for this document to be finished and I am so thankful to have you in my life.

To my family, especially Memaw and Grandad, who made this portion of my education a reality: Thank you for your love, support, encouragement, prayers, and most of all, financial contributions.

To Mr. Wade Barnes: Thank you for being a great supervisor, teacher, and friend.

To the faculty and staff of the Civil and Environmental Engineering Department: Thank you for reinforcing the values, ethics, and knowledege necessary to become a successful, continually developing professional engineer.

To my classmates Wesley Kumfer and Holly Murphy: Thanks for making these last few years truly spectacular. I hope to never forget our ridiculous times in the computer lab, our random excursions, or just how great of friends you guys have been to me.

Table of Contents

List of Tables

List of Figures

Chapter 1
Introduction

Flow in natural channels may cause sediment to move along the bed or in suspension. When the amount of sediment in the water is greater than the transport capacity, channel aggradation or the accumulation of sediments occurs. Whereas the amount of sediment is less than the transport capacity, channel degradation occurs (Graf and Altinakar, 1988). Several factors have traditionally been used to predict and describe sediment transport, and when these factors change, the transport type can change as well. Factors such as flow velocity, bed slope, sediment size, and others are referred to in the literature (Graf and Altinakar, 1988; Sturm, 2010; Yang, 1996). In the experiments described herein, the sediments (rocks) are large enough and the flow is low enough that nearly all transport is assumed to be bed-load.

Because the rocks in the experiments reported are large in relative scale, there is an interest that the rocks will clog one or more culvert models. When a culvert becomes clogged in the real-world, it no longer functions as designed, and may increase the probability of a roadway overtopping or damage. As a result understanding of culvert clogging is an important endeavor unto itself. An definitive photograph of a culvert used for peak streamflow measurement by the U.S. Geological Survey (William H. Asquith, written communication, 2011) is shown in Figure 1.1. The figure shows a triple circular barrel configuration—a geometric configuration used for some of the experimental models reported herein.

A simple way to calculate the volume of rocks moved is to use a bucket of known volume to measure a known volume of rocks upstream of the culvert, then run the experiment and measure the remaining volume using buckets again. The "bucket difference" is the change in volume. There are a few issues with using a bucket:

- Bucket volumes reveal no information about bedforms,

Figure 1.1. Photograph of U.S. Geological Survey Peak-Streamflow Station 08123618 Sulphur Springs Draw near Plains, Texas Courtesy of USGS Lubbock Field Office

- Buckets require physical effort to fill and empty,
- There is a proportional relation between the scale of the experiment and the amount of effort required to reset each experiment,
- In the field, it is exceedingly difficult to standardize each experiment with buckets, and
- The use of buckets requires the establishment of a static datum prior to the experiment.

Instead of using only buckets for measuring sediment-transport volume, this thesis explores two more options: time-lapse photogrammetry during the experiment and an adequate density topographic survey before and after each experiment. Time-lapse photogrammetry would have been an interesting solution, but all necessary data acquisition techniques or equipment were not available to do the photogrammetric analysis. A combination of using buckets and surveying the bedforms was thus chosen to test the viability of surveying sediment transport volumes.

Surveying is used around the world to generate cross sections to calculate cut and fill, but in this thesis, topographic surveys were used, with a surface interpolating software program, to make 3-dimensional (3D) surface models of the top of the observed rock surface. The 3D surfaces then could be subtracted from each other to calculate the volume change. The use of these surveys is compared to measuring with buckets in the Methods section of this thesis.

Ultimately, this thesis is exploring the question:

What general observations can be made about the effects of a culvert system on sediment transport, and can those observations be quantified by some remote sensing technique?

1.1 Background

This thesis is a small part in the larger work of Texas Department of Transportation (TxDOT) Project 0–6549: Hydraulic Performance of Staggered Barrel Culverts for Stream Crossings. The researchers working on TxDOT Project 0–6549 are seeking to "address the issue of solids accommodation in Texas stream crossings, and develop design guidelines to assist in building multiple barrel systems that mimic the necessary stream behavior to facilitate solids migration, yet still provide the sufficient clear-water hydraulic capacity to meet their transportation infrastructure drainage needs" (Cleveland et al., 2009). In order to build the requisite knowledge to achieve the goals described in the contract documents of TxDOT Project 0–6549, the researchers constructed and analyzed a database containing all relevant past work, and physically modeled the culvert system in a laboratory.

1.2 Purpose and Scope

As part of TxDOT Project 0–6549, this thesis is intended to be an exploratory analysis of a relation between select hydraulic properties and sediment transport volume through experimental culvert systems. Also described in this thesis are selected techniques for the measurement of sediment transport volume.

Because this work is a small part of the larger body of work in TxDOT Project 0-6549, the scope is comparatively limited relative to the size of the larger body of work. The

purpose of this thesis can be stated as exploring relations in the experimental apparatus between selected parameters such as:

- Discharge,
- Bed Slope,
- Sediment Transport Volume,
- Culvert Array Configuration and Culvert Barrel Geometry,
- Sediment Size, and
- Bedforms.

Although velocity is important in understanding sediment tranport, and instruments are available to measure velocity, any velocity measurement made in the course of the experiments described herein is outside the scope of this thesis. As a result of the need to measure sediment transport volume and bedform shapes, this thesis is concerned with the techniques used to generate 3D surface models for use in cut and fill calculations.

Chapter 2
Literature Review

2.1 The Importance of Considering Sediment Transport in River-Culvert Systems

Tsihrintzis (1995) states that "The primary function of a drainage culvert—to convey the design flow effectively—is often greatly impaired or completely lost due to the presence of deposited sediments." In that article, a case study was considered that showed just how much of an impact this deposition can have. Clogged or otherwise obstructed culverts can cause serious flooding issues that may lead to financially significant damage.

Financial losses are not the only reason why sediment transport should be considered in river-culvert systems; there is a growing movement to reconsider the impacts of culverts on fish populations. The local hydraulics of culverts can have a deleterious effect on fish habitat and migration. Several of these studies identify sediment transport processes as important to the hydraulics of a culvert, specifically where velocity profiles can be drastically changed. Typically, the main concern is that the design velocities in the culvert do not exceed the swimming ability of juvenile fish (House et al., 2005).

According to Castro (2003), overlooking the geomorphology of streams may cause "well-intentioned and well-planned projects" to become "completely ineffective or detrimental to the stream system and related habitat." It would seem prudent, then, for additional attention to be paid when designing a culvert for a stream crossing so that the culvert performs adequately throughout the wide variety of flows it may encounter. Some important aspects to consider when designing culverts are: excessive scour, a tendency to clog and reduce the flow capacity of the system with bed material, and keeping the velocities in a reasonable range as governed mostly by biotic constraints.

2.2 Potential Causes of Sediment Transport

There are two primary types of transport, bed-load and suspended-load transport (Graf and Altinakar, 1988). Bed load transport is the type of transport where "solid particles glide, roll, or briefly jump, but stay very close to the bed . . . which they may only leave temporarily. The displacement of the particles is intermittent; the random concept of turbulence plays an important role" (Graf and Altinakar, 1988). Because turblulence plays a dominant role in bed-load transport and is characterized by unpredictable variations in velocity, it is necessary to have velocity-monitoring equipment that can measure and record turbulent variations in the reverse current generated by eddies near the streambed. However direct application of velocity data is outside the scope of this thesis.

Many formulas used to predict bed-load transport are empirical in nature, but make considerable use of dimensionless numbers. The use of dimensionless numbers allows experiments to be made in a laboratory, without too much loss of generality to the real world, where conditions can be altered to isolate the key variables being tested by a hypothesis. Through derivation using the fluid density, viscosity, sediment density, sediment characteristic diameter, flow depth, slope, and gravity, Graf and Altinakar (1988), for example, develop the relation: $q_{s_b} = a_s U^{b_s}$, where q_{s_b} is the volumic solid discharge (sediment transport) per unit width, a_s and b_s are coefficients dependent upon the granulometry of the bed. Other examples based on discharge are reported in (Yang, 1996, p. 98). The average velocity, U, and the related streamflow discharge are key parameters in the computation of sediment transport.

Yang (1996) discusses the Schoklitsch formulas (Schoklitsch, 1934), which are formulas only dependent upon slope and particle size. In general, with increased channel slope, the streamflow discharge and attendant velocity increase for all other hydraulic properties being equal.

Sturm (2010) describes two different methods of accounting for sediment transport. The first approach separates the bed-load and suspended-load, while the second approach directly relates the total sediment discharge to hydraulic variables.

> "In either approach, issues of water temperature, the effect of fine sediment, bed roughness, armoring, and the inherent difficulties of measuring total sediment discharge can cause significant deviations between estimates and measurements (Sturm, 2010)."

It is important to systematically address the hydraulic variables that can be feasibly measured in the experimental apparatus so that the results can reflect the estimates.

In developing equations similar to those already stated, some simplifying assumptions were made. Sturm (2010, p. 442–447) describes these assumptions as:

> The bed itself was considered to be movable with bed forms, but on average, the bed was assumed not to be undergoing significant changes in elevation on an engineering time scale, which may be on the order of several years. In the short term, however, sediment storage (plus or minus) compensates for imbalance in the inflow and outflow sediment discharges for a river reach.

Klingeman (2003) identifies a less often considered period of sediment transport, the recession limb of a runoff event. This is most likely attributable to sediments that have entered a state of equilibrium at a higher flow, and as the water drains downstream faster than it is replenished, some supercritical flow occurs. This extra velocity causes the equilibrium bedforms to be broken and erode away. This concept needs to be evaluated during the shutdown procedures of the experiment. It is conceivable that the supercritical flows during the recession limb may cause culverts to unclog and/or gravel bars to wash out.

2.3 Effects of Sediments on Open Channel Flow

Intuitively, if the sediments that comprise a streambed are mobile, the channel is experiencing a change in geometry. A change in geometry can cause a change in flow area, that necessarily causes a change in velocity. Much of the literature was concerned with either channel stability or aggradation and degradation (incision) Castro (2003), Graf and Altinakar (1988).

Sediments also have an effect on the channel roughness, a major component of Manning's Equation. A rough channel slows down the velocity, whereas a smooth channel would increase the velocity. Higher velocities, in turn, correspond with more sediment being transported.

2.4 Different Types of Culverts

Culverts exist in many different shapes, styles, and configurations. Hotchkiss and Frei (2007) provides Table 2.1. Some culvert shapes are more hydraulically efficient, whereas other culvert shapes may be more cost effective or easier to install. The culvert configurations studied in this thesis are circular, box, and multi cell.

Table 2.1. Advantages and Disadvantages of Different Culvert Shapes for Fish Passage Installations

Shape	**Advantages**	**Disadvantages**
Bridge	Usually the best alternative for fish passage.	Cost
Circular	Structurally and hydraulically efficient. Greater depth of fill allowable for given span, and easier installation (in reference to Arch or Pipe Arch)	More prone to clogging at high flows. Flexible walls in large culverts require special care during backfill construction.
Pipe-Arch and Elliptical	Wider section available for low flows with less height	For buried culverts, installation can be difficult.
Arch	Very good fish passage when sized adequately. Allow natural streambed material to be maintained in new installations.	Expensive installation. Not practical when stable footings cannot be created.
Structural Plate (Round or Arched)	Can be placed on the bedding and partially backfilled with top plates left off.	Distortion during compaction can lead to problems joining final pieces. Structural plate pipes should not be backfilled until all plates are completed and bolts tightened.
Box	Easily adaptable to a variety of situations.	Not as structurally and hydraulically efficient as other shapes due to angled corners.
Multi Cell	Allow adequate capacity in low profile situations. Lower road bed elevation.	Prone to clogging due to area between the barrels and smaller individual culvert size.

2.5 Effects of Culverts on Open Channel Flow

Wargo and Weisman (2006) compared the effects of using single barrel and multiple barrel culverts in a laboratory flume. The study asserted that because the use of single barrel culverts effects the hydraulic dimensions of a stream and causes a change in the active channel during normal and near-normal flow conditions, the culvert can cause sediment to deposit upstream of the culvert. Also, perching of the outlet can prevent fish passage, and scour at the outlet can lead to accelerated erosion throughout the reach. Multiple barrels allow higher depths of flow at low-flow conditions than a single barrel with an overall equivalent cross-sectional area, and should also have smaller scour pool sizes, and lower backwater depths at bankfull flows. Further discussion on culverts can be found in (Sturm, 2010, p. 246–261).

2.6 Prior Experimentatal Investigations

A study by House et al. (2005) looked at the velocity distributions in countersunk (depressed) "streambed simulation" (gravel bed) culverts. The purpose of the House et al. study was to determine what the velocity distributions in a culvert look like, and how the velocities might impact salmonid migrations during spawning. The study also looked at arch culverts with a gravel bed with velocity measurements taken at the middle and outlet cross sections of the study culverts. The mechanical-meter equipment used to measure velocities were incapable of measuring reverse currents, but because the flow is approximately uni-directional, the lack of reverse current detection was not an issue.

Based on the literature, the most important parameters in determining the amount of sediment transported through a culvert is dependent upon:

- Sediment size,
- Bed slope,
- Culvert configuration and geometry, and
- Flow velocity.

The exploratory work in this thesis is focused on relating the discharge to the volume of solids transported for a given sediment size, bed slope, and culvert configuration.

Chapter 3
Methods

3.1 Lab Setup

At the Texas Tech University East Loop Research Facility (East Lab), there is a 48-foot long, 8-foot wide, and 4-foot tall flume used for the experiments reported in this thesis. Water is pumped from a large water-storage reservoir (approximately 20,000 gallon) into a head tank, with a stage-discharge rated chute that flows into the flume. Inside the flume is an "energy ramp," which is a ramp that redirects the flowing water downstream so that the water does not pool upstream and diminish capacity, and prevents damage to the model floor. Figure 3.1 shows a view of the experimental apparatus as viewed looking upstream from the downstream end.

The model in the flume is a trapezoidal channel that is constructed of wood with outdoor carpet glued to the sides to increase the friction. In the channel are two culverts for which the upstream culvert is the experimental model and the downstream culvert acts as a backwater control and rock trap. The experimental model was fabricated to have interchangeable barrels in order to have a reasonably efficient to modify experimental setup. After the flow encounters the two culverts, it continues into a rock bin, where the rocks that pass the downstream culvert are ultimately trapped and prevented from entering the water-storage reservoir.

For the experiments reported herein, eight different culvert configurations (systems) were tested. A naming convention for the culvert configurations was established and is listed in Table 3.1. Figures 3.2 through 3.9 are representations of the models tested in this thesis from a perspective looking upstream. The culvert system was 29 inches wide from culvert entrance to exit, and the roadway was 84 inches long and spanned from bank to bank.

Table 3.1. Short Alphanumeric Codes Used for the Experimental Culvert Setups

Culvert Code	Description
SB-I	Staggered barrels with inverts equal
SB-C	Staggered barrels with crowns equal
M-6-C	Multiple 6-inch circular barrels
S-6-C	Single 6-inch circular barrel
M-4-C	Multiple 4-inch circular barrels
S-4-C	Single 4-inch circular barrel
M-R	Multiple rectangular barrels
S-R	Single rectangular barrel

The channel model was made of painted wood. It was discovered during preliminary experiments that the smooth painted wood along the sides of the channel were forming unrealistic velocity distributions. Therefore, the sides of the walls covered in carpet to

Figure 3.1. Flume Experimental Apparatus Looking Upstream

increase the friction in the channel. The solids in the channel were leveled at 0.2 feet from the model floor upstream of the culvert where there was a 0.1 foot "boundary roughness layer" of rocks held in place by an aluminum grate. The solids in the channel downstream of the experimental model were leveled at 0.3 feet from the model floor with special attention made not to have a sediment layer above the invert of the outlet-sections of the culvert barrels at the beginning of each experimental run.

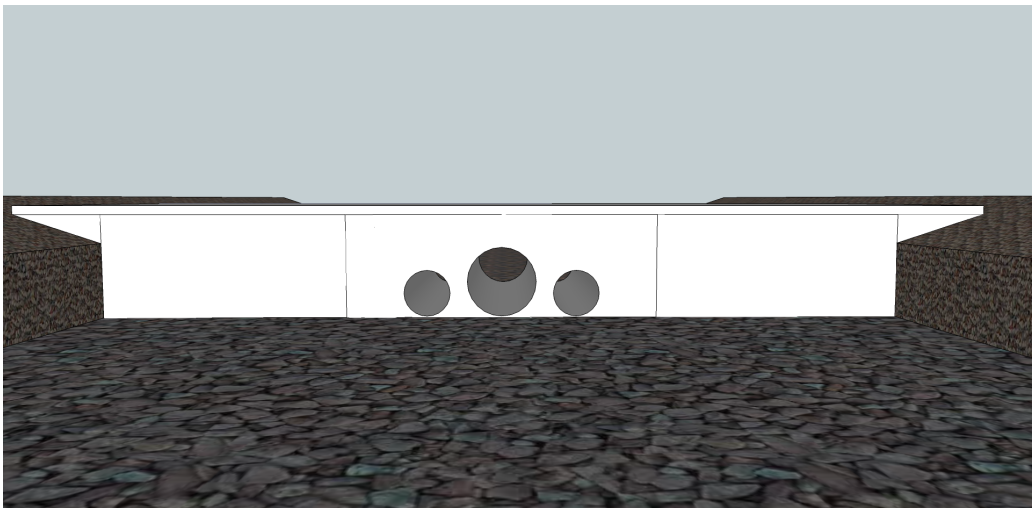

Figure 3.2. Diagram of Experimental Model SB-I (The outside barrels are 4 inch diameter and the middle barrel is 6 inch diameter)

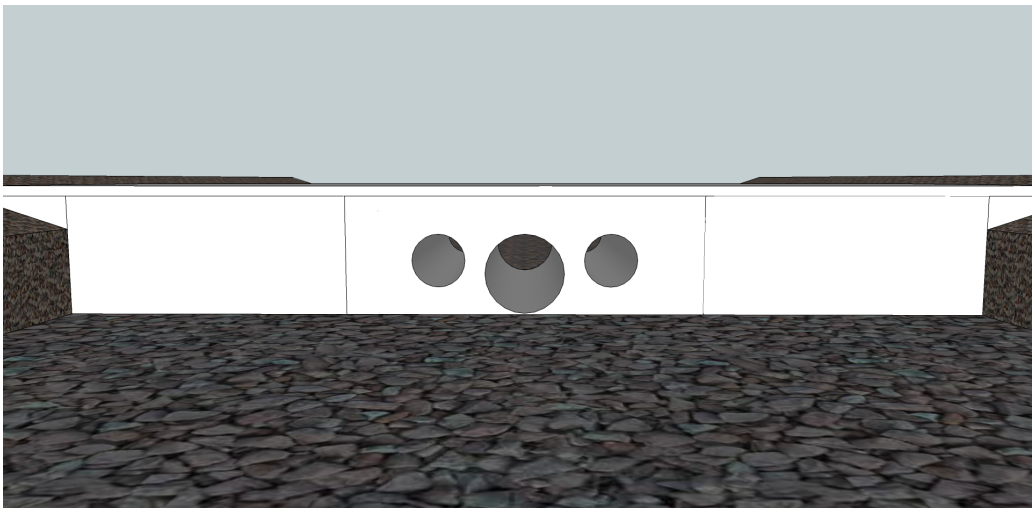

Figure 3.3. Diagram of Experimental Model SB-C (The outside barrels are 4 inch diameter and the middle barrel is 6 inch diameter)

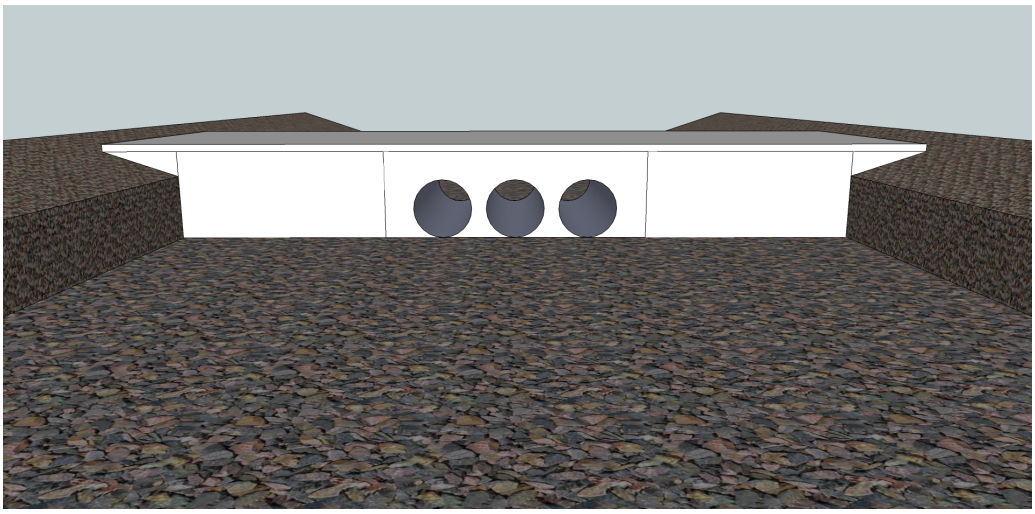

Figure 3.4. Diagram of Experimental Model M-6-C (The identical barrels are 6 inch diameter)

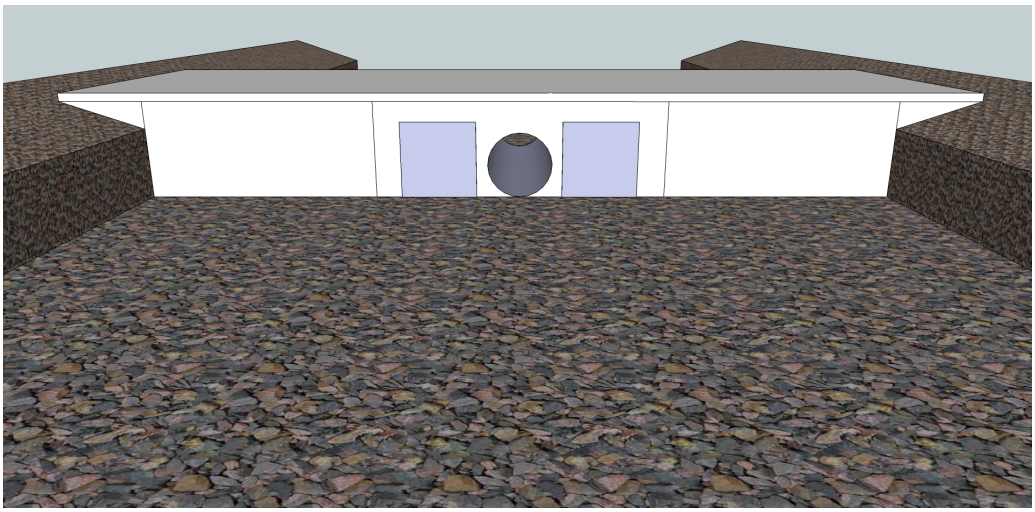

Figure 3.5. Diagram of Experimental Model S-6-C (The barrel is 6 inch diameter)

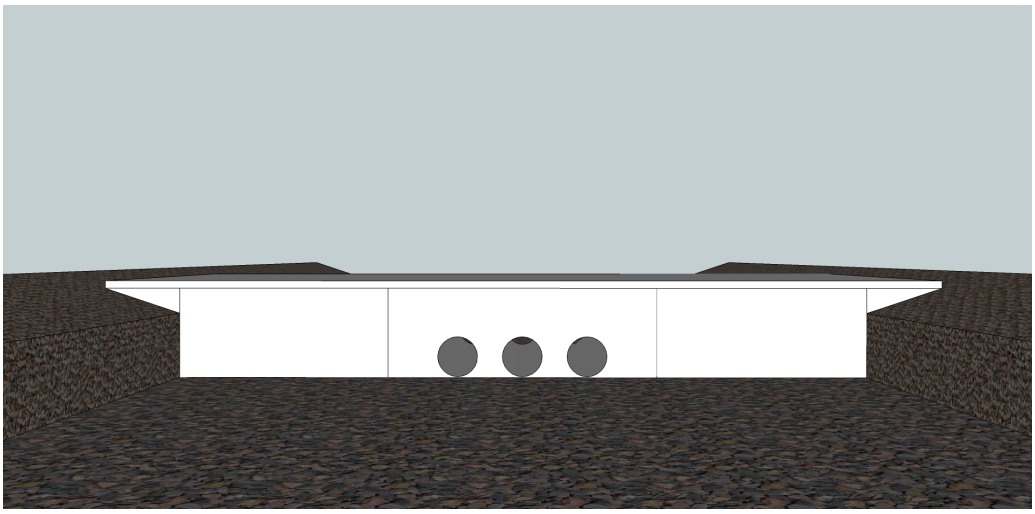

Figure 3.6. Diagram of Experimental Model M-4-C (The identical barrels are 4 inch diameter)

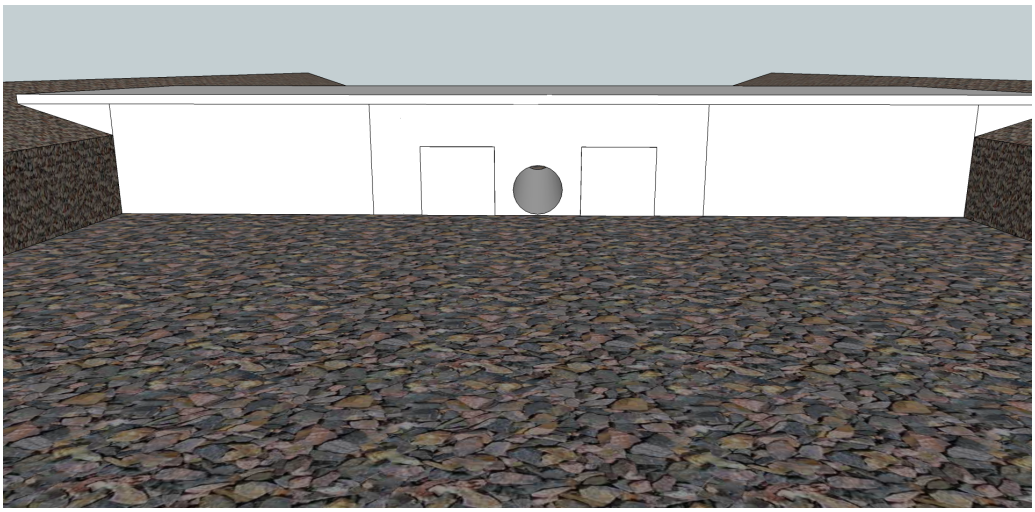

Figure 3.7. Diagram of Experimental Model S-4-C (The barrel is 4 inch diameter)

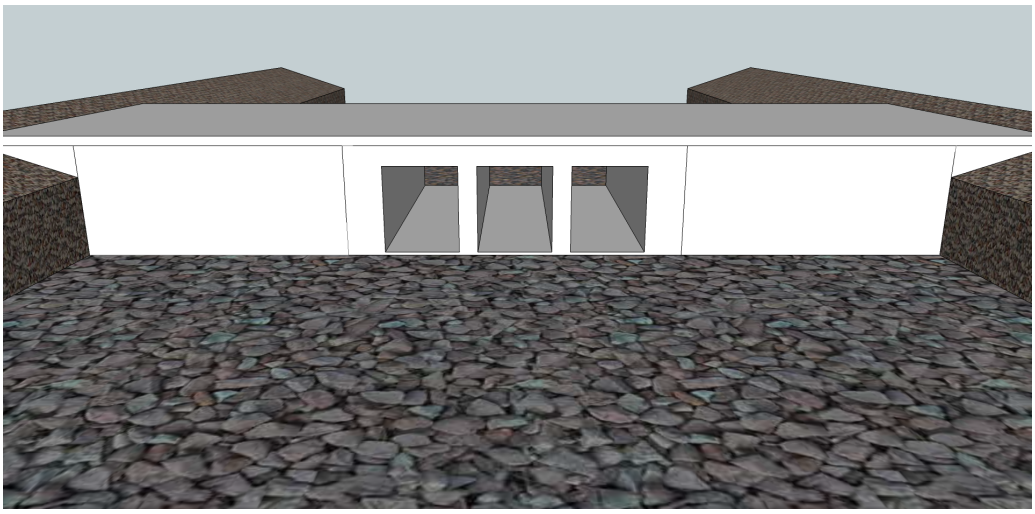

Figure 3.8. Diagram of Experimental Model M-R (The identical barrels are 6$\times$7 inches)

Figure 3.9. Diagram of Experimental Model S-R (The barrel is 6×7 inches)

3.2 Experiment Standard Operating Procedures

There were two different types of rocks used—the large rocks were approximately 3/4 inch diameter and the small rocks were approximately 3/8 inch diameter. The two different rock sizes resulted in slightly differing experimental techniques. Because the smaller rocks tended to move at lower flow rates, the standard operating procedures had to be modified to run for a comparable amount of time. The standard operating procedure was:

1. A measured volume of rocks are placed upstream of the culvert model—this known volume provides a 0.2 foot deep layer of rocks available for transport,
2. Place all 3 MicroADV probes in the appropriate location,
3. Turn the pump on at 24 Hz and let it stabilize,
4. Increase the pump to 32 Hz and let it stabilize for 15 minutes,
5. Increase the pump by 1 Hz every five minutes until 38 Hz is reached,
6. Take three bursts on each ADV probe for each new pump speed,
7. Increase the pump by 1 Hz every 10 minutes until 40 Hz is reached,
8. Increase the pump by 1 Hz every 15 minutes until 42 Hz is reached,
9. Take a burst every 15 minutes on 42 Hz, and if there has been no noticeable bed movement after 30 minutes, increase to 43 Hz,
10. Increase the pump by 0.5 Hz if no bed movement has occurred in 30 minutes time. Repeat as necessary until the culvert has clogged, and
11. Run the pump at the last Hz setting for 1 hour after the clog is first noticed and then shut the pump down.

The standard operating procedure for the smaller rocks was similar but with lower flow rates. Increased flume slope allowed the sediments to transport more easily, therefore the flow needed to be adjusted accordingly. Further comparison between experiment duration, rock size, and flume slope are listed in a comma delimited file in the Appendix.

3.3 Quantifying Flow

3.3.1 Discharge

The head-tank chute was rated using various direct and temporary weir computations to form a head-discharge relation. The head-discharge relation (rating curve) was used to calculate the flow coming from the head-tank chute. Head in the tank was measured by a staff-plate mounted in proximity to a sight glass, shown in Figure 3.10. The intitial rating curve (William H. Asquith, U.S. Geological Survey written communication, 2010) is read by entering the graph on the vertical axis with the measurement of the staff plate, finding the intersection of the rating curve with the value, and then looking up the corresponding discharge value on the horizontal axis. The rating curve for the head tank chute is shown in Figure 3.11. The rating curve used in this thesis was made by digitizing the given rating curve in order to establish the discharge as a function of head. The rating curve used to calculate discharge in this thesis is shown in Figure 3.12.

Figure 3.10. Sight Glass Used to Measure Head in the Head Tank

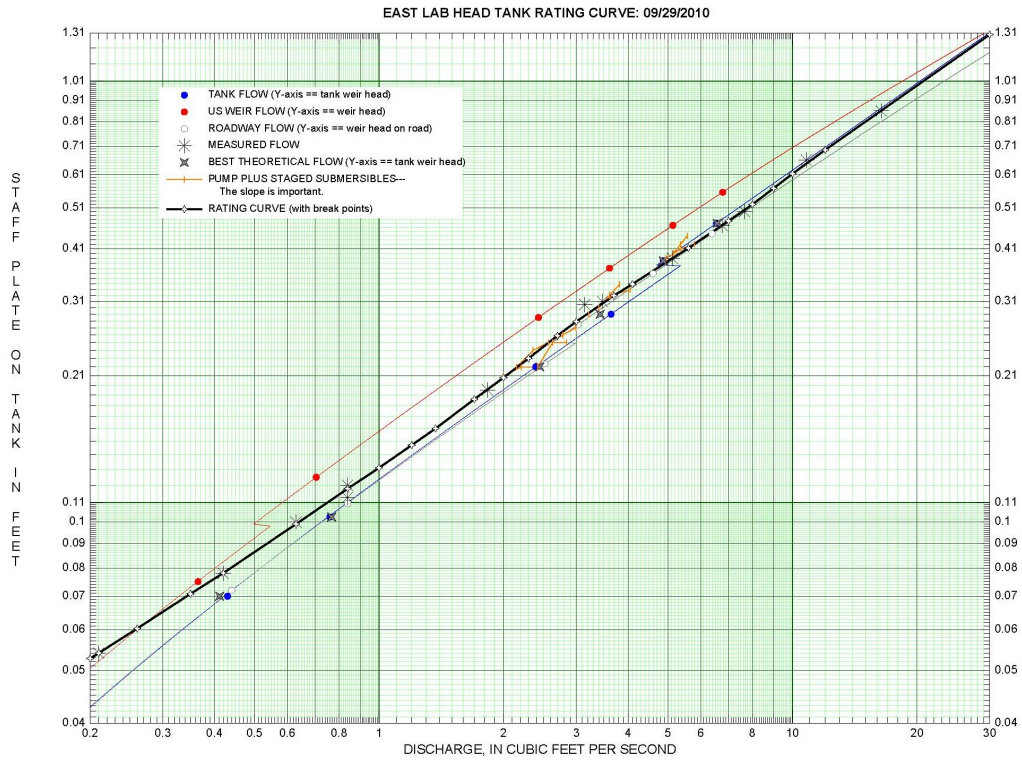

Figure 3.11. Head-Discharge Relation for the Head Tank

In general, the rating curve for the experimental runs is considered very reliable. The rating curve was developed by measuring the head in the head tank and relating that head to measurements of discharge in the flume made by different operators. Because the rating curve is considered very reliable, the digitized rating curve is also considered very reliable for determining the discharge in the flume.

Table 3.2. Rating Curve Values Digitized from Figure 3.11—Data are shown in Figure 3.12

Discharge $(\mathrm{ft}^3/\mathrm{s})$	**Staff Plate Reading** (ft)
0.199	0.055
.209	.057
.259	.065
.349	.078
.419	.086
.630	.112
.839	.134
.999	.149
1.196	.168
1.366	.183
1.695	.213
2.001	.239
2.299	.264
2.697	.296
2.990	.318
3.700	.365
4.103	.388
5.596	.467
6.985	.537
7.979	.585
8.981	.636
9.989	.687
11.999	.778
17.831	1.008
30.000	1.415

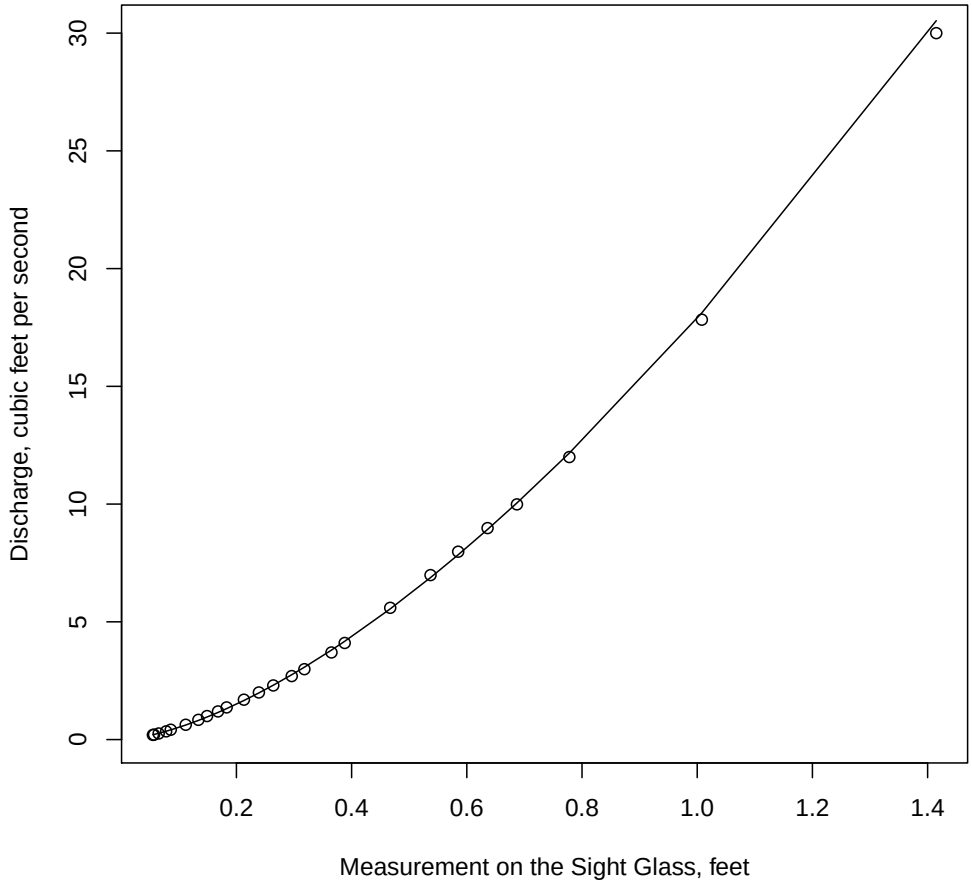

Figure 3.12. Rating Curve for the Head Tank—Values listed in Table 3.2

3.3.2 Velocity Measurements

Acoustic Doppler Velocimeters (ADVs) were used to measure the velocity in the channel. All ADV operations were conducted in accordance with the MicroADV Operations Manual Dixon (2011), shown in the Appendix. The ADVs were mounted on aluminum rods that spanned the width of the flume. The rods had an adjustable clamping system that allowed measurements to be taken in the same place, even after resetting from different locations.

During experiments, the ADVs were used for two purposes: to record entrance and exit velocities in the culvert barrels, and to determine when the culvert was clogged. In the sediment transport experiments, the middle barrel of the array was monitored at the inlet and outlet for velocity. If the array had multiple barrels, the third ADV was used to measure the outlet of the right bank-side barrel. If the array was a single barrel, the third ADV was used to monitor the velocity just above the streambed approximately eight feet downstream from the culvert outlet. The data acquired using the ADVs is outside the scope of this thesis and is not considered further herein.

3.4 Quantifying Solids

It is important to measure the amount of solids that pass through the culvert because these values are necessary to fully understand the interaction between the channel, sediments, and culvert. In order to estimate the volume available for transport, the simple method of counting buckets was used. The bucket count was a quick and reliable way to ensure that the same volume of rocks are available for each experiment. The bucket count was made using a 5-gallon bucket.

The bucket counts provide a rough approximation that is acceptable because this study is primarily concerned with what moves into and through the culvert. Solids in the culvert are extracted and weighed to measure the real weight, and a topographic survey is made downstream of the model. The purpose for measuring the weight of solids stuck in the barrel was to be able to account for differences between the bucket-determined volume and the surveyed volume. The solids that remained upstream of the culvert after the experiment were measured to the nearest $1/4$ bucket, and the difference between the measured upstream volume and the total bucket volume should approximate the volume transported to and through the culvert. The measurements of the 5-gallon bucket and the

survey results were compared for the larger rock size. The comparison shows 0.665 cubic feet per bucket and 0.668 as the defined conversion factor from 5 liquid gallons to cubic feet. The comparison was made only on the experimental results that did not have rocks trapped in the culvert barrel. The data are shown in Figure 3.13 and listed in Table 3.3. For the experiments with the larger size of rock, the bucket count is 11.5, whereas the smaller rock size has a bucket count of 12.

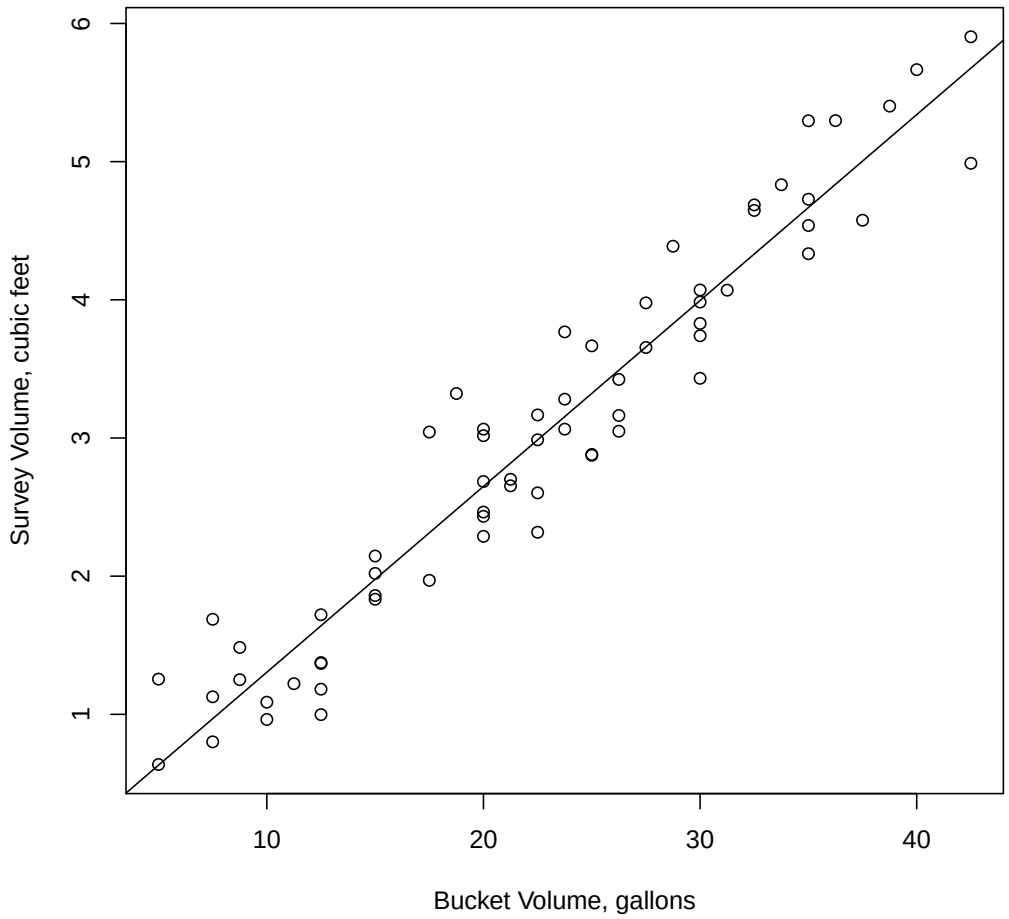

Figure 3.13. Relation Between Bucket-Determined Volume and Surveyed and Kriged Volume and a Superimposed Regression Line—Data are Listed in Table 3.3.

Table 3.3. Comparison Between Bucket-Determined Volume and Surveyed and Kriged Volume—Data are Shown in Figure 3.13

Buckets	**Survey** (ft^3)	**Buckets**	**Survey** (ft^3)	**Buckets**	**Survey** (ft^3)
4	2.464	4 1/4	2.654	6 1/2	4.687
5 3/4	4.388	6	3.984	6 3/4	4.833
8 1/2	5.904	4	2.288	6 1/4	4.070
8 1/2	4.988	1	1.255	7	4.728
8	5.666	2 1/2	0.998	5 1/4	3.163
7	4.334	2	1.088	4	2.685
7	5.296	2 1/2	1.375	5 1/4	3.049
7 1/2	4.576	1	0.637	1 3/4	1.484
5	2.881	1 1/2	1.127	3	1.860
4	3.064	2	0.963	3	1.833
4 1/2	2.987	2 1/2	1.721	4 3/4	3.281
4 1/2	2.318	2 1/2	1.182	4 1/4	2.701
4	3.017	5 1/2	3.655	4 3/4	3.064
5 1/4	3.424	7	4.538	2 1/4	1.222
3	2.146	7 1/4	5.297	1 1/2	0.801
3 1/2	1.970	7 3/4	5.402	1 1/2	1.688
3	2.020	6	3.740	4	2.433
6	4.071	4 3/4	3.768	2 1/2	1.368
6	3.829	6	3.432	1 3/4	1.251
4 1/2	3.167	5 1/2	3.978	3 1/2	3.043
4 1/2	2.603	5	3.667	3 3/4	3.322
5	2.875	6 1/2	4.647	--	--

3.4.1 Solids That Have Passed Through the Culvert Models

The preliminary plan for measuring sediment transport volume was to use time-lapse photogrammetry. Several issues arose that prevented this type of measurement:

- Photogrammetric cameras could not measure sediment within (trapped or clogging) the culvert,
- Surface waves caused too much refraction,
- Water was too murky to distinguish individual particles,
- Camera equipment was not suitable for photogrammetric measurement, and
- Image processing softwares were not available as anticipated.

In lieu of time-lapse photogrammetry, a Sokkia total station was used to generate an appropriate resolution survey of the topography. A x-y-z coordinate system was established within the lab with benchmarks off of the flume itself. A Carlson Surveyor field computer was used to perform resection (3D triangulation) to bring each survey into vertical and horizontal control using approximately 4 to 6 points. A list of benchmarks is provided in the Appendix, and the benchmark known as `pumpbolt3` is shown in Figure 3.14. Non-coincident topographic points were measured for each experiment, in two sets, the before and the after set. The region surveyed prior to an experimental run was entirely dependent upon how far the rocks were anticipated to move. The collected points were exported in a text file and imported into a Excel spreadsheet, which was subsequently converted into a Surfer grid file. By differencing the before and after surfaces, an approximation of the solids passed through the culvert models could be calculated. Surveys were performed in accordance with the specifications and recommendations of Sokkia Topcon (2009). Davis et al. (1981) also provides some useful commentary on topographic surveying theory.

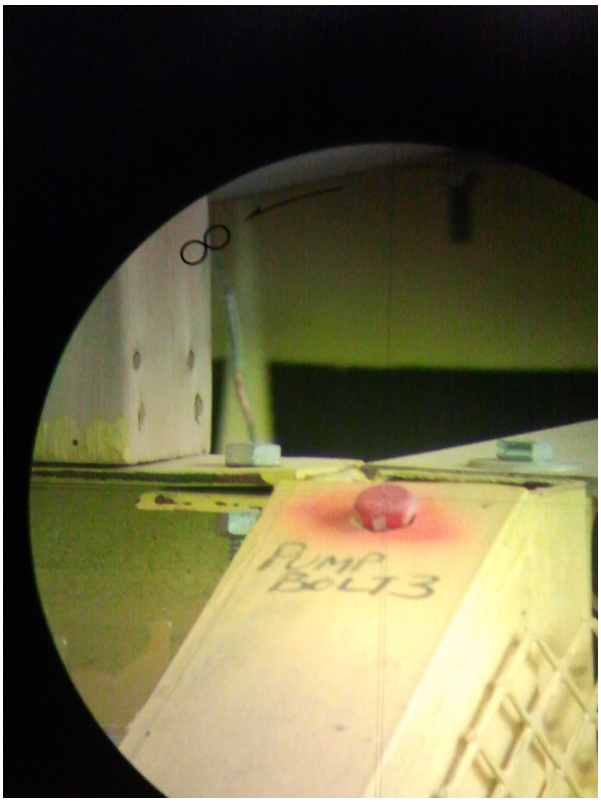

Figure 3.14. Benchmark `pumpbolt3` as Seen Through the Eyepiece of the Total Station

The surveys were initially conducted according to the standard operating procedures that follows:

1. Setup the instrument downstream of the bedforms and level it,
2. Resection using points that are easily identifiable and facing the instrument,
3. Place the survey grid alignment tool approximately 1 inch away from the right bank,
4. Survey each point along the grid proceeding downstream on the right bank side, then upstream on the left bank side,
5. Move the survey grid alignment tool towards the left bank by a distance equivalent to twice the width of the tool,
6. Repeat steps 4 and 5 until the full width of the channel has been surveyed,
7. Move the survey grid alignment tool downstream by a distance equivalent to the length of the tool if there is more bedform to survey, and

8. Pack up the instrument when finished with the full survey.

One of the drawbacks of this method was the amount of motion required of the operator. For every 4 foot survey, the operator had to move past the total station 5 times without disrupting the total station or the bedforms. In an effort to reduce the amount of time spent between experiments on surveying, the previous setup (from the post-experiment survey of the prior experiment) was used for the pre-experiment survey of the next experiment. E.g. for experiment 2011/02/14, the setup from the "after survey" was used for the "before survey" for experiment 2011/02/15. This method did not always work, because the total station may have been inadvertently bumped or otherwise shifted from its original resectioned position. In the case of a shift in position, the total station was releveled and returned to vertical and horizontal control through resection.

An example of the survey method with the data points plotted and connected in the order with which they were collected is shown in Figure 3.15. It is important to note that this figure shows that the grid is not exactly uniform. The points were not surveyed in the same location for each survey. The portion at the bottom of the graph is where the survey grid alignment tool was turned sideways to extend the survey further downstream.

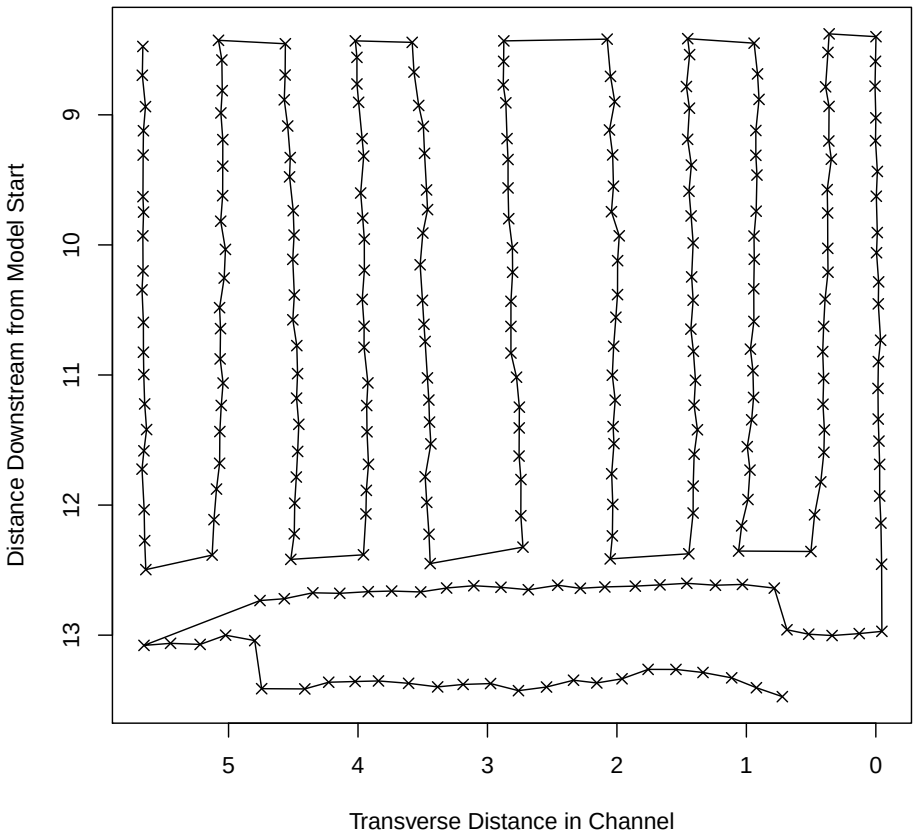

Figure 3.15. Example of the Initial Surveying Technique—Semi-Uniform spacing

The survey grid alignment tool is a 3-link section of orange construction fence that has been painted along the outside edges to be more visible to the operator. It is simply a tool to keep a semi-uniform spacing throughout the survey and otherwise guide the operator (the author). The tool is shown in Figure 3.16.

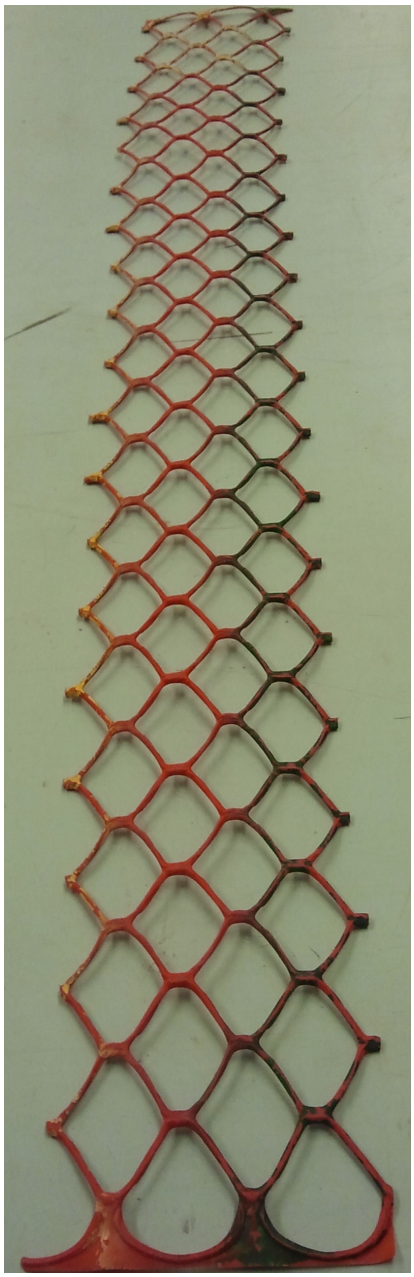

Figure 3.16. Survey Grid Alignment Tool Used to Keep the Survey Structured

The original x-y-z coordinate system of the survey was not established in a manner that would easily allow the algorithms of Surfer (Golden Software, 2002) to create appropriately sized surfaces. By default, Surfer takes the 4 most extreme X and Y values and creates a rectangular area to represent the extents of the surface. Because neither axis was parallel to the primary flow direction, a rotational conversion was needed. The coordinate system was also translated so that the origin was located on the beginning of the right bank of the model. The positive x-direction was made to be in the direction of flow, the positive y-direction was made to be perpendicular to the flow, into the left bank, and the positive z-direction was in the opposite direction of gravity. Visually, the axes were rotated about 30 degrees. The parameters of coordinate transform were determined at the end of experiments. Specifically a few points were measured and the coordinate transforms were based on the measured values of the beginning of the model floor on the right bank and left bank.

In order to determine the actual angle of rotation with respect to the desired coordinate system, the difference between the X values of reference marks known as `pumpbolt1` and `pumpbolt2` were set to zero. A change of basis was established and GoalSeek was used to find the angle that made the difference in X values zero. Equations 3.1 and 3.2 show the coordinate transform calculations.

$$x' = x\cos\theta + y\sin\theta \tag{3.1}$$

$$y' = x\sin\theta + y\cos\theta \tag{3.2}$$

Following coordinate transformation, Surfer could be effectively used. However, an error message that "the grids may be incompatible" kept appearing. A series of boundary points were measured by the total station and were used as bounding points in the grid file. The grid cell spacing was set to 0.05 feet and the error message disappeared. The next task was to decide which method of gridding yielded the most applicable results. The methods chosen to compare were:

- Kriging,
- Inverse distance to a power, and
- Simple arithmetic mean.

A brief comparison of the results is given in Table 3.4. The kriging method volume results were typically nearer to the bucket volume than the inverse distance results. Also, the kriging method produces the most faithful representation of the surface based on photographs taken just after the experiments. Figures 3.17 and 3.18 show the surface output generated by Surfer. Figure 3.19 is a photograph of the actual surface model with yellow string simulating contour lines. The simple arithmetic mean is similar to the volume of the interpolated methods, as well as to the bucket volumes. This evidence supports that the surveying technique and interpolation methods are done adequately. In the figures 3.17, 3.18, and 3.19, as well as all similar figures have an arrow that provides the direction of flow in relation to the picture.

Table 3.4. Comparison of Calculated Volume Transported in Cubic Feet

Date	Model	Buckets	Kriging	Inverse Distance	Simple mean
2011/03/22	M-R	5.653	5.904	5.939	4.305
2011/04/01	S-6-C	2.993	2.987	3.110	2.749
2011/05/20	S-R	0.665	0.637	0.574	0.654
2011/07/22	M-R	3.658	3.655	3.709	3.118
2011/08/05	S-6-C	2.660	2.685	2.769	3.401

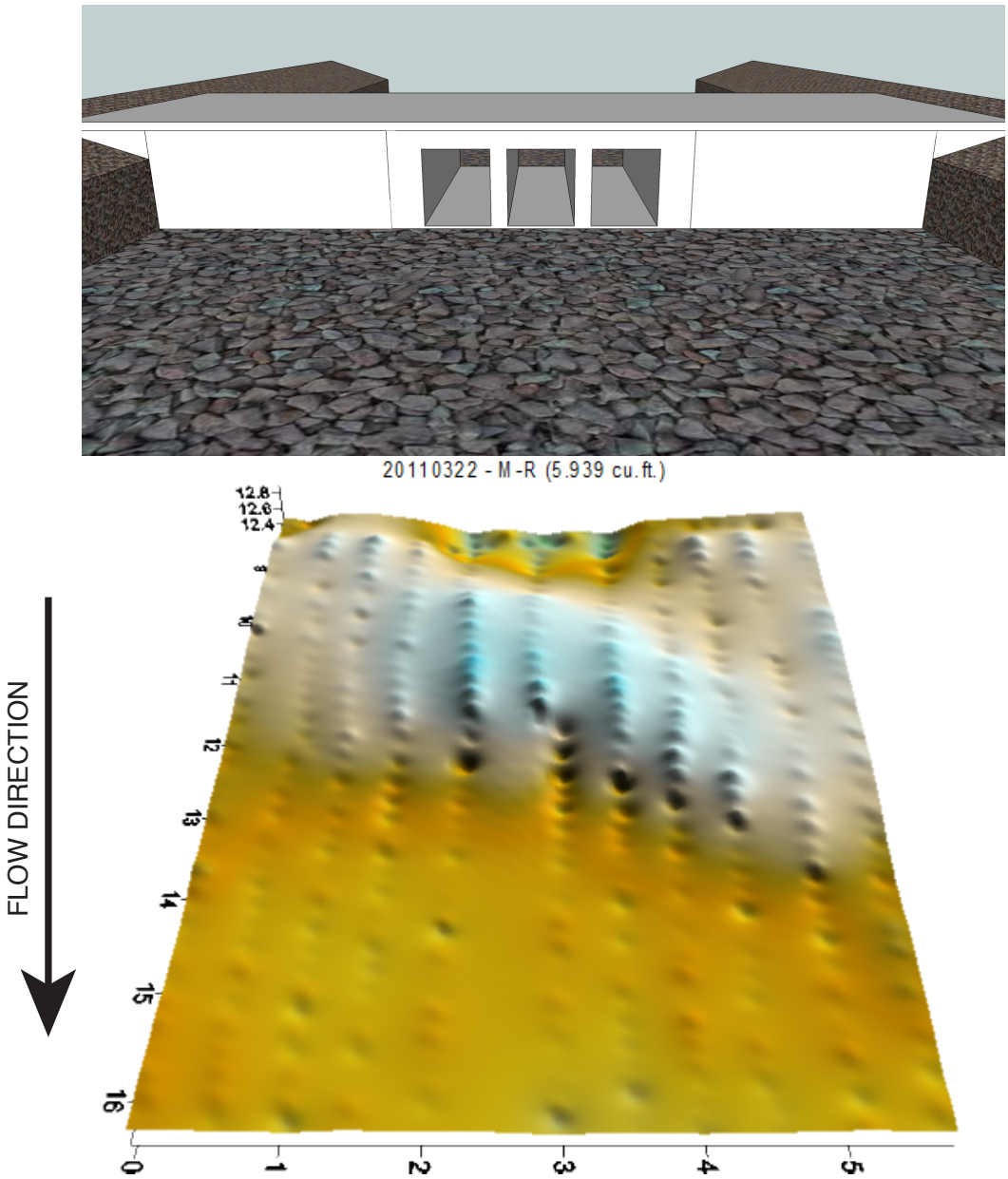

Figure 3.17. Surface Generated by the Inverse Distance Method for Experiment on 2011/03/22, Experimental Model M-R—Culvert Diagram Not to Scale

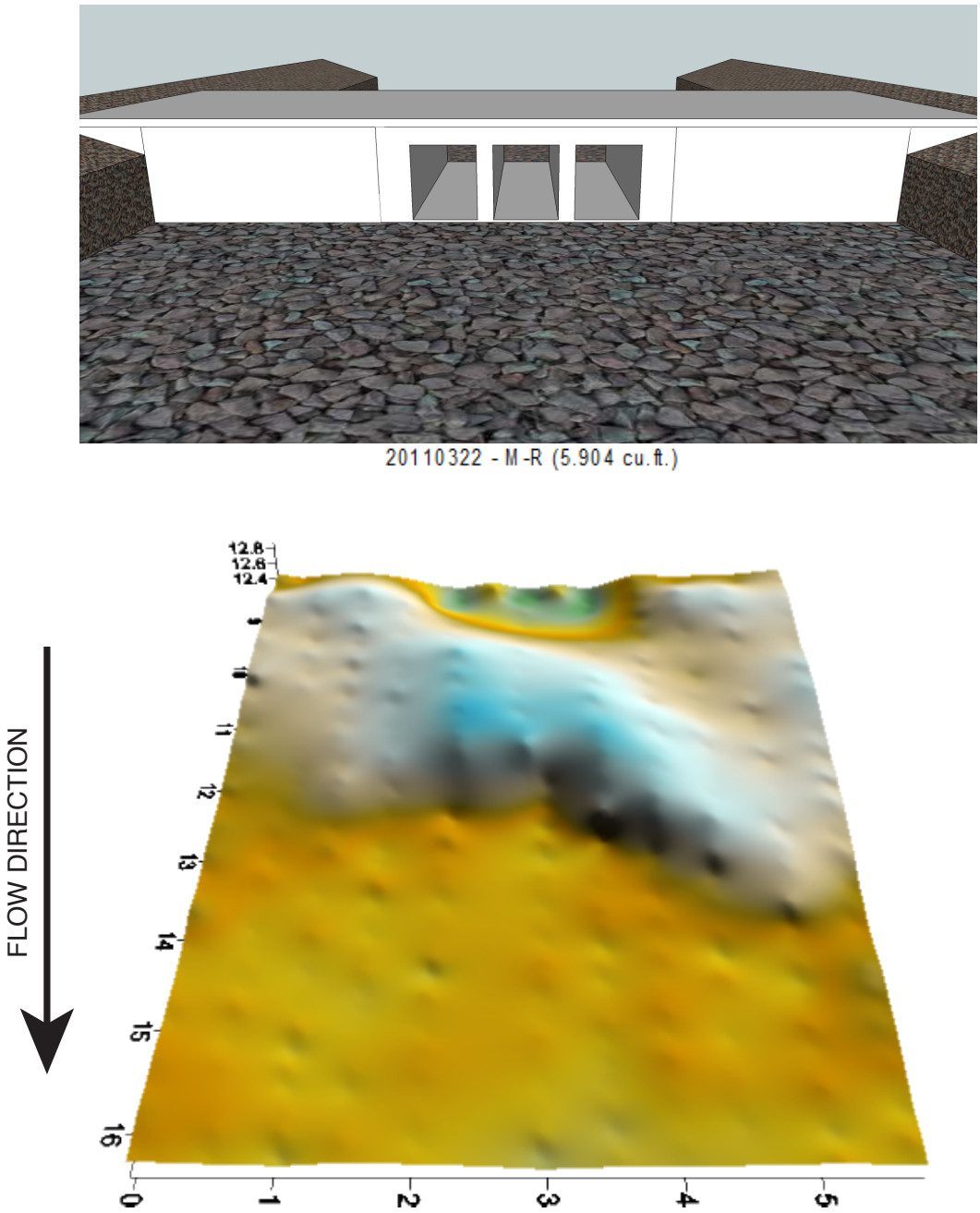

Figure 3.18. Surface Generated by the Kriging Method for Experiment on 2011/03/22, Experimental Model M-R—Culvert Diagram Not to Scale

Figure 3.19. Photograph of Downstream Bedform Following Experiment on 2011/03/22, Experimental Model M-R

Whereas the bedform can still be determined in both surface modeling methods, the inverse distance method has a tendency to produce "bumps" where the data points were acquired, though the kriging surface appears to have less of that effect. Figures 3.20, 3.21, and 3.22 lead toward the same conclusions:

- The inverse distance method produces bumps in the surface,
- The kriging method has an overall smoother appearance, and
- The volumes represented in both methods are comparable.

Therefore, kriging is chosen as the selected method because it produces a more faithful representation of the surface. This parallels Chapter 4 of Golden Software (2002), which states "Kriging is the default gridding method because it generates a good map for most data sets." The author concludes for the surface data considered herein that the quotation is appropriate and applicable.

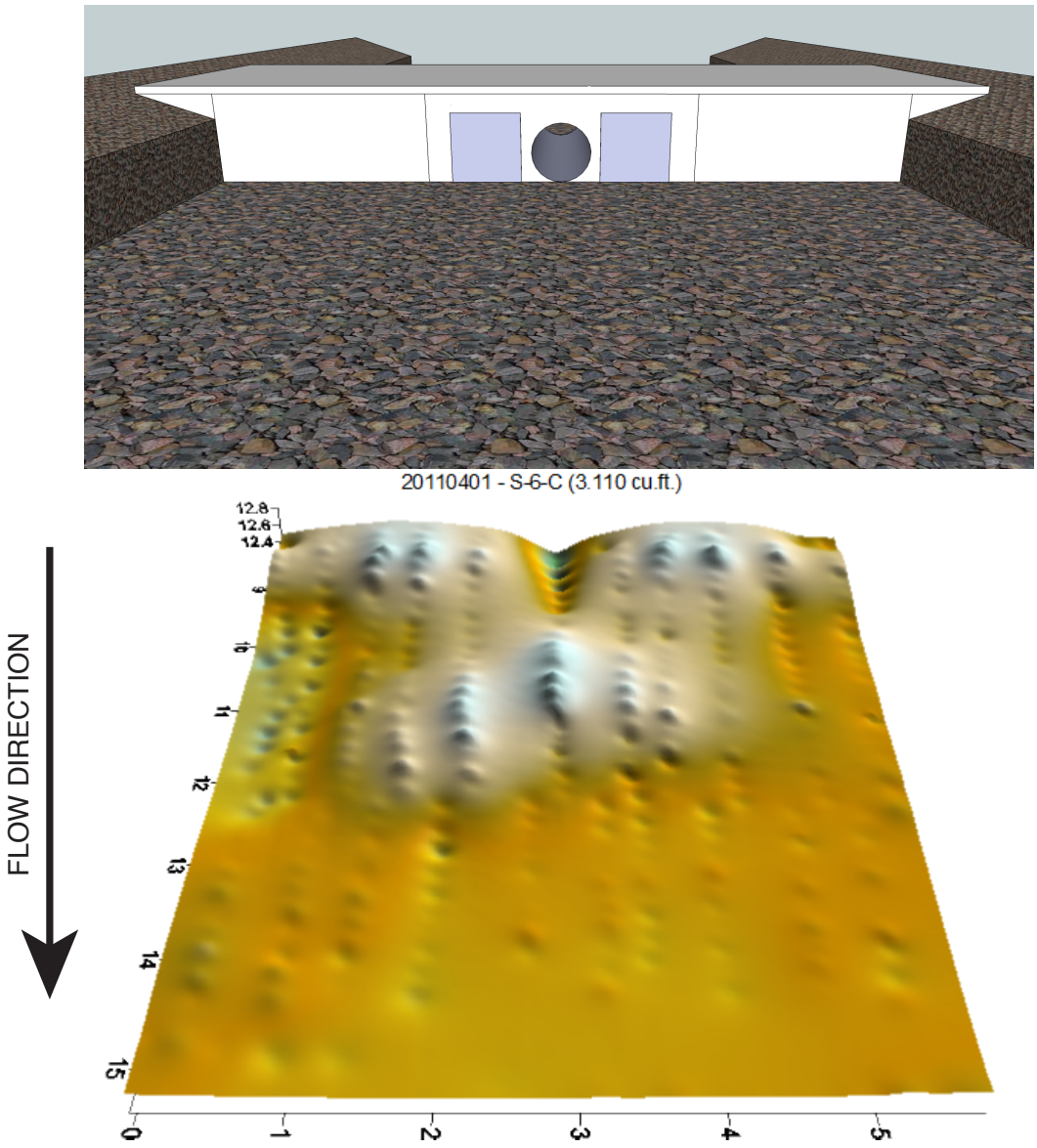

Figure 3.20. Surface Generated by Inverse Distance Method for Experiment on 2011/04/01, Experimental Model S-6-C—Culvert Diagram Not to Scale

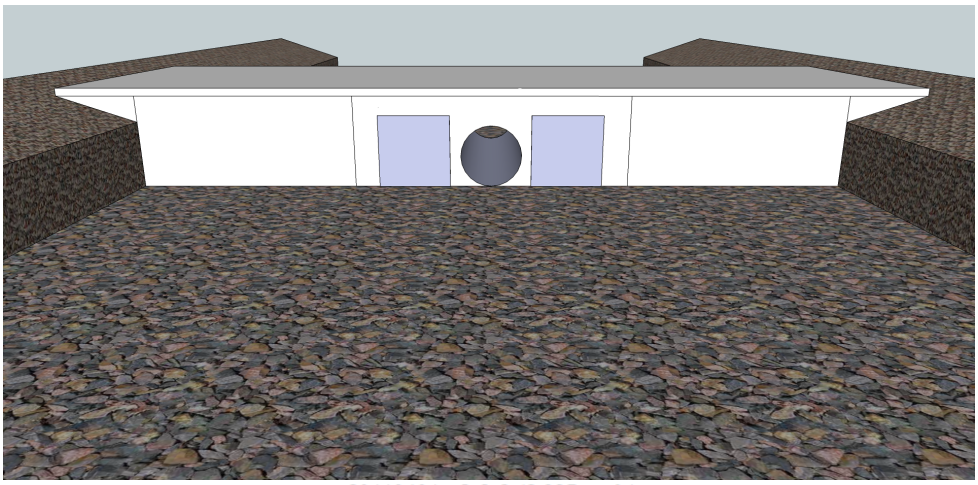

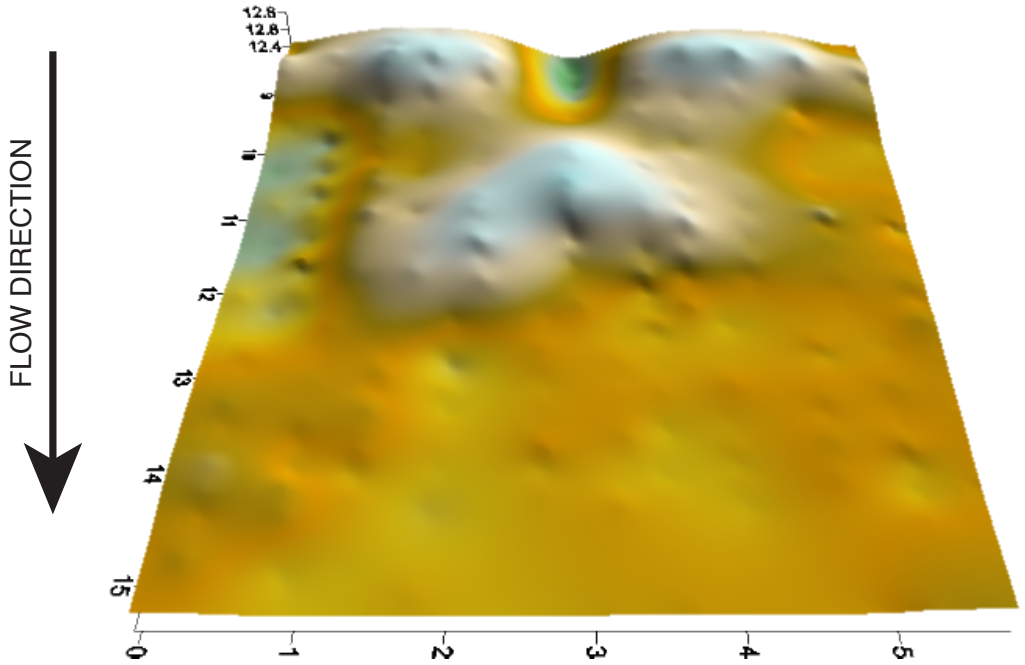

Figure 3.21. Surface Generated by Kriging Method for Experiment on 2011/04/01, Experimental Model S-6-C—Culvert Diagram Not to Scale

Figure 3.22. Photograph of Downstream Bedform Following Experiment on 2011/04/01, Experimental Model S-6-C

The surveying technique was refined during the break between experiments dated 2011/05/25 and 2011/07/22. The previously used technique required significant movement by the operator to survey strictly according to the grid mesh. The new technique removed that restriction so that the operator could survey more points without having to move as much—for a 4 foot survey the operator had to move past the total station without disturbing the bedforms a maximum of 3 times. The thought process was that the unnecessary movement of the operator to reset the grid for each new line meant that there was more opportunity for the instrument to be bumped or otherwise shifted out of plane. The technique developed now allows the operator to "freehand" the survey based on the detected prominent features of the bedform.

An example of the new survey method with the data points plotted and connected in the order with which they were collected is shown in Figure 3.23. The survey started at the farthest downstream extents of the bedform.

The new survey method Standard Operating Procedures are based on a length of grid to be measured. The total number of points is 220 for a 4-foot section, 270 for a 5-foot section, and 320 for a 6-foot section. These values are based on the old survey method, in order to have the same number of points from the before survey as the after survey. The before survey is done in the old style, with the more structured grid approach, but the after survey is done by the new method. Overall, the new method saves the operator time by not requiring the operator to move as much. The new survey method becaume a standard operating procedure as follows:

1. Setup the instrument on the downstream culvert and level the instrument,
2. Resection using points that are easily identifiable and facing the instrument (typically `pumpbolt1`, `pumpbolt2`, `pumpbolt3`, and `pipedotlb`),
3. Place the survey grid alignment tool so that its long side is perpendicular to the flow direction and is approximately four feet downstream of the culvert model,
4. Survey each point along the grid on the downstream edge, then on upstream edge,
5. Survey any potential scour upstream of the survey grid alignment tool,
6. Survey along the toe of the gravel bar,
7. Survey along the crest of the gravel bar,
8. Survey between the crest and toe of the gravel bar,
9. Survey extra intermediate points until approximately 20 points remain,

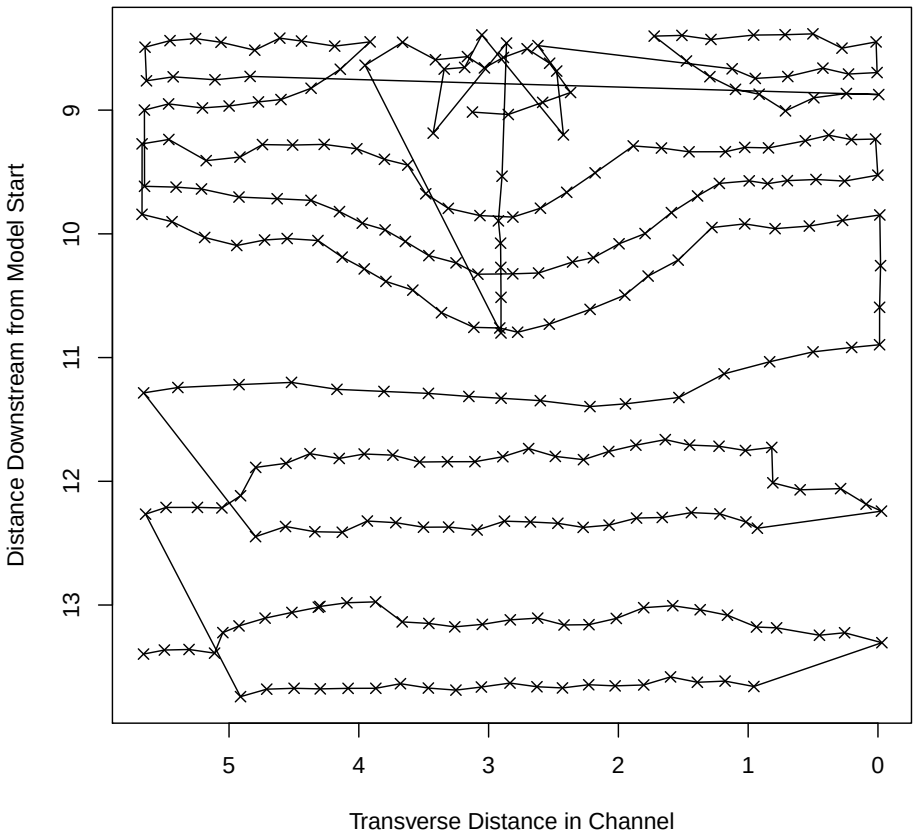

Figure 3.23. Example of the New Surveying Technique

10. Move any portion of the gravel bar if it is preventing the farthest upstream rocks from being surveyed, and
11. Survey the final points and pack up the instrument.

Figures 3.24, 3.25, and 3.25 especially highlight the new surveying technique used on the smaller rock size. The kriging method smoothed the bumps that are very obvious in the inverse distance models.

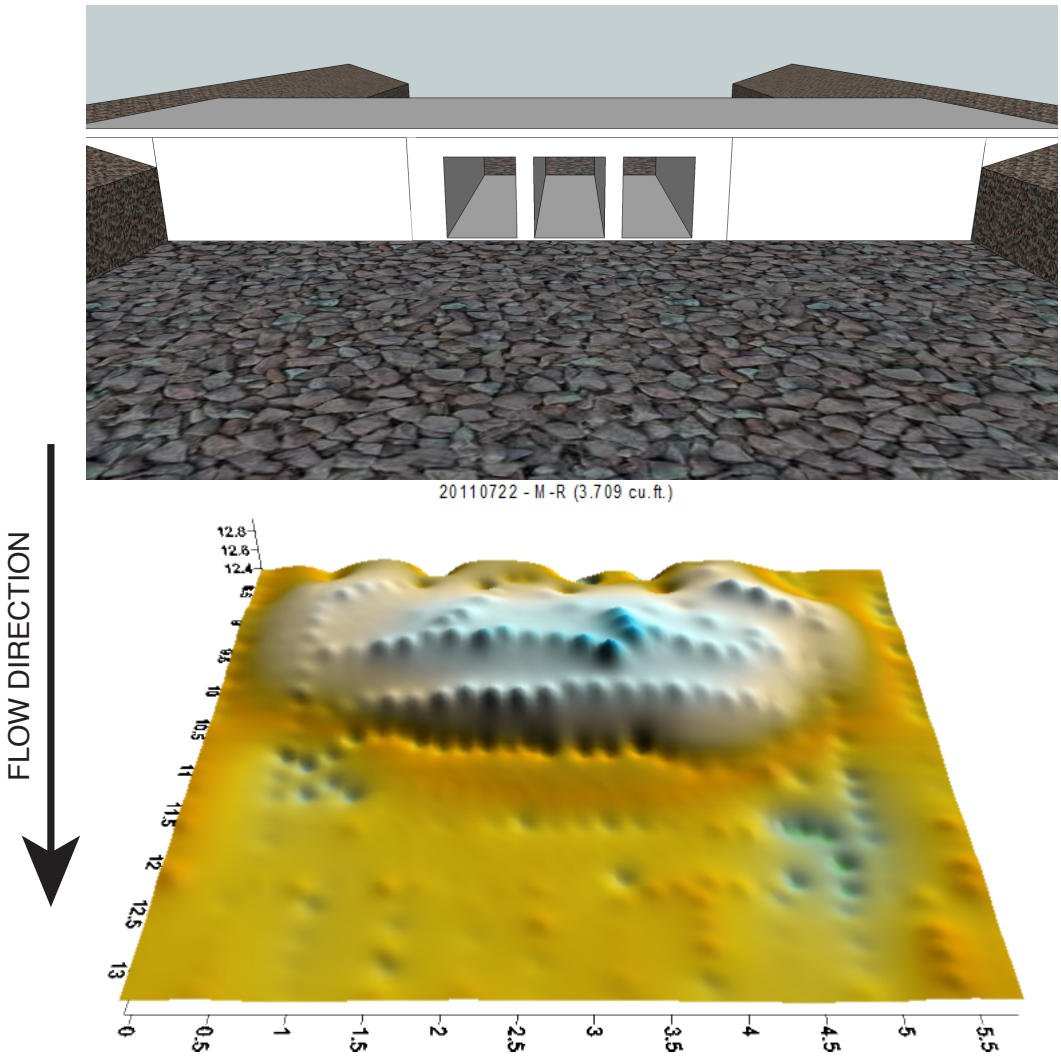

Figure 3.24. Surface Generated by Inverse Distance Method for Experiment on 2011/07/22, Experimental Model M-R—Culvert Diagram Not to Scale

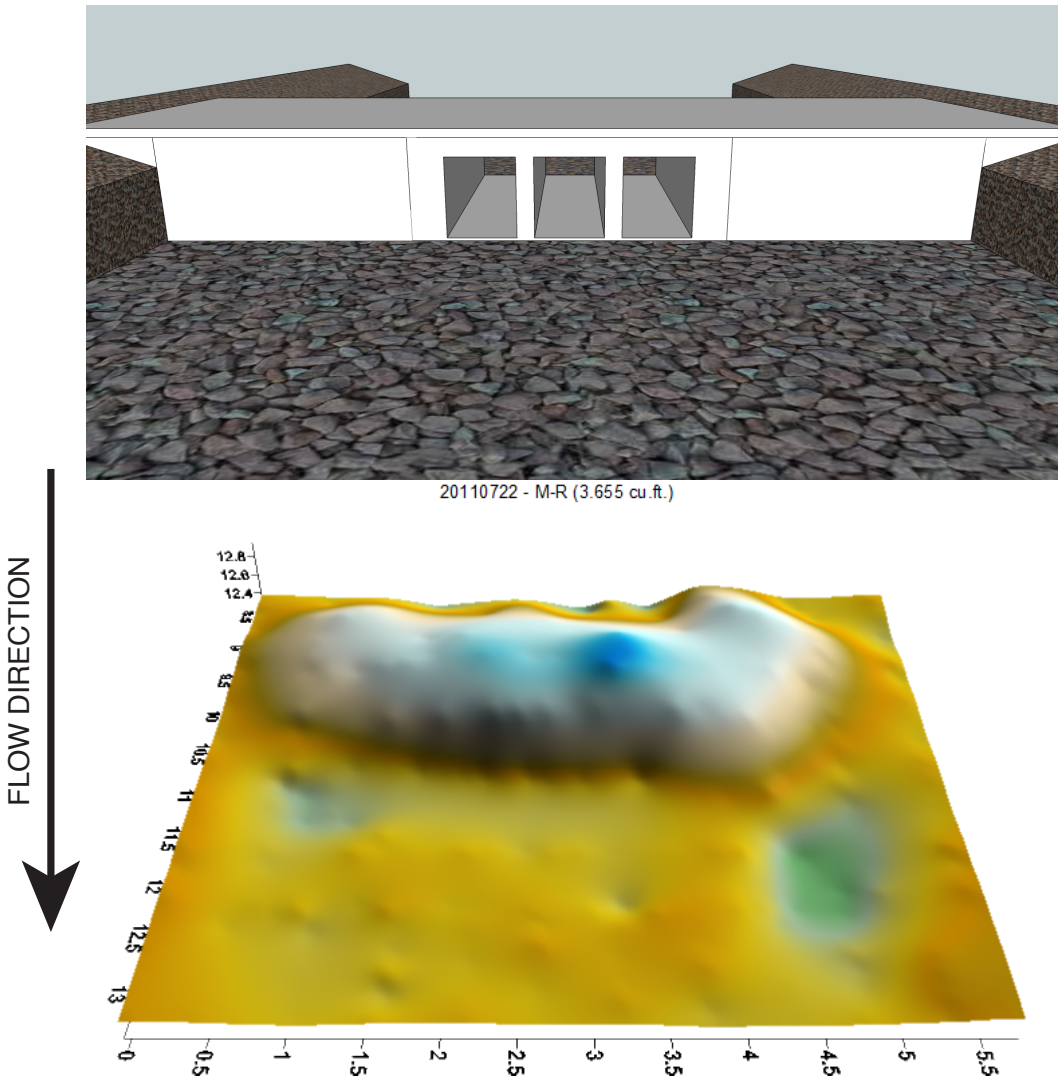

Figure 3.25. Surface Generated by Kriging Method for Experiment on 2011/07/22, Experimental Model M-R—Culvert Diagram Not to Scale

Figure 3.26. Photograph of Downstream Bedform Following Experiment on 2011/07/22, Experimental Model M-R

3.4.2 Solids Stuck in the Culvert

After each experiment, the rocks that are retained in the culvert barrel(s) are removed and weighed on a digital scale. The scale can read different values based on where the bucket is placed, so multiple readings are taken. If the readings match, then the weight of rocks is assumed to be correct at that value.

Not every experiment had a substantial amount of rocks remaining in the culvert barrel(s), but the experiments that did are shown in Table 3.5. These weights are solely included to give an estimate of the size of the clog in the barrels.

Table 3.5. Weights of Rocks Measured on Experiments with Substantial Volume Remaining in the Barrels

Date	**Configuration**	**Weight** (lbs)	**Date**	**Configuration**	**Weight** (lbs)
2011/01/24	SB-I	30.0	2011/05/12	M-6-C	24.8
2011/01/25	M-4-C	41.6	2011/05/13	M-6-C	16.8
2011/01/27	M-4-C	29.6	2011/05/14	M-6-C	13.0
2011/01/28	M-4-C	44.0	2011/05/16	M-R	24.2
2011/02/05	S-4-C	16.4	2011/05/17	M-R	36.2
2011/02/07	S-4-C	14.6	2011/05/18	M-R	14.4
2011/02/10	S-4-C	16.2	2011/08/11	M-4-C	7.6
2011/02/14	S-6-C	23.4	2011/08/12	M-4-C	6.2
2011/02/15	S-6-C	29.2	2011/08/13	M-4-C	8.0
2011/02/16	S-6-C	17.4	2011/08/17	SB-I	10.4
2011/02/17	M-6-C	18.6	2011/08/19	M-6-C	7.4
2011/02/18	M-6-C	50.8	2011/08/20	M-6-C	15.0
2011/02/19	M-6-C	42.8	2011/08/21	M-6-C	8.7
2011/02/21	M-R	35.4	2011/08/23	SB-C	6.4
2011/02/22	M-R	25.8	2011/08/25	M-R	32.2
2011/02/23	M-R	17.0	2011/08/25	M-R	35.4
2011/02/28	S-R	12.2	2011/08/26	M-R	35.2

Chapter 4
Results

One of the notable results of the experiments was that there were apparently specific bedforms created by each culvert arrangement. Single barrel arrangements tended to have two very pronounced scour pits downstream and to the outside of the main bedform that formed downstream of the culvert barrel. Multiple identical barrel arrangements tended to have one large mound that would nearly span the channel width. The staggered barrel arrangements showed a tendency for what appeared to be early stages of erosion of the built up formation.

The staggered barrel configurations exhibited bedforms that were not all that different from the multiple barrel configurations with the exception that there seemed to be an orientation of the sediments. The orientation of the sediments would tend to indicate flow going around the largest portion of the bedform as the flow exits the culvert barrel. Further experimentation should be performed on this result.

The following results show images that were generated in Surfer (Golden Software, 2002) using the survey data. The color ramp, shown in Figure 4.1, is normalized for all experiments, and the colors represent the same elevation in each picture. The numbers in the top of each picture show the difference in volume between the before surface and the after surface.

4.1 Staggered Barrels with Inverts Equal (SB-I)

Figure 4.2 shows that the surveyed bedform has very slight accumulation and there is mild scour evidence.

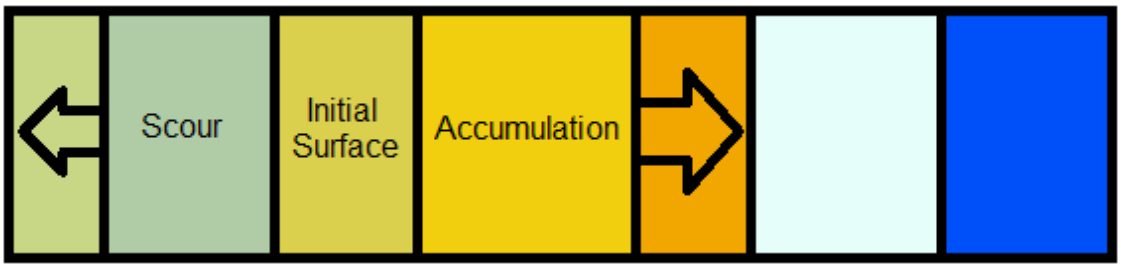

Figure 4.1. Color Ramp Used to Assist in the Evaluation of Surface Models

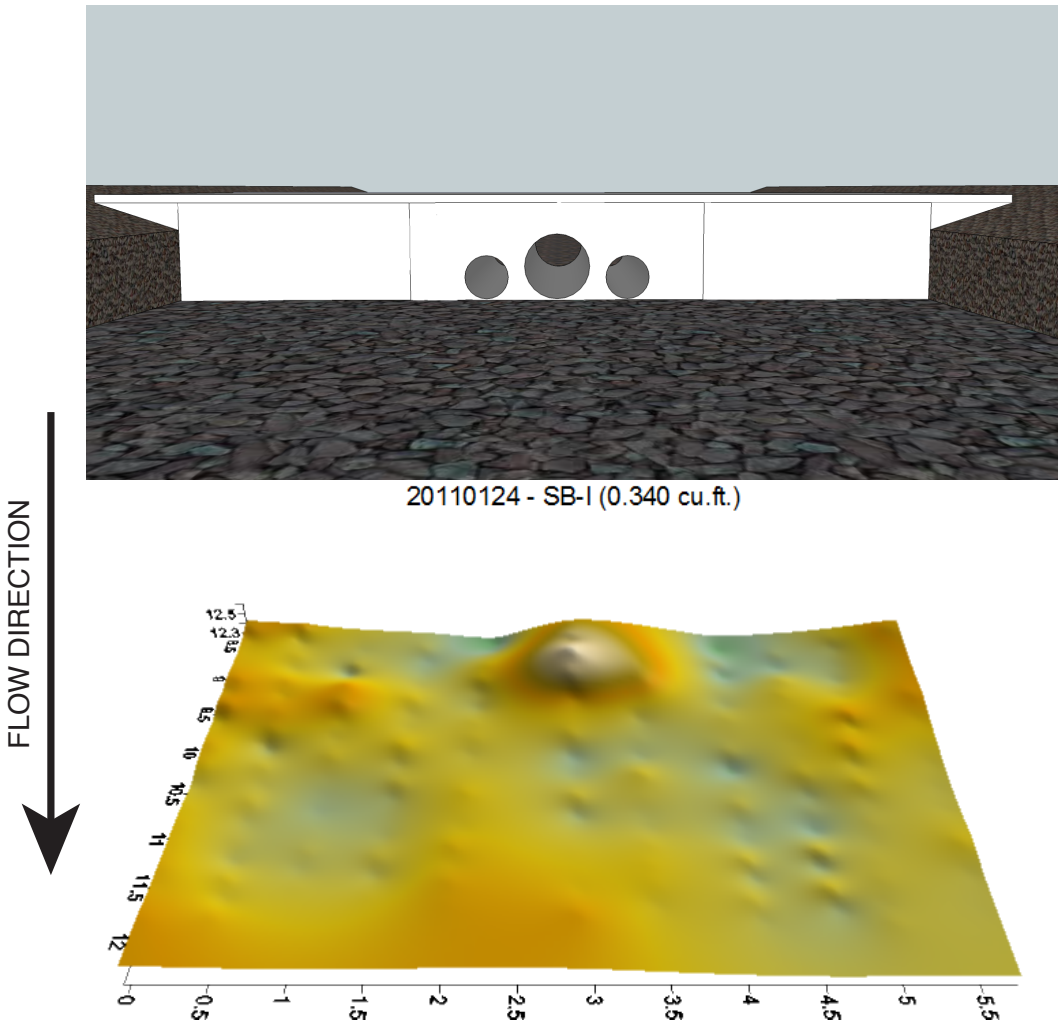

Figure 4.2. Typical Downstream Surface Model for Experimental Model SB-I for 0.3 Percent Slope with Large Rocks

Figure 4.3 shows a "U-shaped" gravel bar with a slight wing toward the right bank and a larger wing toward the left bank.

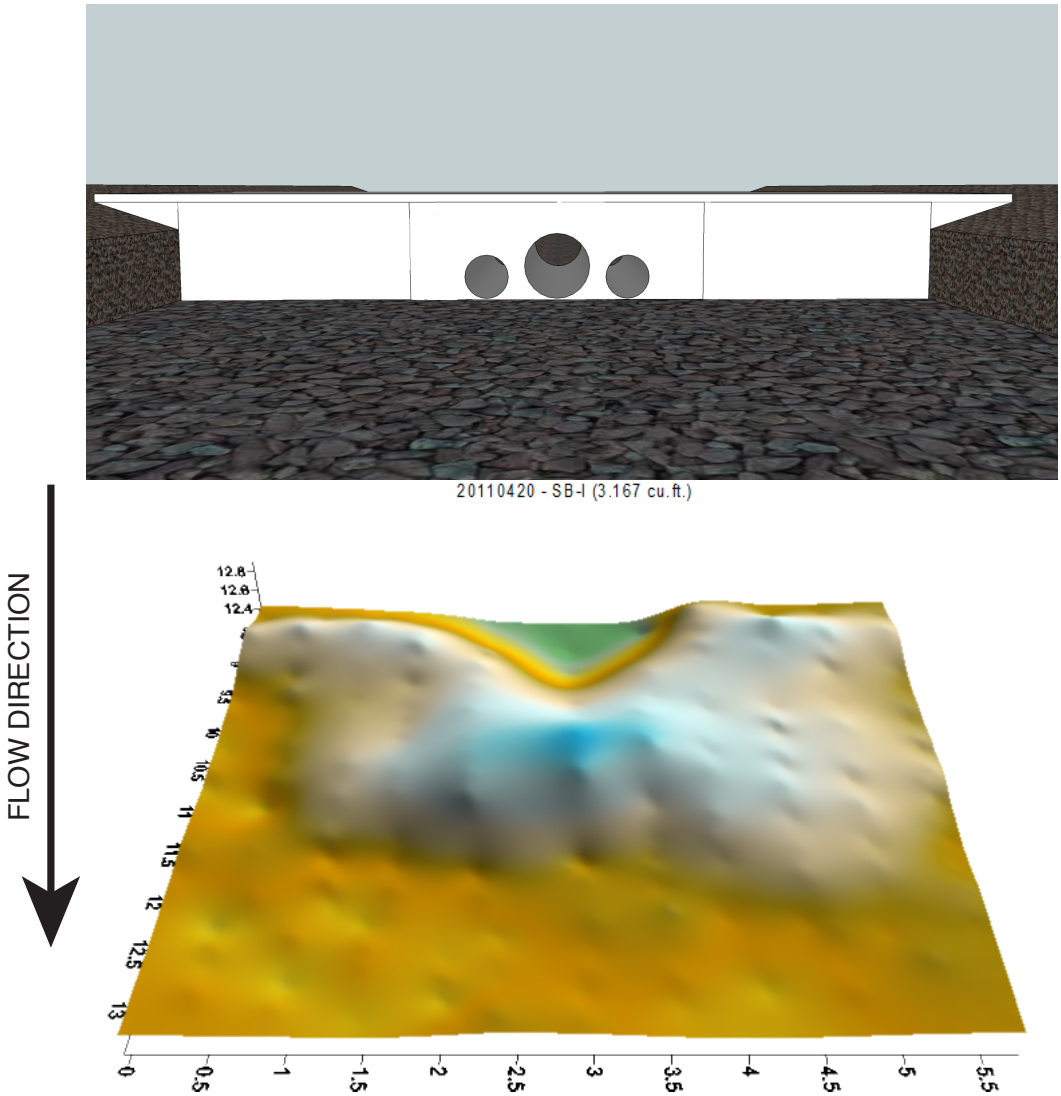

Figure 4.3. Typical Downstream Surface Model for Experimental Model SB-I for 1.0 Percent Slope with Large Rocks

Figure 4.4 shows a gravel bar just downstream of the culvert with noticeable scour downstream and towards the banks.

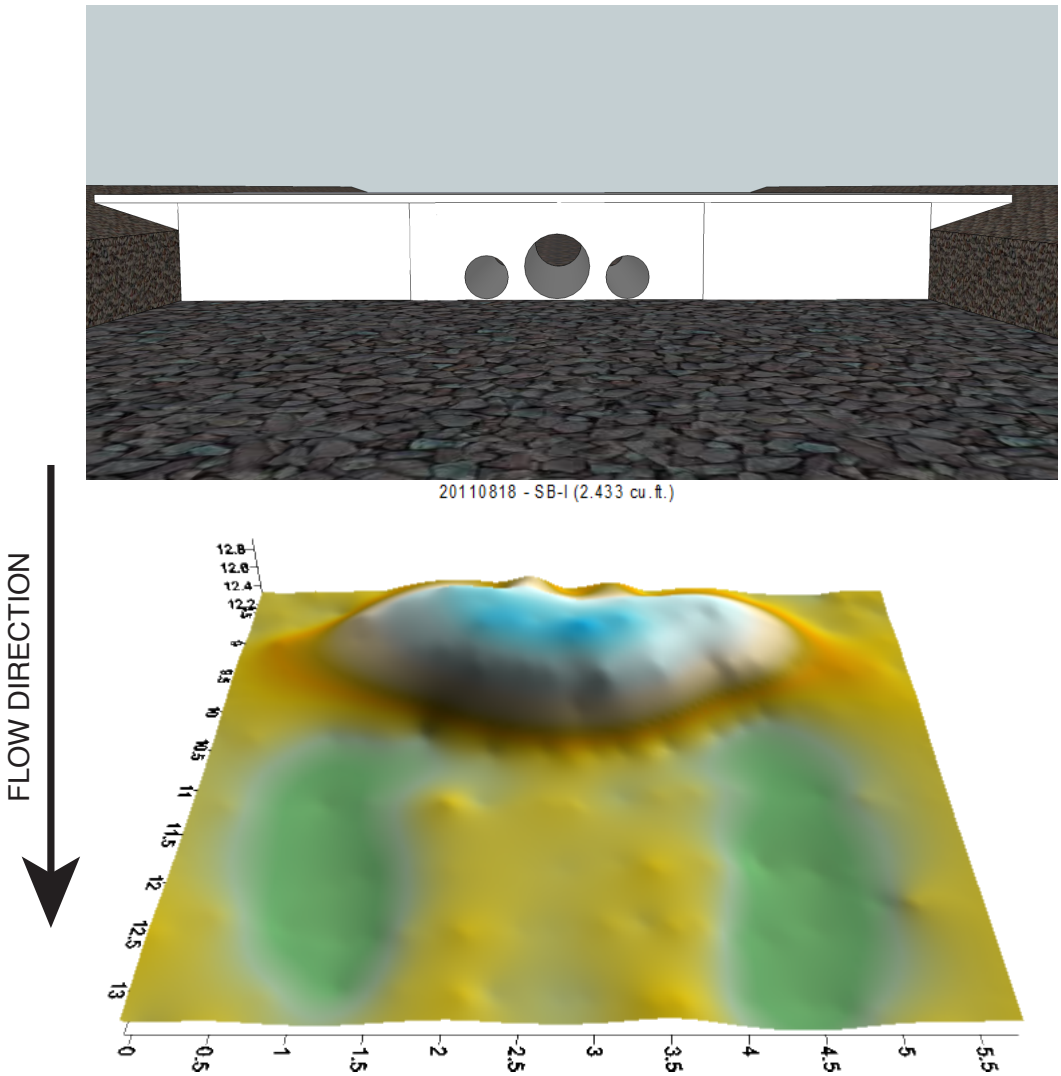

Figure 4.4. Typical Downstream Surface Model for Experimental Model SB-I for 0.3 Percent Slope with Small Rocks

4.2 Staggered Barrels with Crowns Equal (SB-C)

Figure 4.5 shows a gravel bar with mild scour downstream of the bedform and some mild accumulation near the culvert headwall.

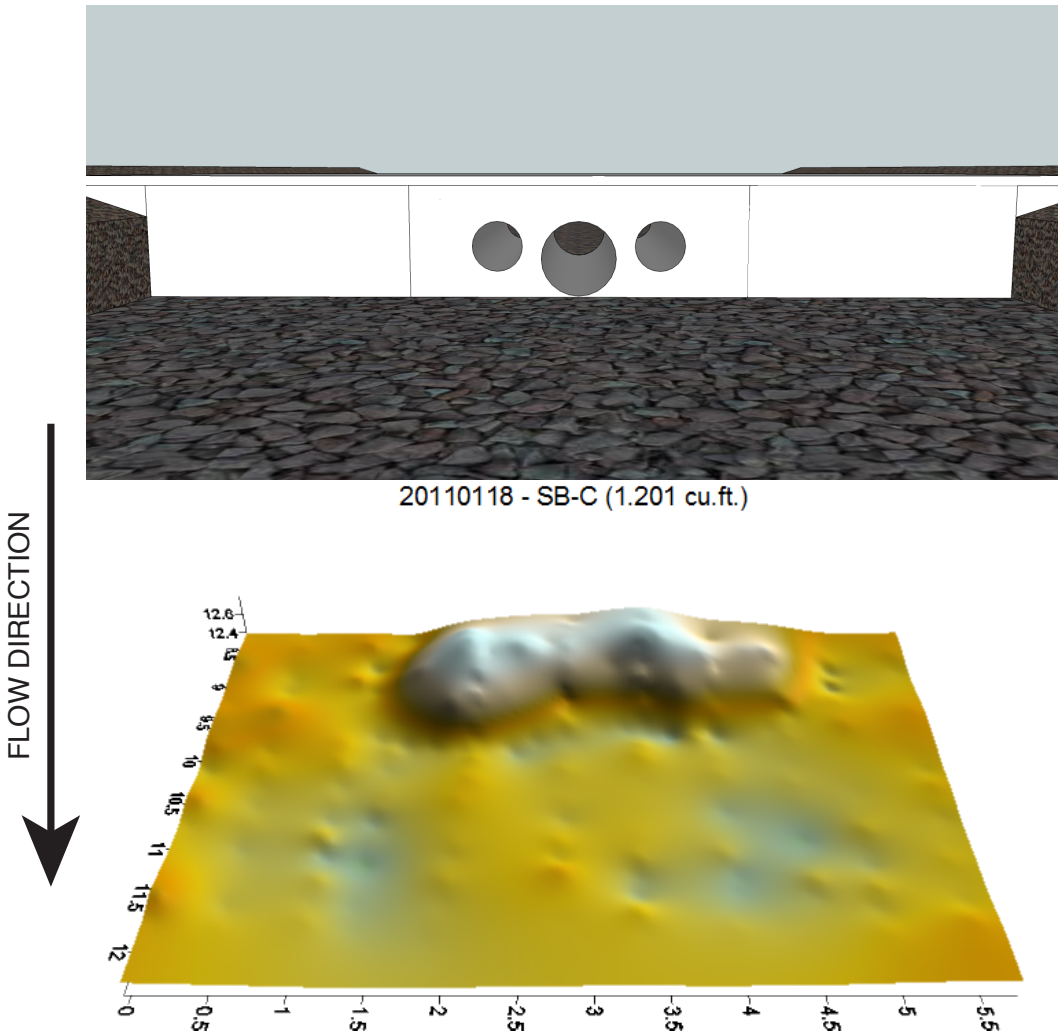

Figure 4.5. Typical Downstream Surface Model for Experimental Model SB-C for 0.3 Percent Slope with Large Rocks

Figure 4.6 also shows a gravel bar, but has obvious evidence of scour along the left bank.

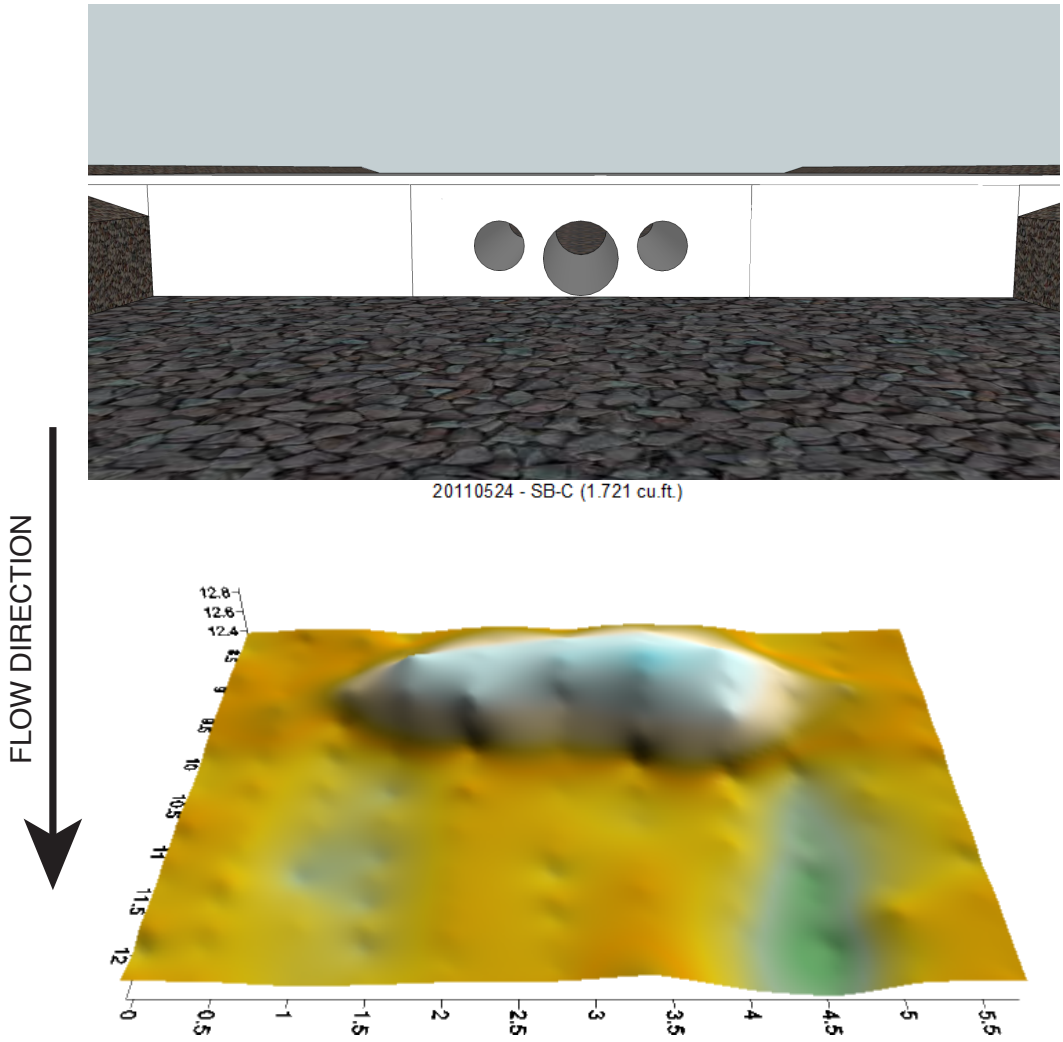

Figure 4.6. Typical Downstream Surface Model for Experimental Model SB-C for 0.6 Percent Slope with Large Rocks

Figure 4.7 shows a U-shaped gravel bar with the sides washed out into wings, as well as some accumulation near the culvert headwall.

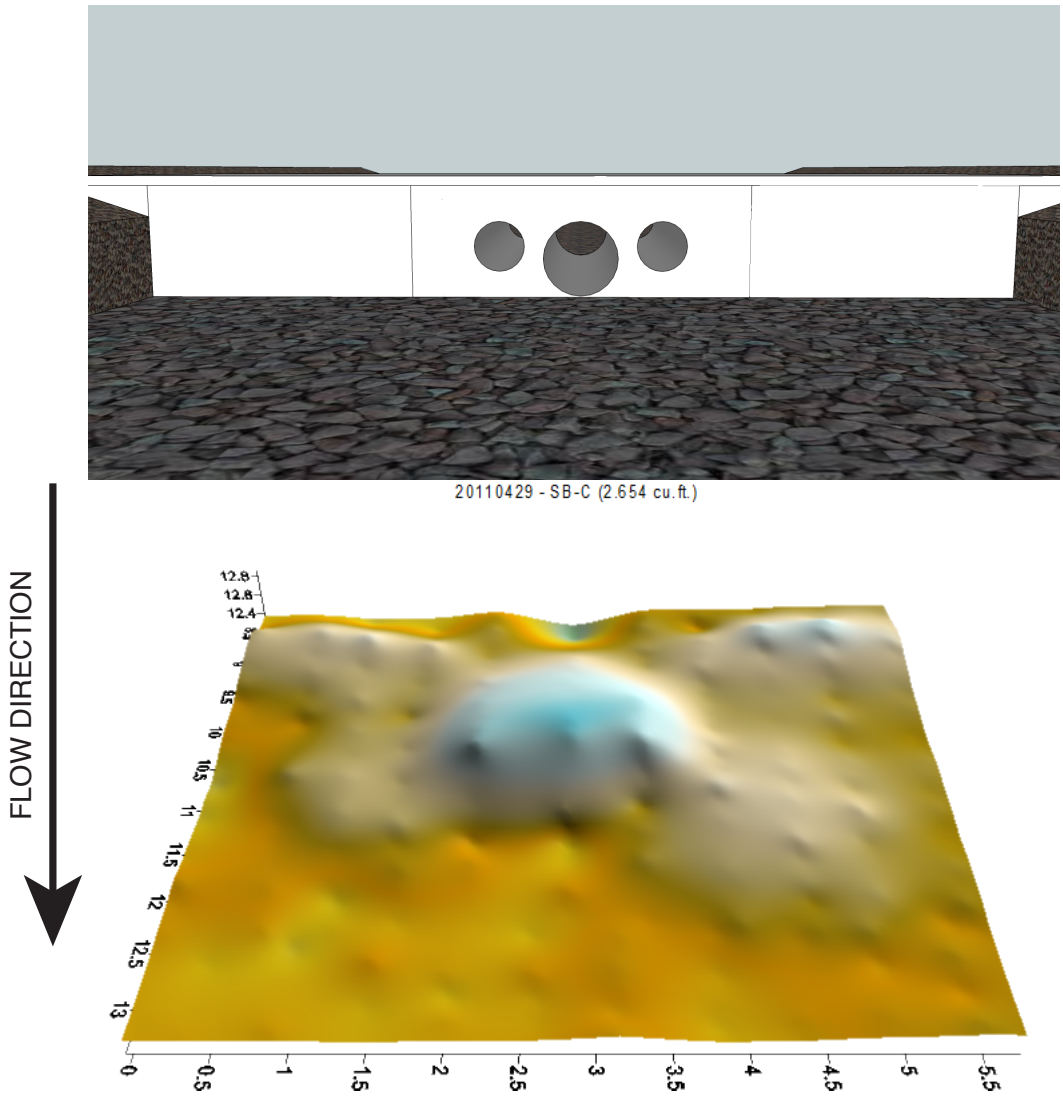

Figure 4.7. Typical Downstream Surface Model for Experimental Model SB-C for 1.0 Percent Slope with Large Rocks

Figure 4.8 shows a gravel bar with noticeable scour downstream and towards the banks.

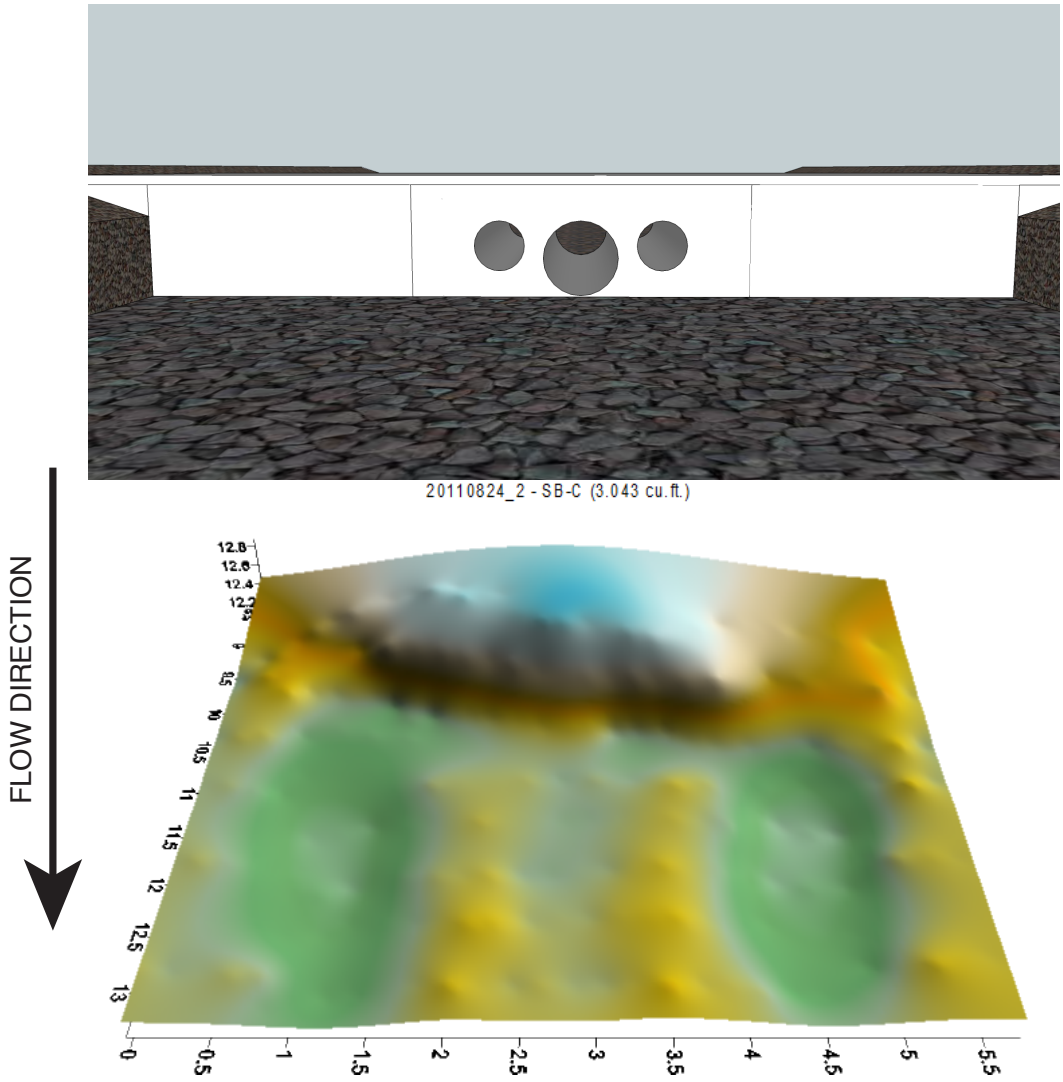

Figure 4.8. Typical Downstream Surface Model for Experimental Model SB-C for 0.3 Percent Slope with Small Rocks

Figure 4.9 shows an gravel bar with a pronounced wing on the left bank and a lesser wing on the right bank.

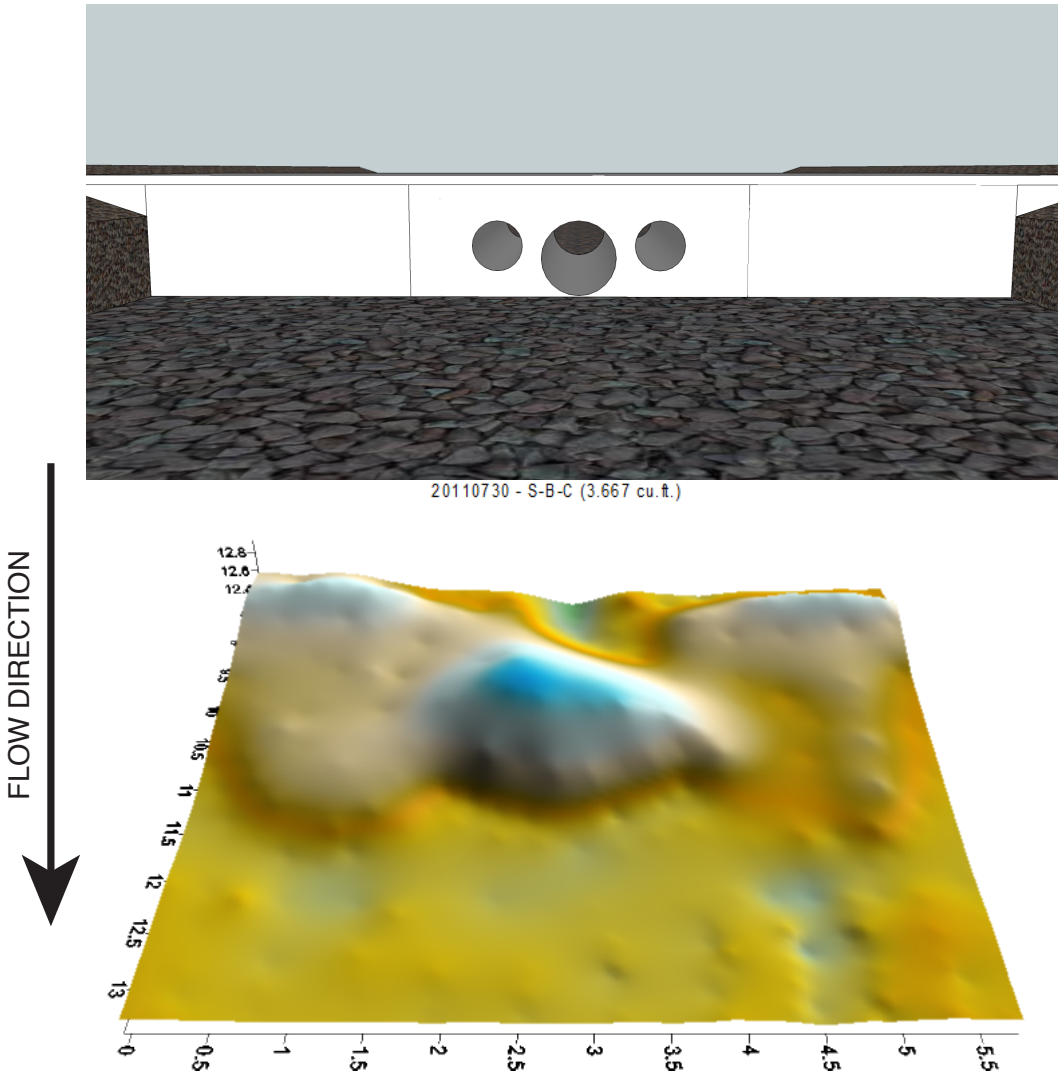

Figure 4.9. Typical Downstream Surface Model for Experimental Model SB-C for 0.6 Percent Slope, with Small Rocks

4.3 Multiple 4-inch Circular Barrels (M-4-C)

Figure 4.10 shows a slight mound with some scour immediately surrounding the mound.

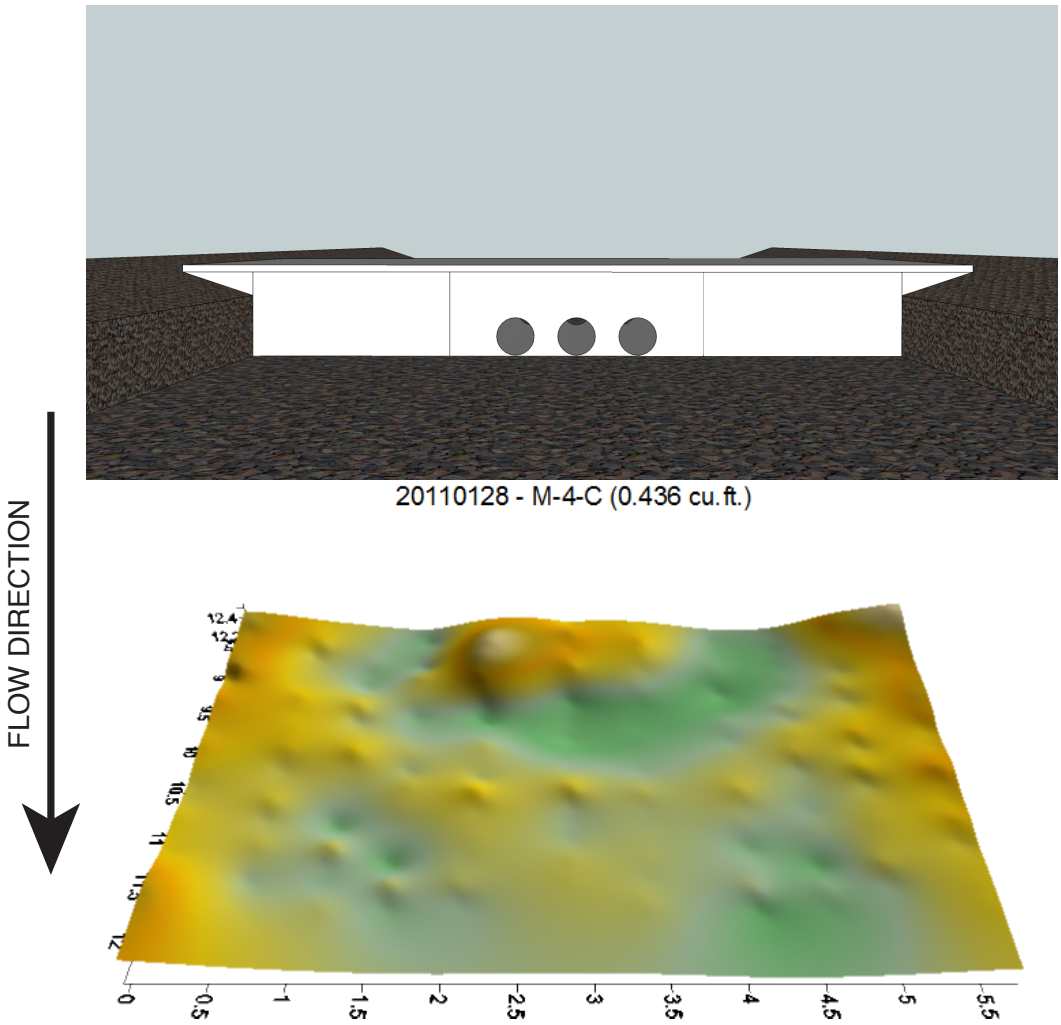

Figure 4.10. Typical Downstream Surface Model for Experimental Model M-4-C for 0.3 Percent Slope with Large Rocks

Figure 4.11 shows a flat gravel bar across the channel that has been built up significantly from the beginning of the experiment. Note the green shades near the culvert exit that signify scour.

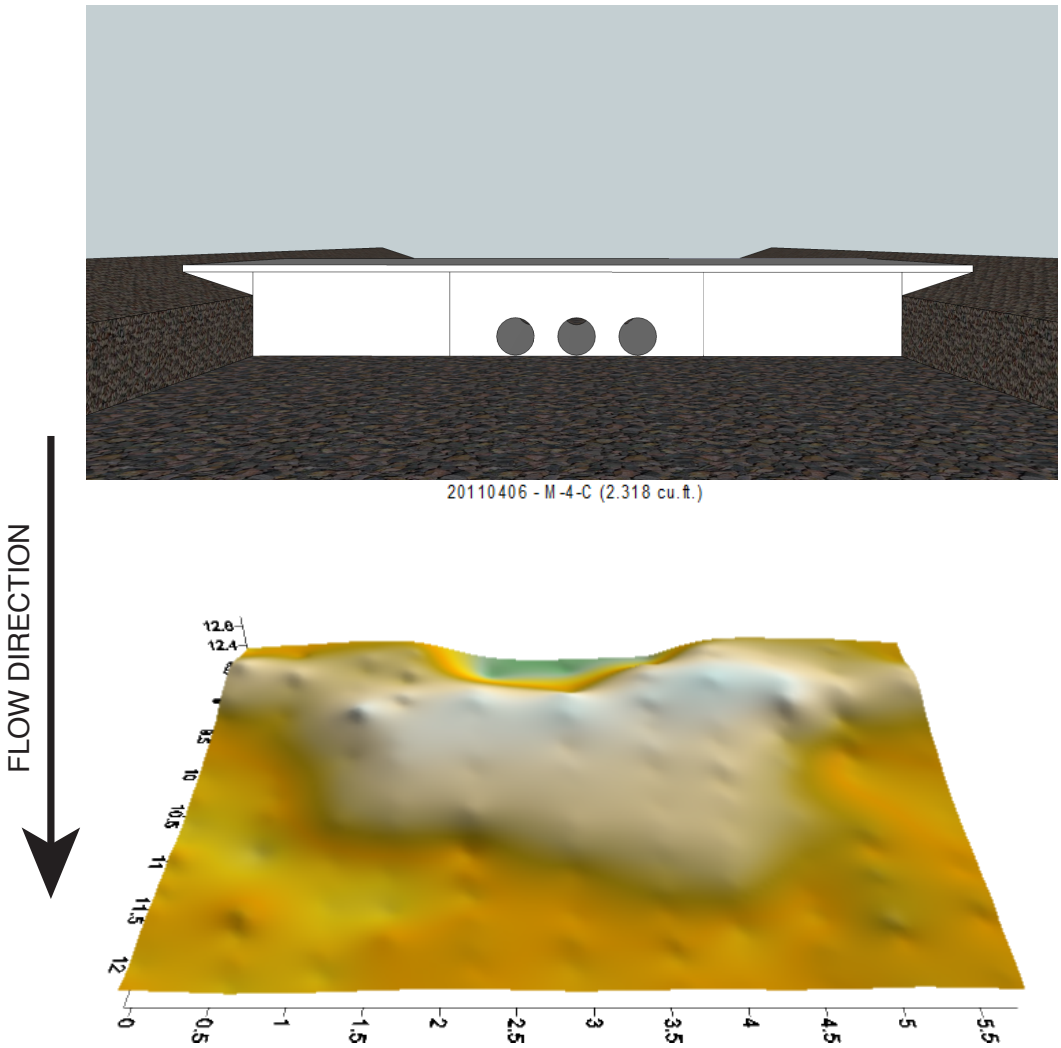

Figure 4.11. Typical Downstream Surface Model for Experimental Model M-4-C for 1.0 Percent Slope with Large Rocks

Figure 4.12 shows a flat gravel bar that spans most of the channel. There is also some significant scour present downstream.

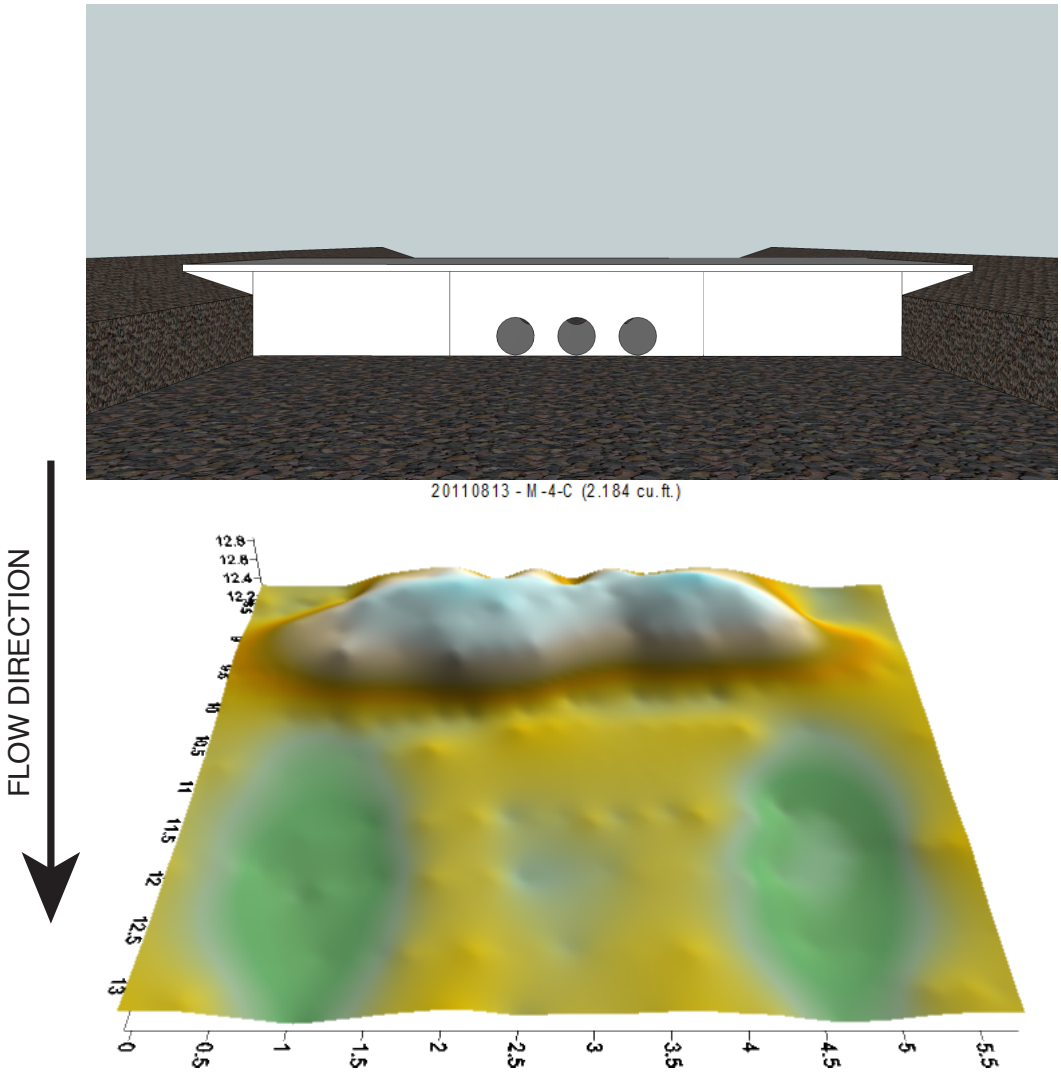

Figure 4.12. Typical Downstream Surface Model for Experimental Model M-4-C for 0.3 Percent Slope with Small Rocks

Figure 4.13 also shows a flat gravel bar extending across the channel and scour is pronounced near the banks.

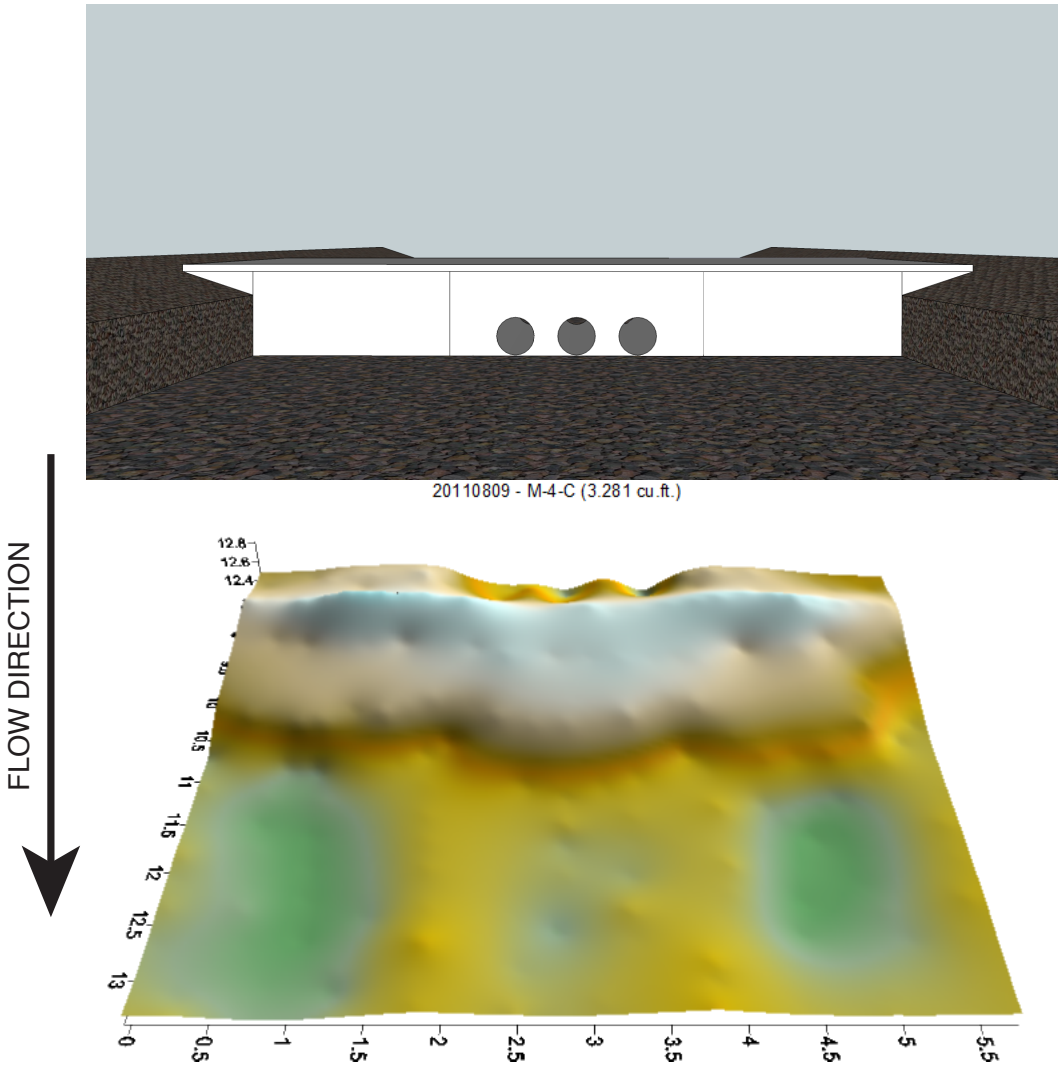

Figure 4.13. Typical Downstream Surface Model for Experimental Model M-4-C for 0.6 Percent Slope with Small Rocks

4.4 Single 4-inch Circular Barrel (S-4-C)

Figure 4.14 shows two mounds, one just downstream of the culvert outlet near the centerline, and the other between the centerline and the left bank. This dual mounding is especially interesting because it implies that there is significant eddy action near the culvert exit or sediment is being transported over the culvert model.

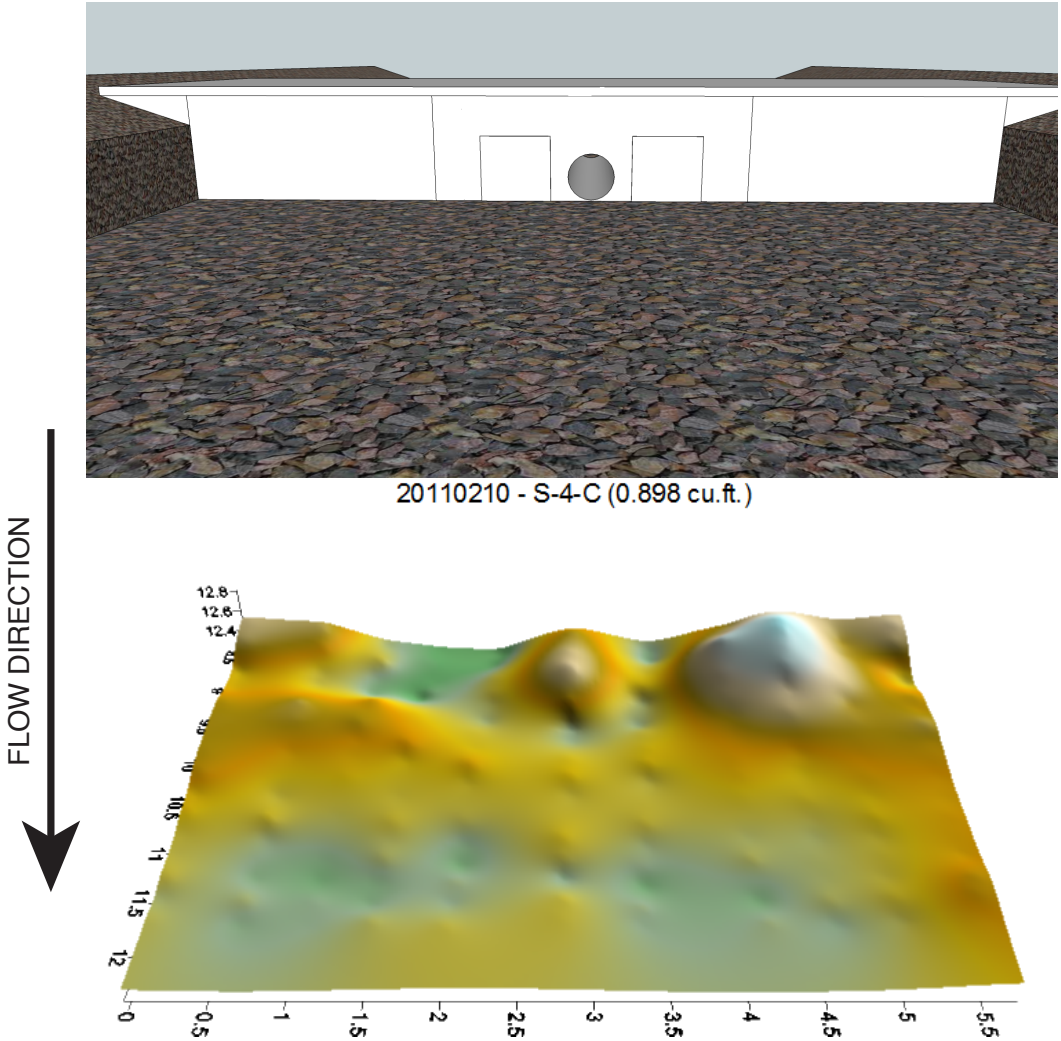

Figure 4.14. Typical Downstream Surface Model for Experimental Model S-4-C for 0.3 Percent Slope with Large Rocks

Figure 4.15 shows a U-shaped gravel bar with some scour on the outside banks.

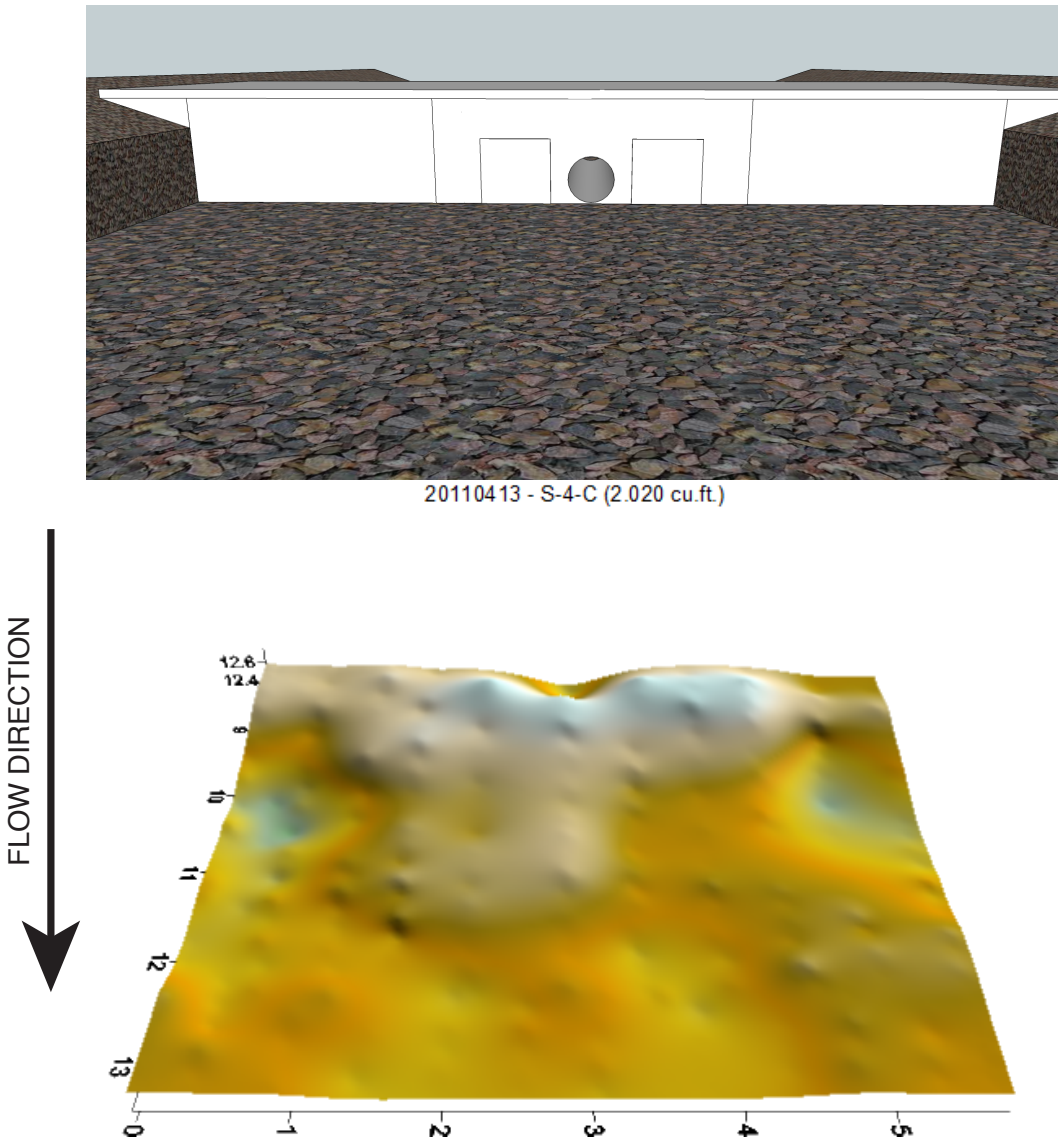

Figure 4.15. Typical Downstream Surface Model for Experimental Model S-4-C for 1.0 Percent Slope, with Large Rocks

Figure 4.16 shows a small mound downstream of the model, with smaller mounds against the model on the sides. These extra mounds corroborate the implications of the discussion about local eddies near the culvert exit in Figure 4.14.

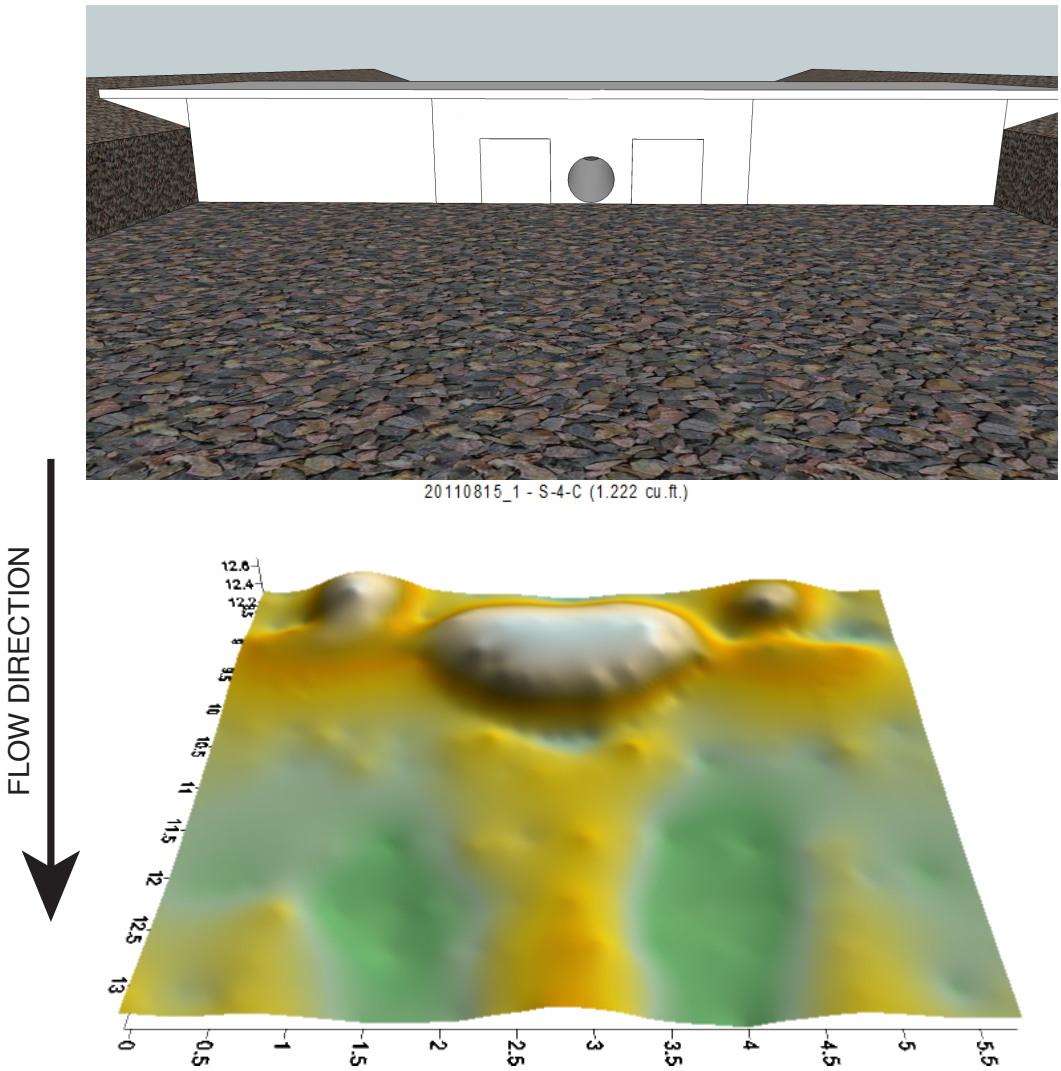

Figure 4.16. Typical Downstream Surface Model for Experimental Model S-4-C for 0.3 Percent Slope with Small Rocks

Figure 4.17 shows a flat mound the spans the channel, with scour downstream of the mound and at the culvert exit.

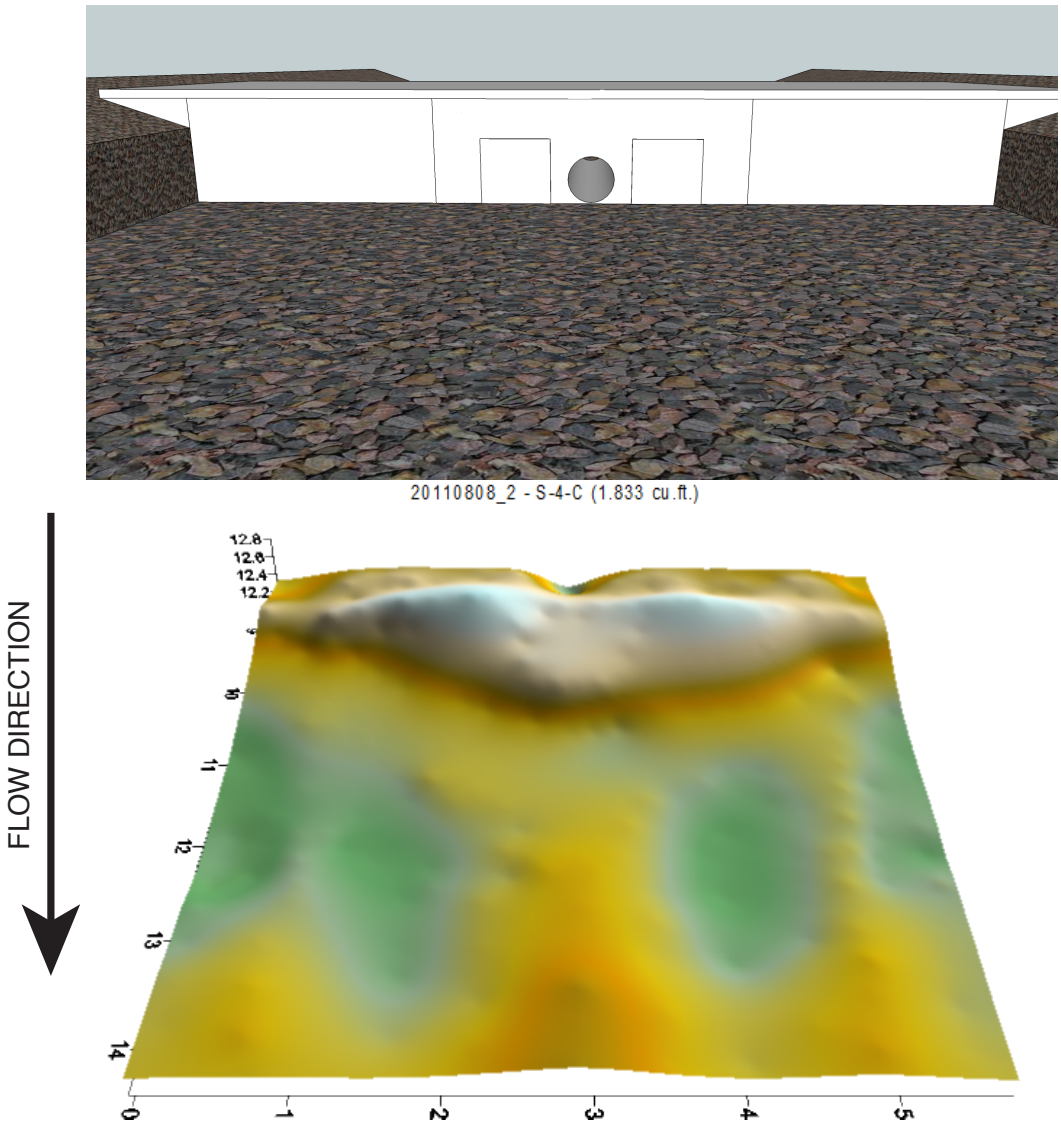

Figure 4.17. Typical Downstream Surface Model for Experimental Model S-4-C for 0.6 Percent Slope with Small Rocks

4.5 Multiple 6-inch Circular Barrels (M-6-C)

Figure 4.18 shows a small, flat gravel just downstream of the culvert near the headwall.

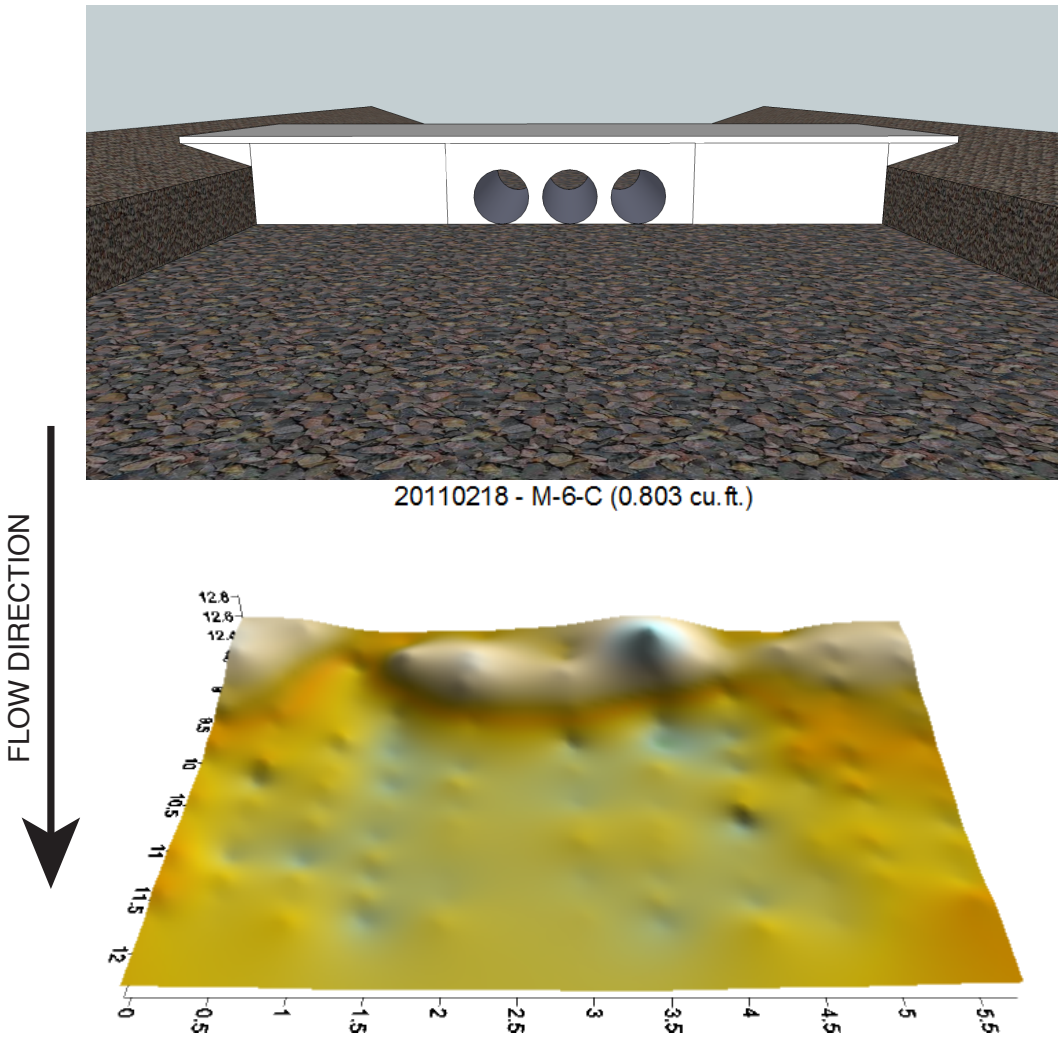

Figure 4.18. Typical Downstream Surface Model for Experimental Model M-6-C for 0.3 Percent Slope with Large Rocks

Figure 4.19 shows a flat gravel bar downstream of the culvert, but there is also some scour downstream of the bar and towards the right bank.

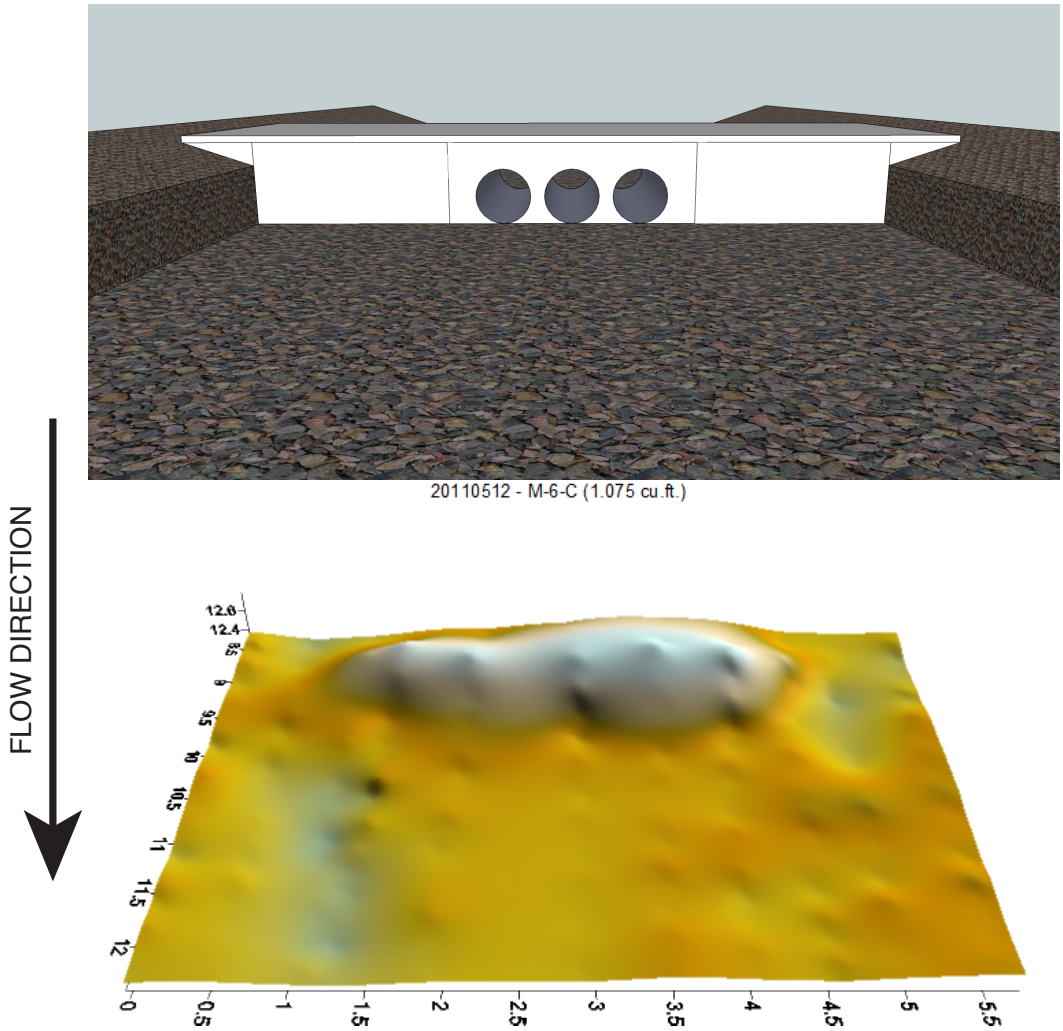

Figure 4.19. Typical Downstream Surface Model for Experimental Model M-6-C for 0.6 Percent Slope with Large Rocks

Figure 4.20 shows a U-shaped gravel bar that has notable scour at the culvert outlet and wings on both sides of the centerline. Note the accumulation in the corners by the headwall.

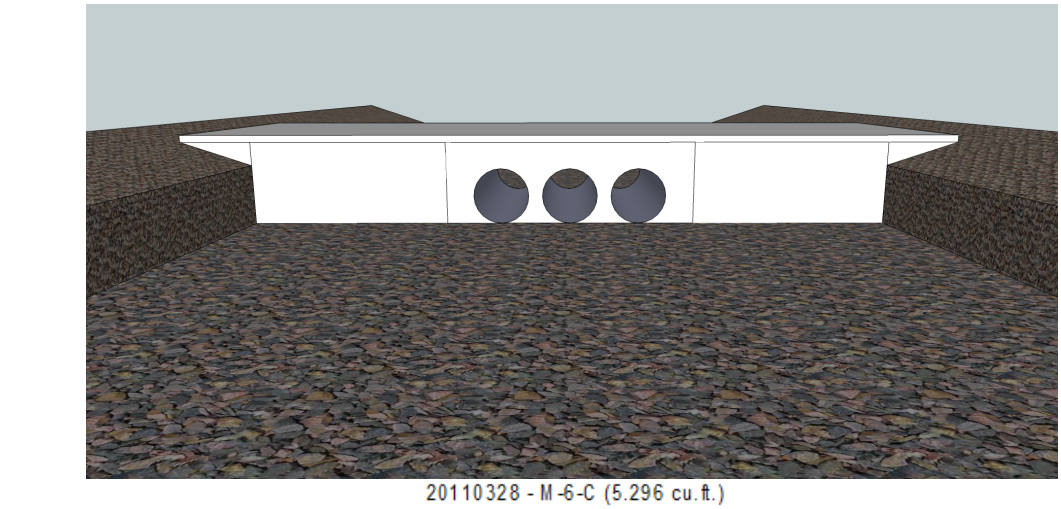

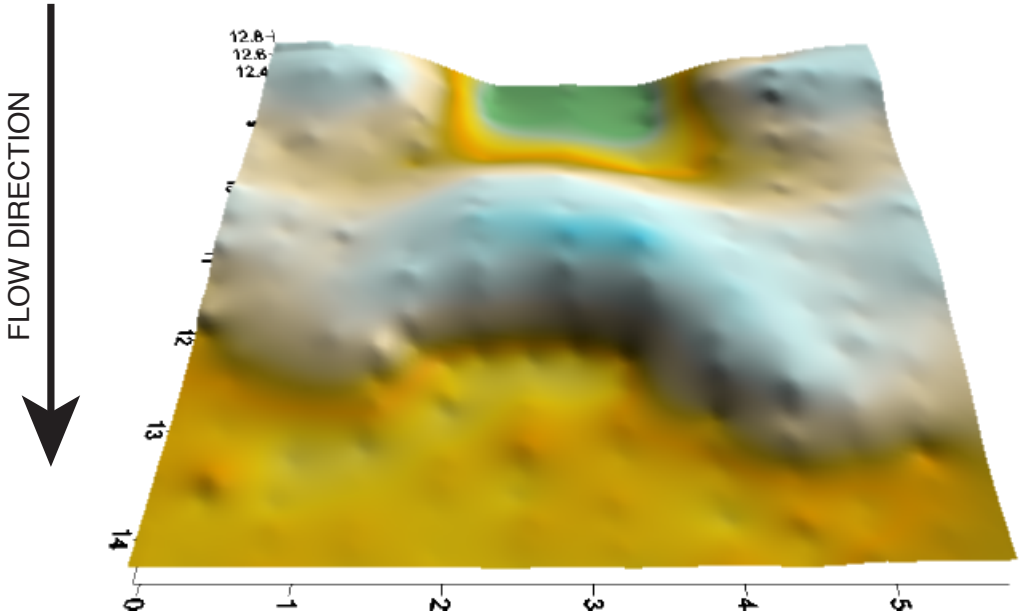

Figure 4.20. Typical Downstream Surface Model for Experimental Model M-6-C for 1.0 Percent Slope with Large Rocks

Figure 4.21 shows a flat gravel bar with three scour holes downstream.

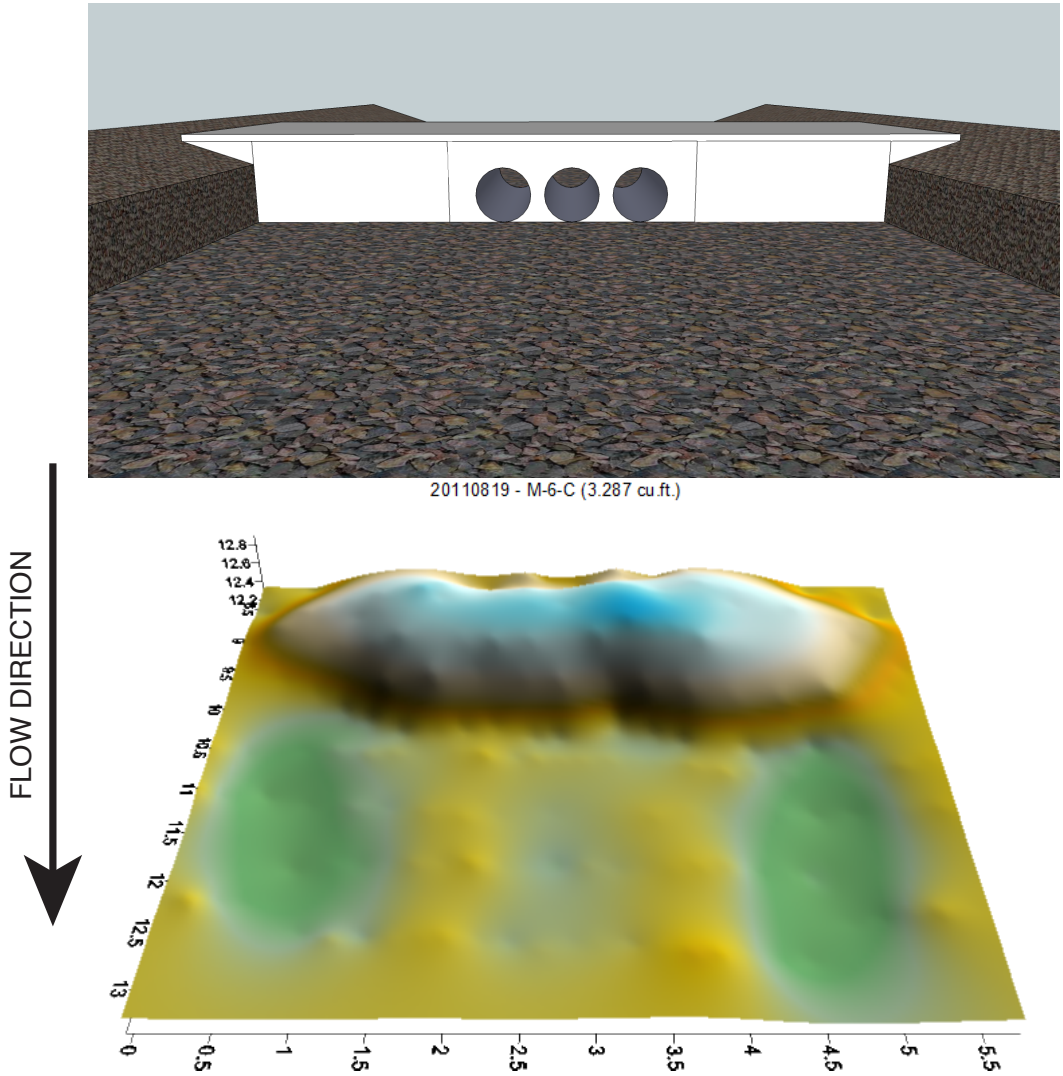

Figure 4.21. Typical Downstream Surface Model for Experimental Model M-6-C for 0.3 Percent Slope with Small Rocks

Figure 4.22 shows a U-shaped gravel bar with slight scour downstream and at the culvert exit.

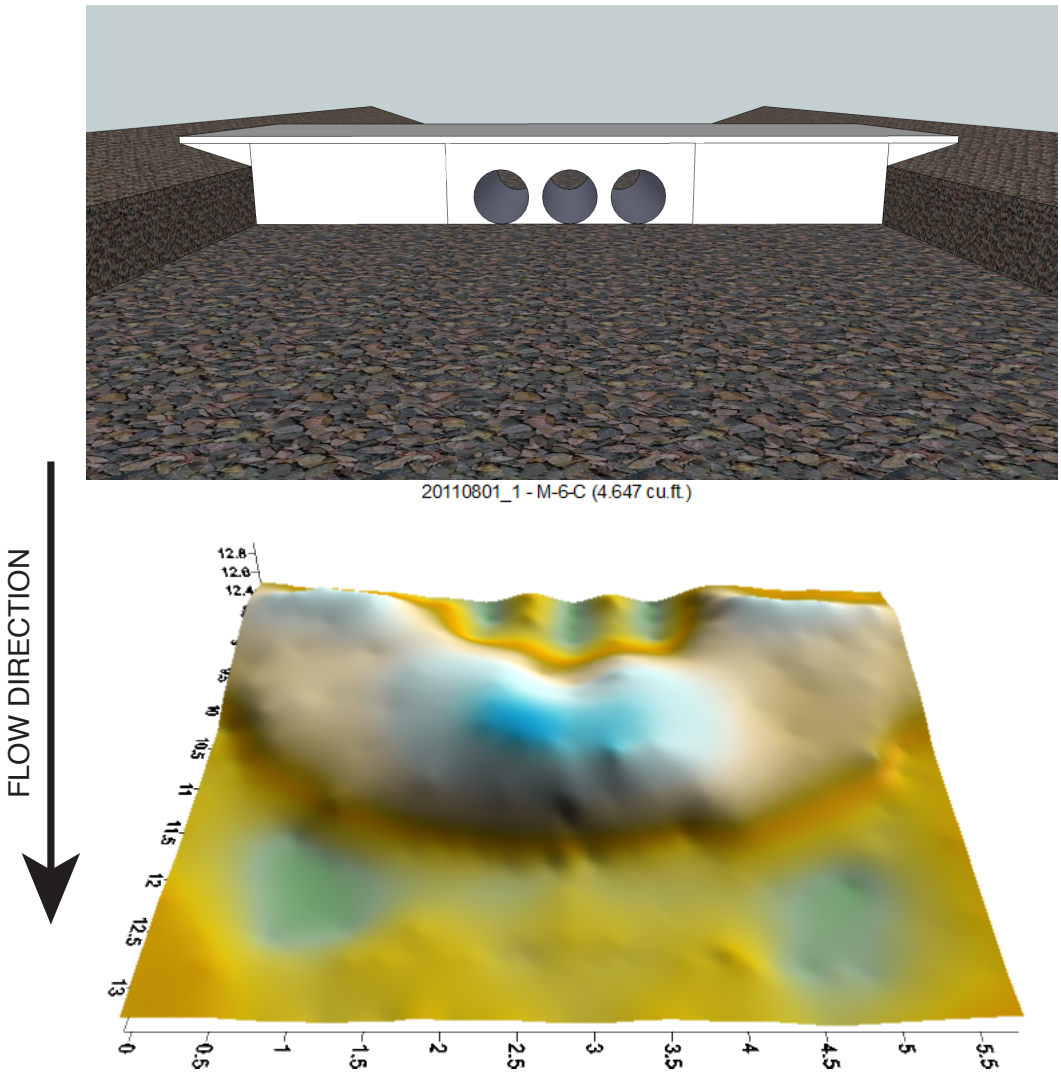

Figure 4.22. Typical Downstream Surface Model for Experimental Model M-6-C for 0.6 Percent Slope with Small Rocks

4.6 Single 6-inch Circular Barrel (S-6-C)

Figure 4.23 shows a mound just downstream of the culvert outlet.

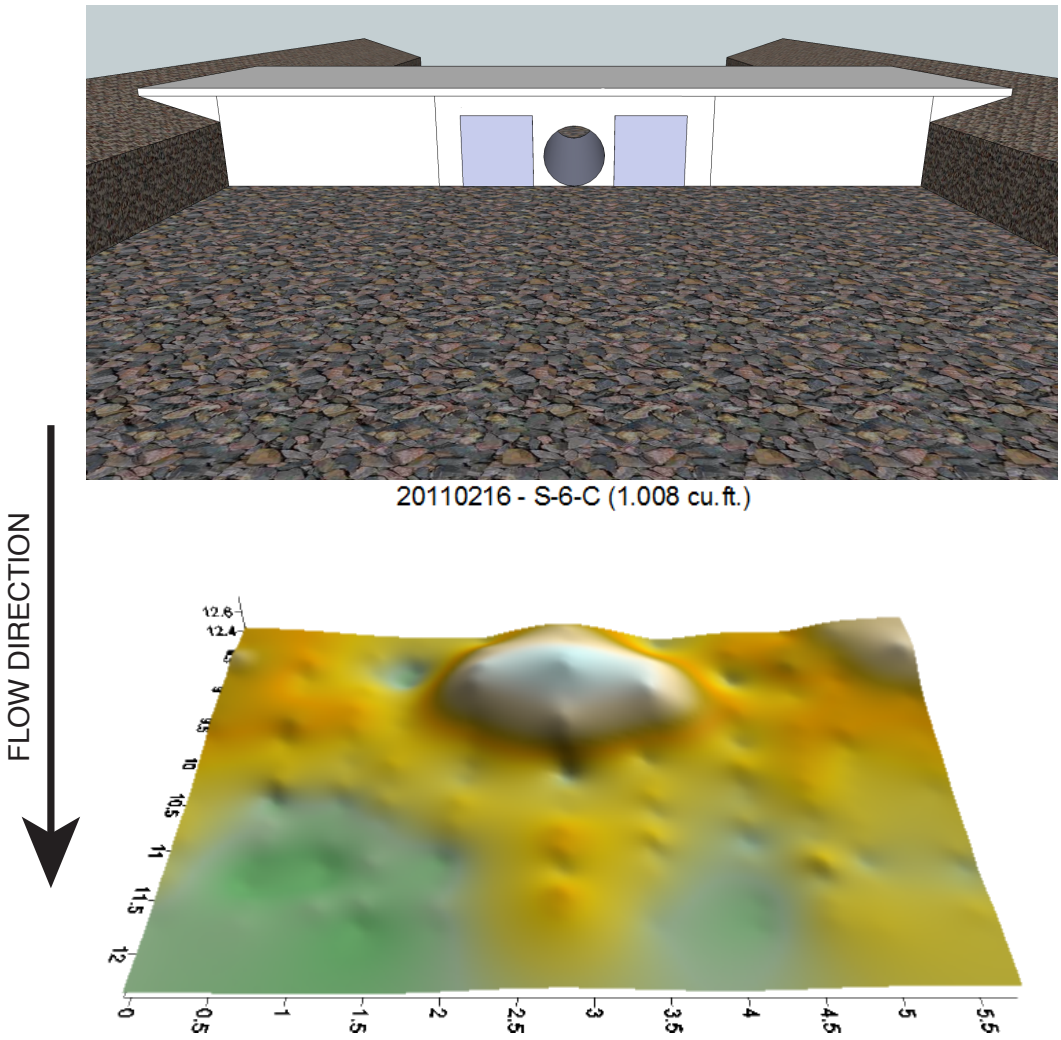

Figure 4.23. Typical Downstream Surface Model for Experimental Model S-6-C for 0.3 Percent Slope with Large Rocks

Figure 4.24 shows a flat gravel bar that nearly spans the channel and has mild scour downstream of the bar.

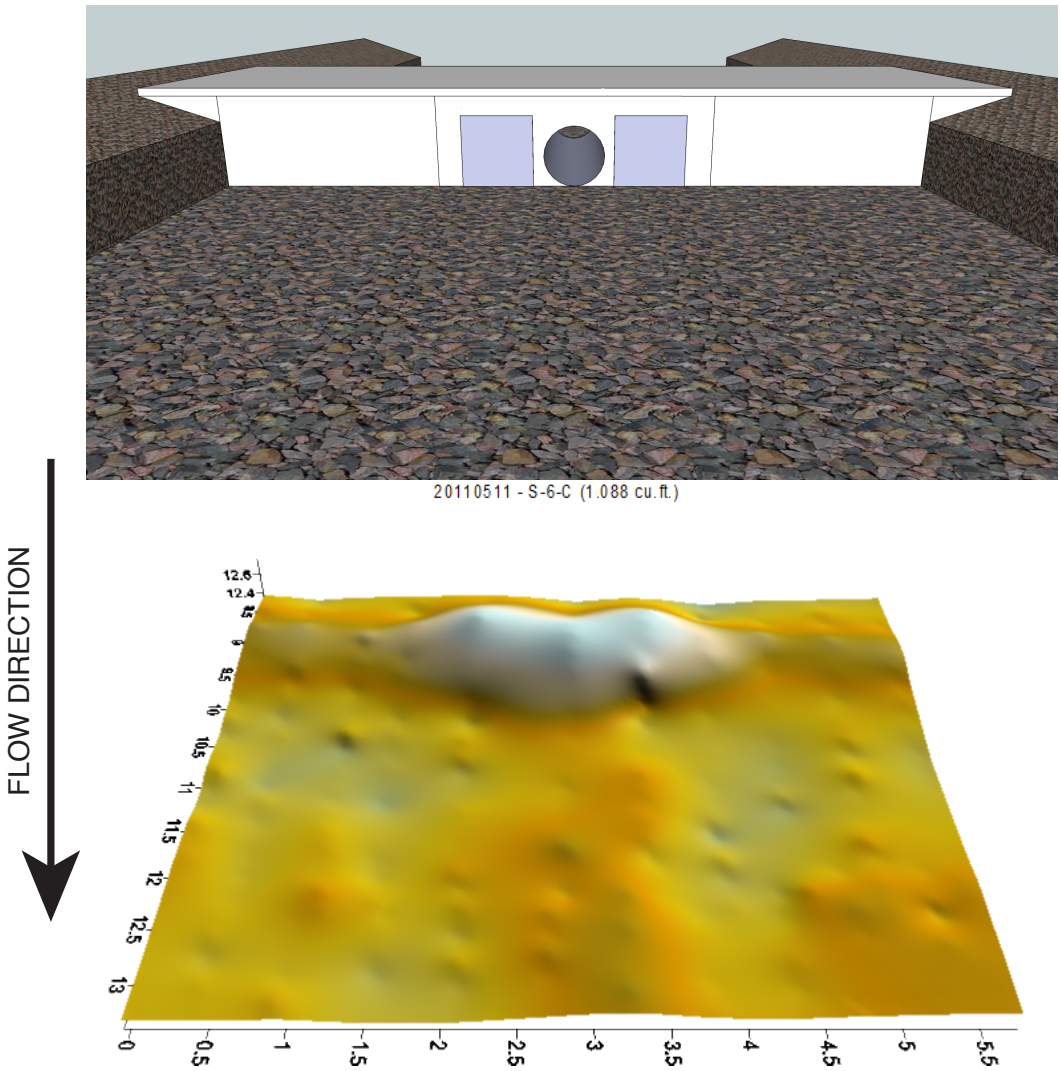

Figure 4.24. Typical Downstream Surface Model for Experimental Model S-6-C for 0.6 Percent Slope with Large Rocks

Figure 4.25 shows a gravel bar with a long wing and a some scour on the right bank. There are also mounds in the corners near the headwall.

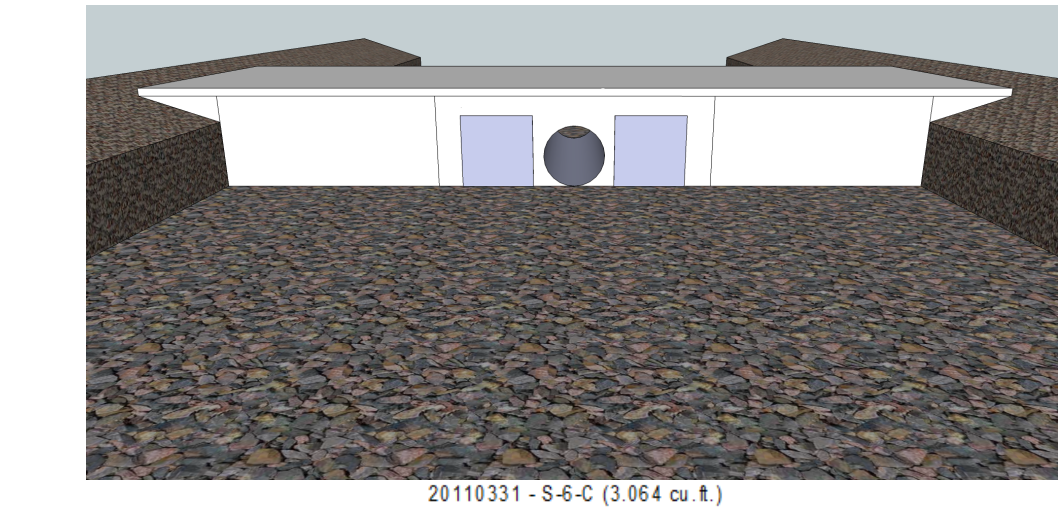

Figure 4.25. Typical Downstream Surface Model for Experimental Model S-6-C for 1.0 Percent Slope with Large Rocks

Figure 4.26 shows a flat gravel bar with scour downstream and towards the banks. There is a continuous line of rocks from bank to bank on the upstream side of the gravel bar. This line is not an artifact of the survey or the interpolation method, but rather it was present in the bedform as observed.

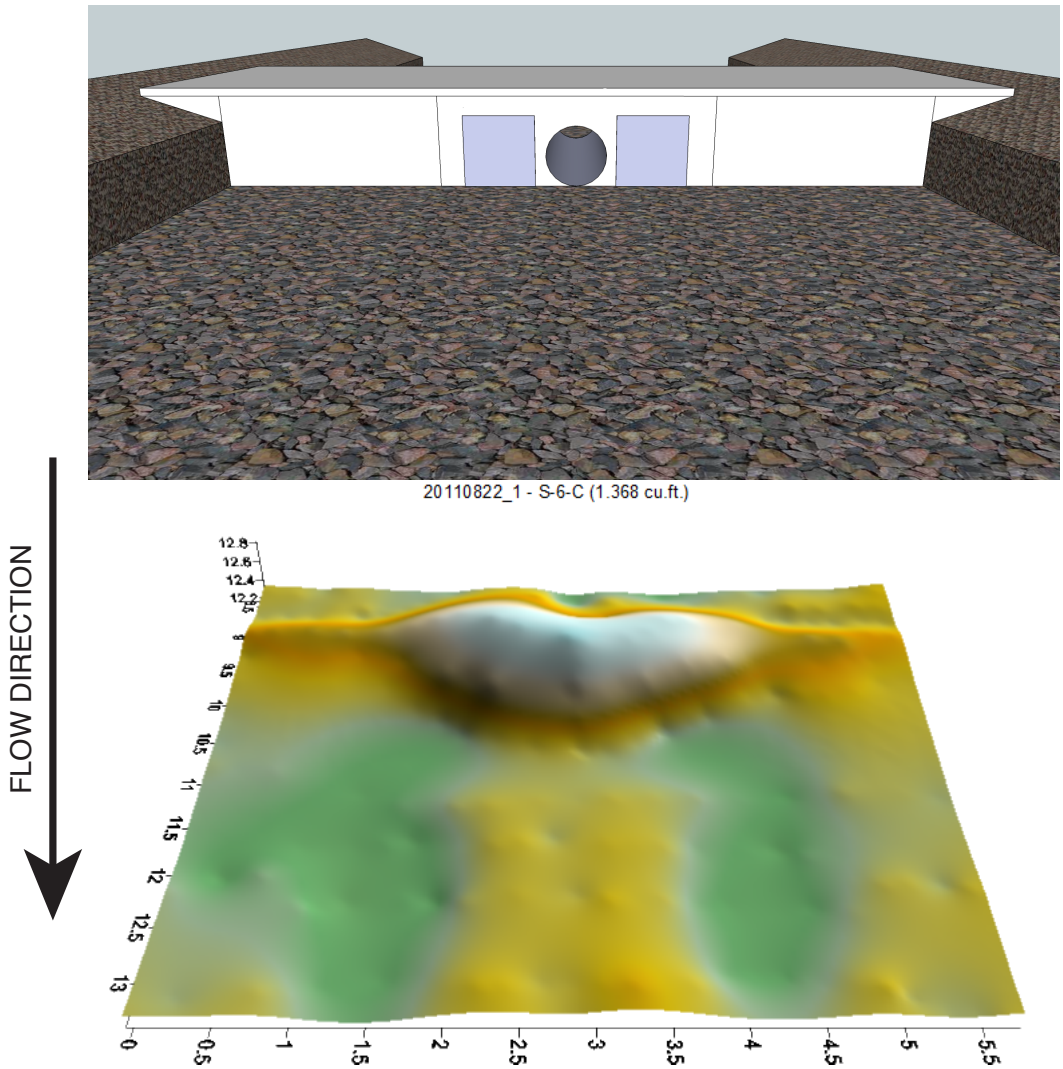

Figure 4.26. Typical Downstream Surface Model for Experimental Model S-6-C for 0.3 Percent Slope with Small Rocks

Figure 4.27 shows a flat gravel bar with a wing towards the left bank and scour downstream on the right bank.

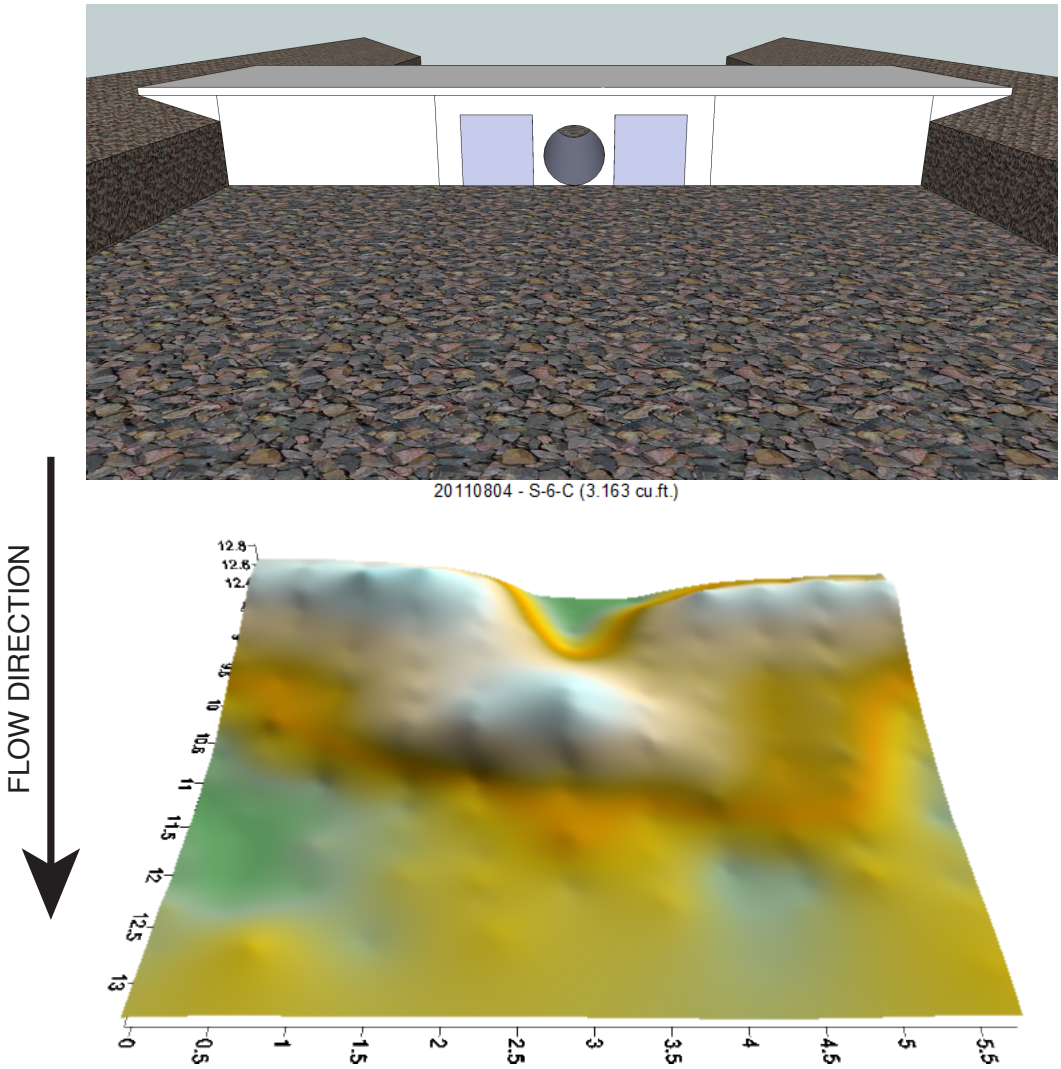

Figure 4.27. Typical Downstream Surface Model for Experimental Model S-6-C for 0.6 Percent Slope with Small Rocks

4.7 Multiple Rectangular Barrels (M-R)

Figure 4.28 shows a small mound immediately downstream of the outlet, with slight scour downstream of the mound and accumulation in the corners near the headwall.

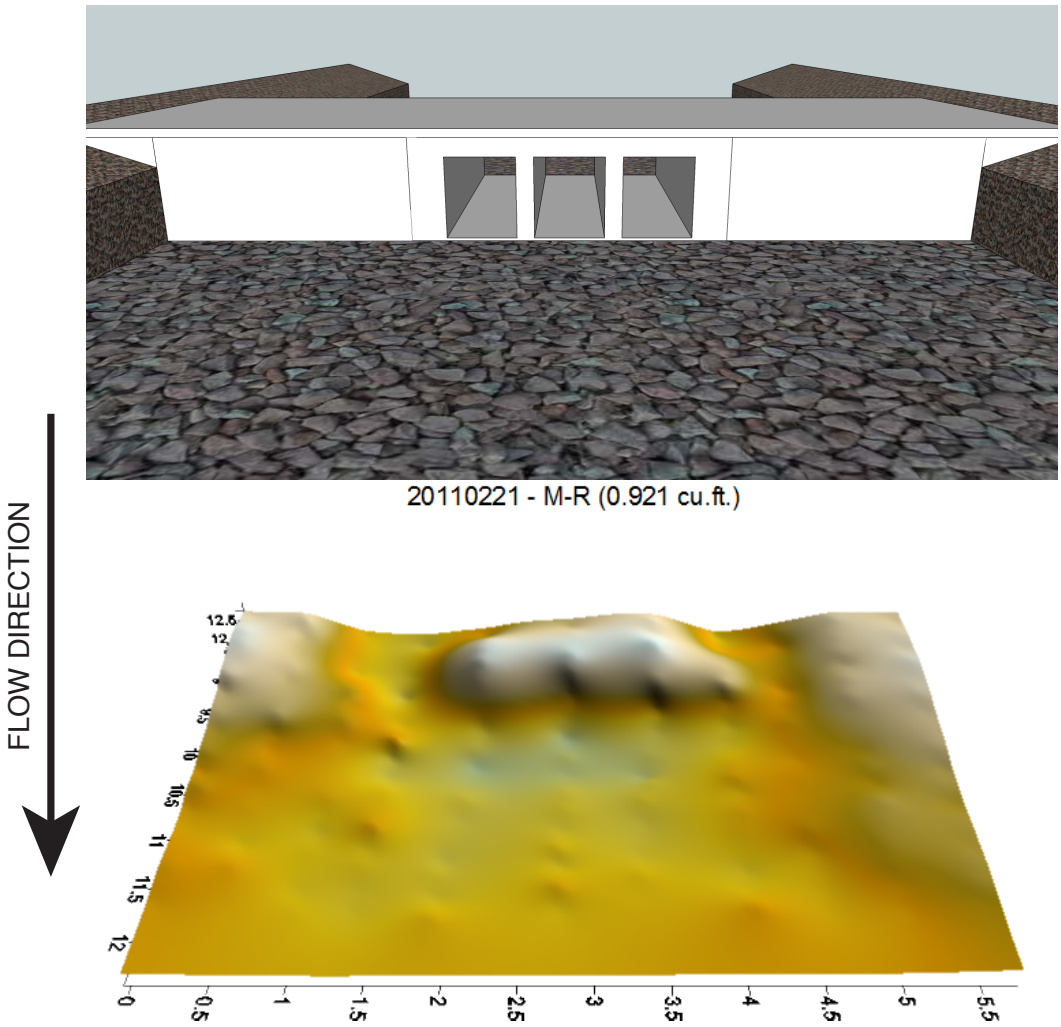

Figure 4.28. Typical Downstream Surface Model for Experimental Model M-R for 0.3 Percent Slope with Large Rocks

Figure 4.29 shows a gravel bar just downstream of the culvert outlet, with very slight scour.

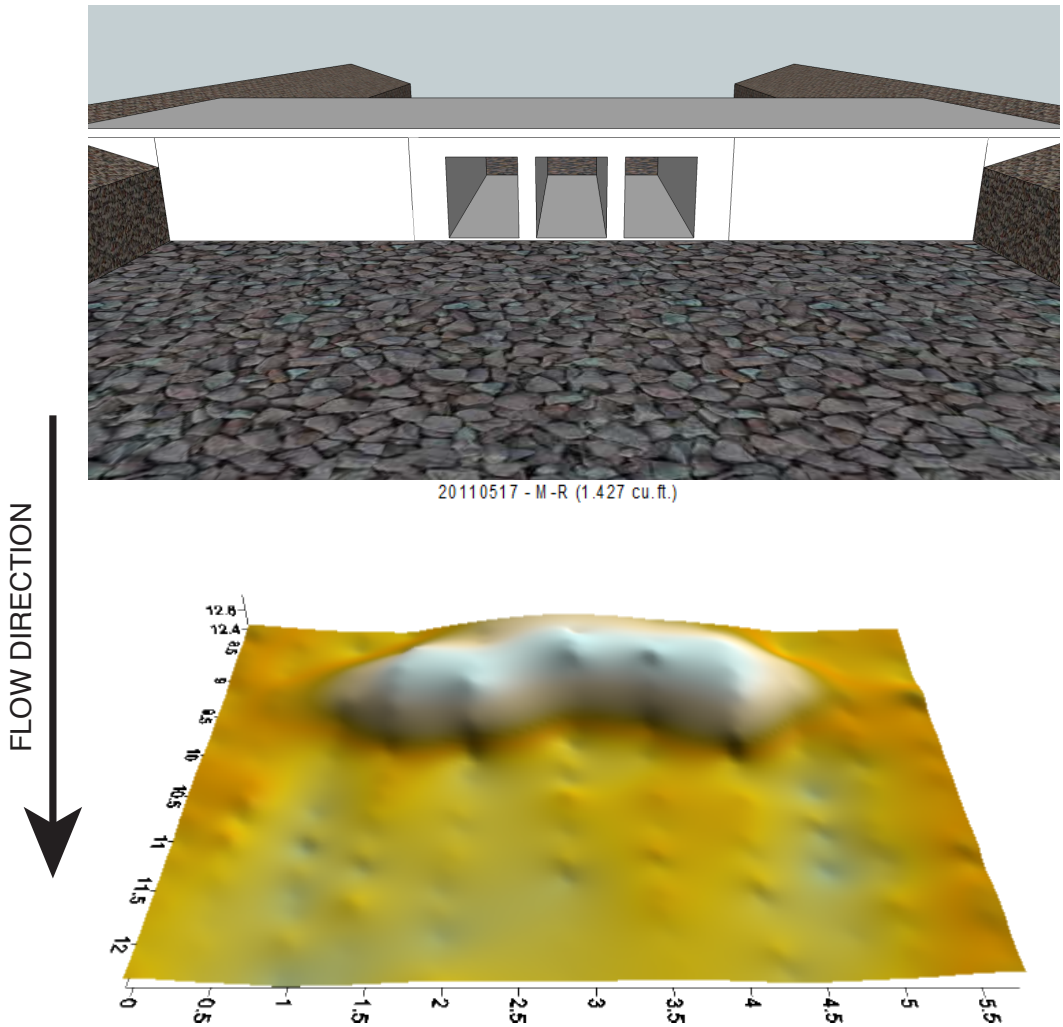

Figure 4.29. Typical Downstream Surface Model for Experimental Model M-R for 0.6 Percent Slope with Large Rocks

Figure 4.30 shows a U-shaped gravel bar with a wing on the left bank side of the bar. There is also scour near the culvert outlet.

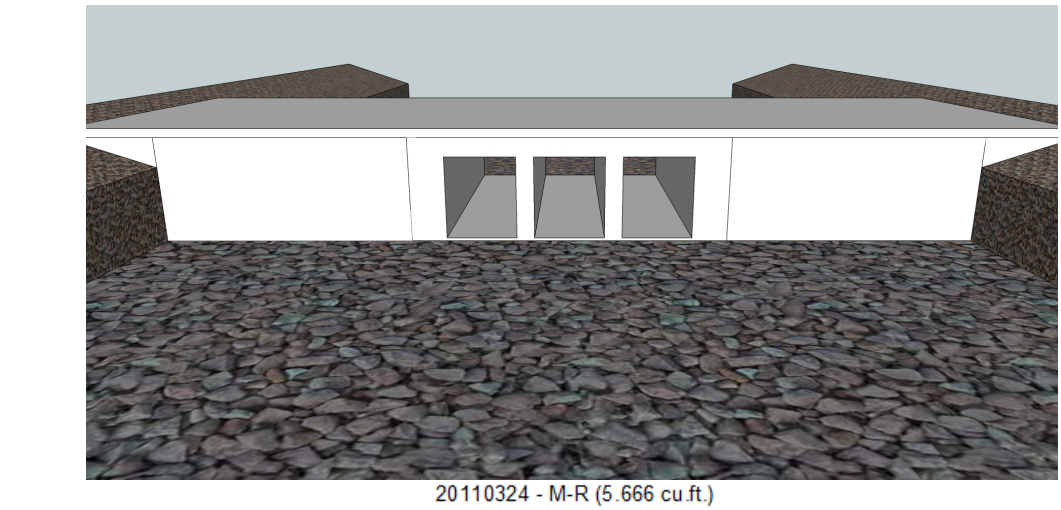

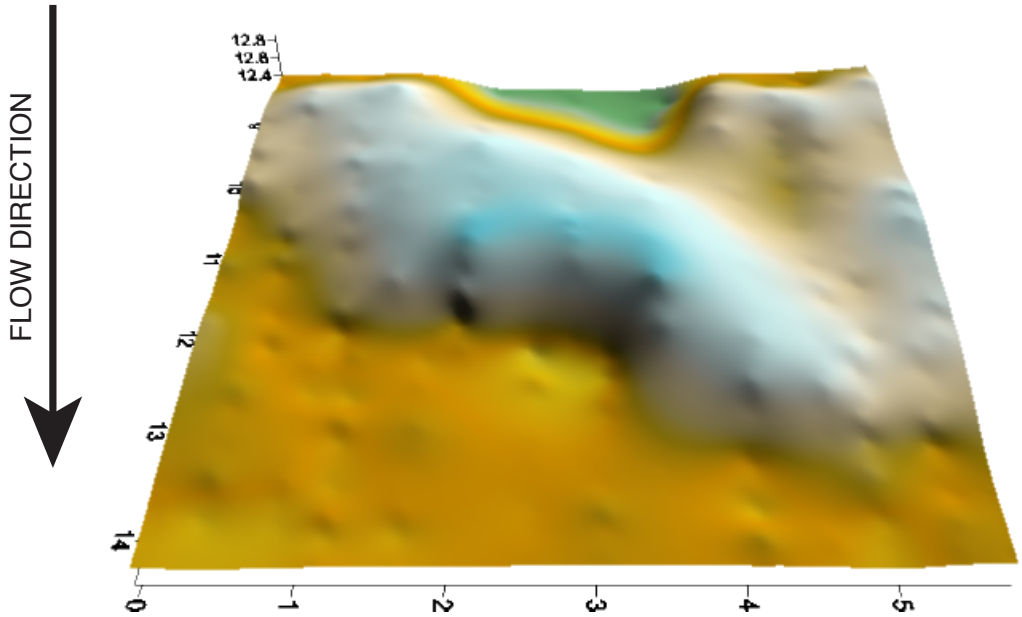

Figure 4.30. Typical Downstream Surface Model for Experimental Model M-R for 1.0 Percent Slope with Large Rocks

Figure 4.31 shows a gravel bar just downstream of the outlet with scour holes downstream.

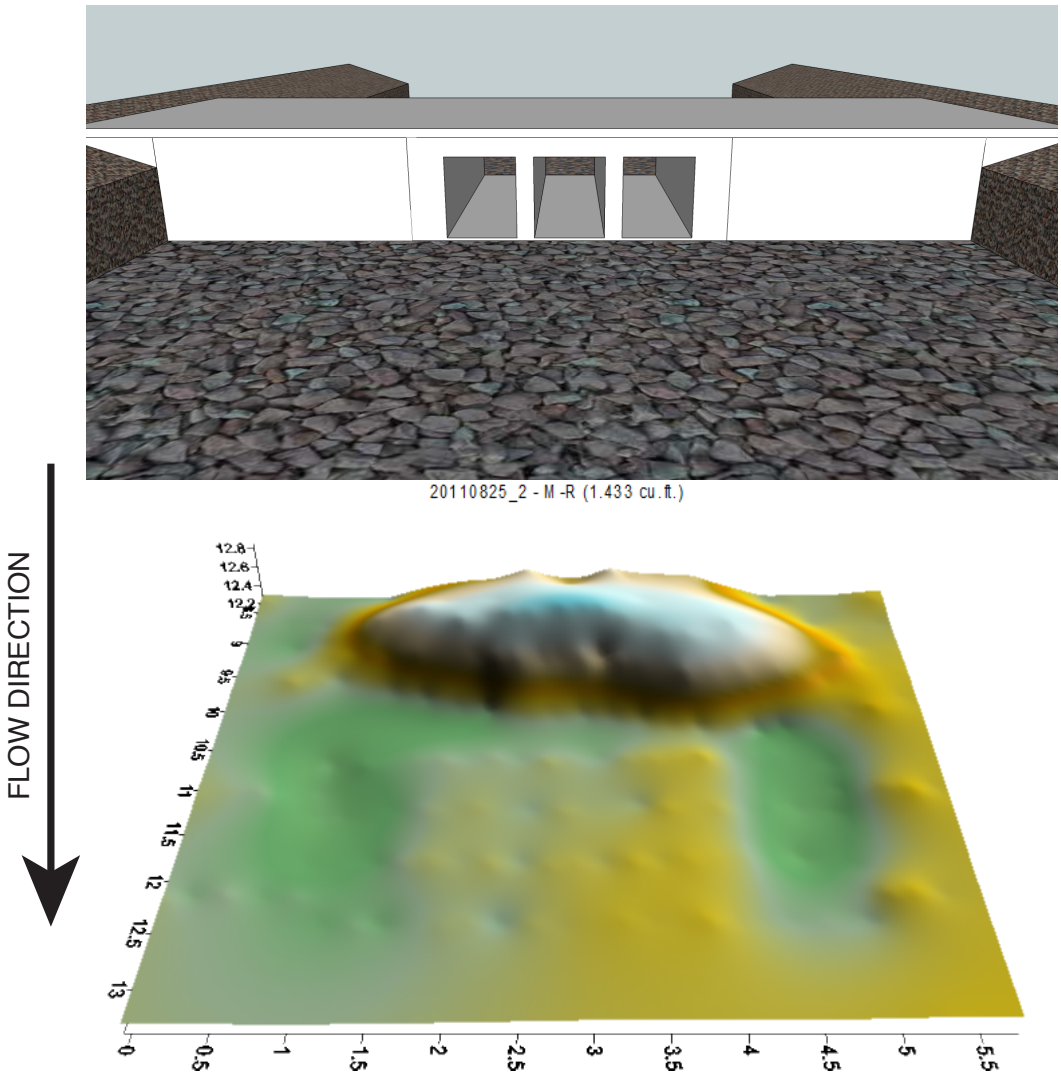

Figure 4.31. Typical Downstream Surface Model for Experimental Model M-R for 0.3 Percent Slope with Small Rocks

Figure 4.32 shows a U-shaped gravel bar with a wing on the left bank side of the bar. There is also scour near the culvert outlet.

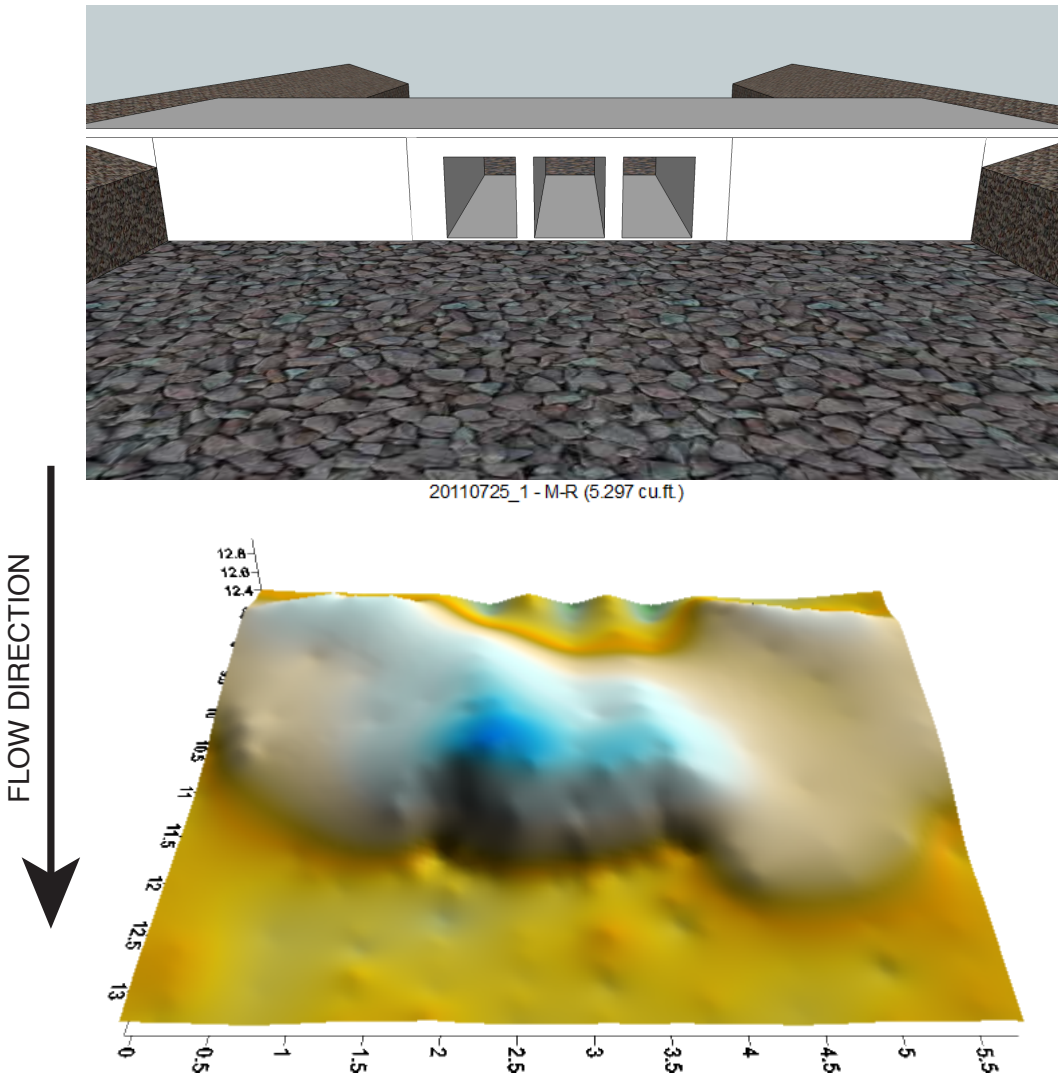

Figure 4.32. Typical Downstream Surface Model for Experimental Model M-R for 0.6 Percent Slope with Small Rocks

4.8 Single Rectangular Barrel (S-R)

Figure 4.33 shows a small mound downstream of the culvert with slight scour and mounds in the corner by the headwall

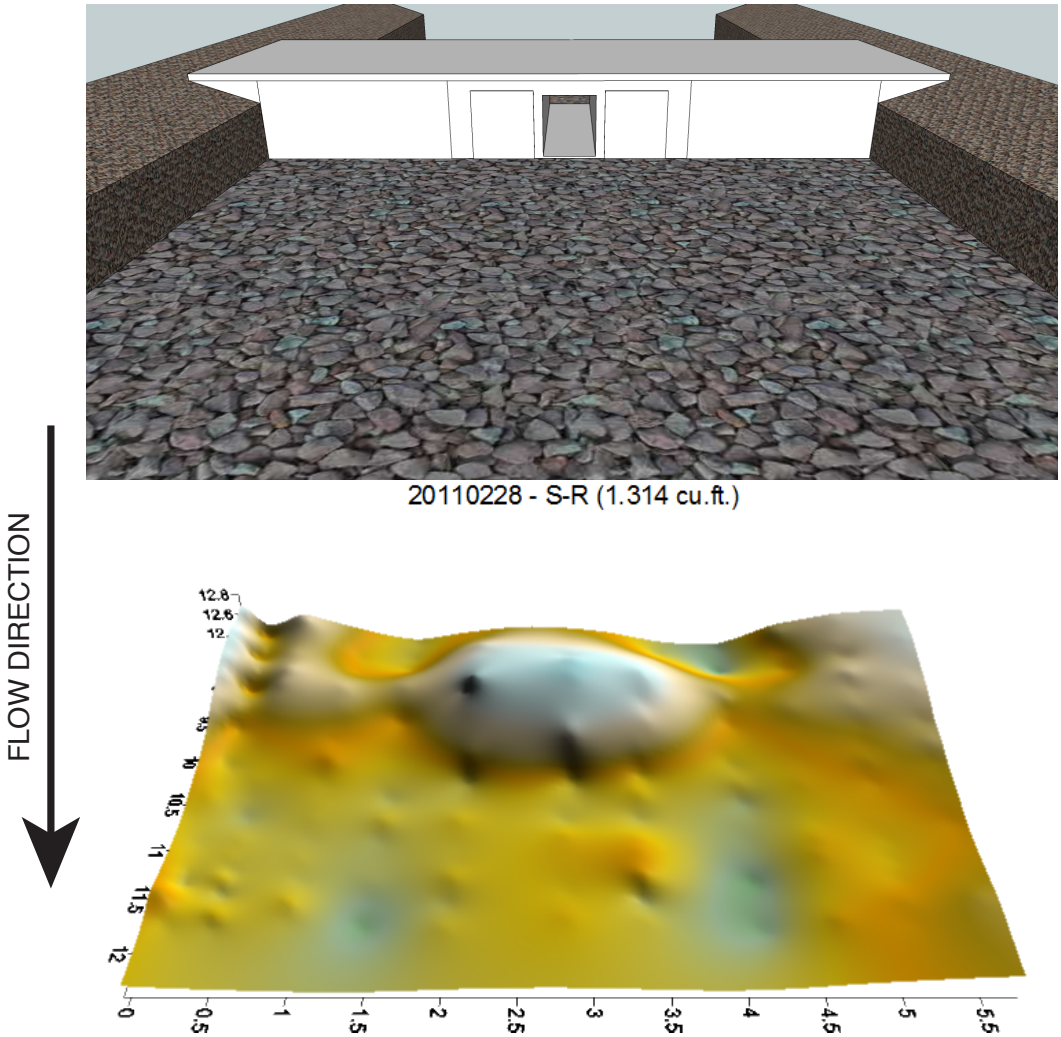

Figure 4.33. Typical Downstream Surface Model for Experimental Model S-R for 0.3 Percent Slope with Large Rocks

Figure 4.34 shows a small mound with little scour downstream of the mound.

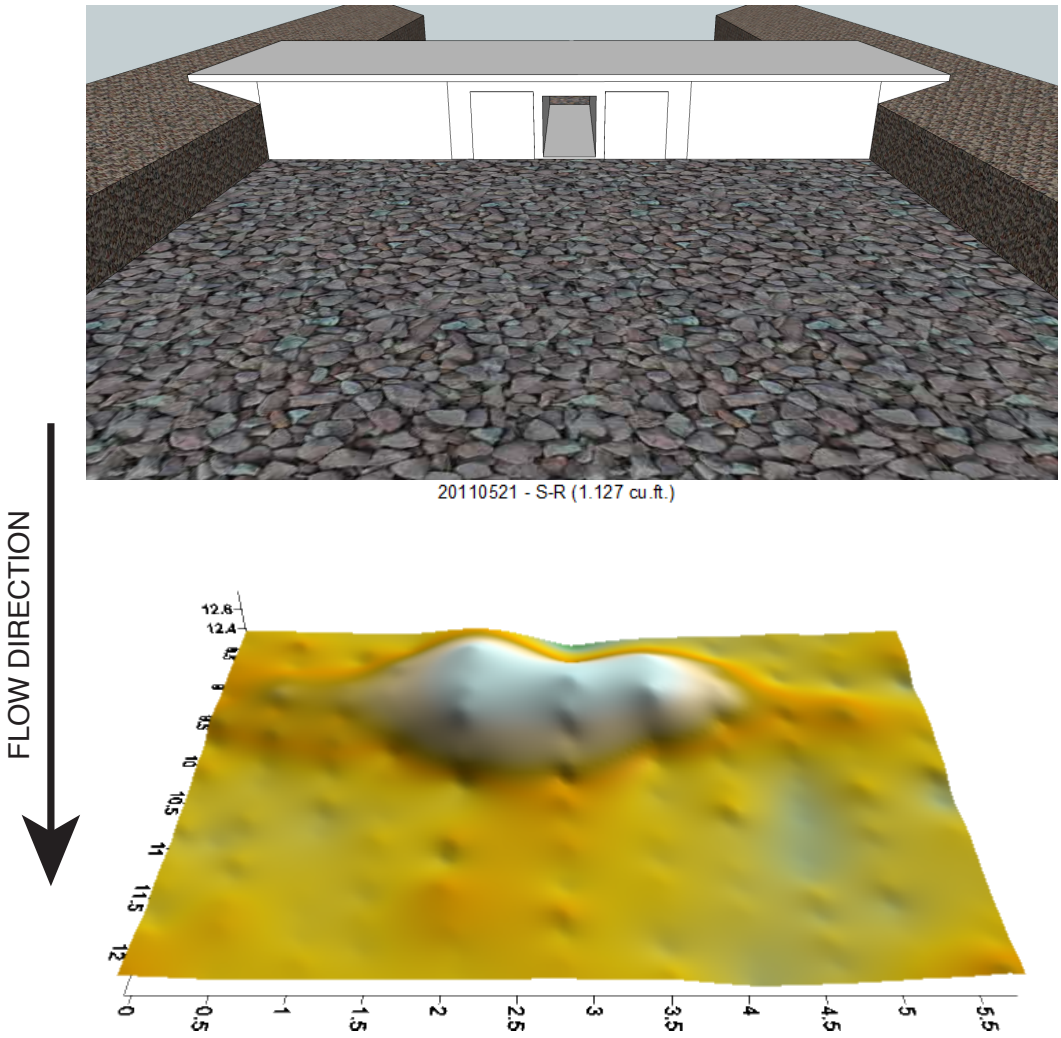

Figure 4.34. Typical Downstream Surface Model for Experimental Model S-R for 0.6 Percent Slope with Large Rocks

Figure 4.35 shows a U-shaped gravel bar with a wing on the left bank side and some minor scour at the culvert exit.

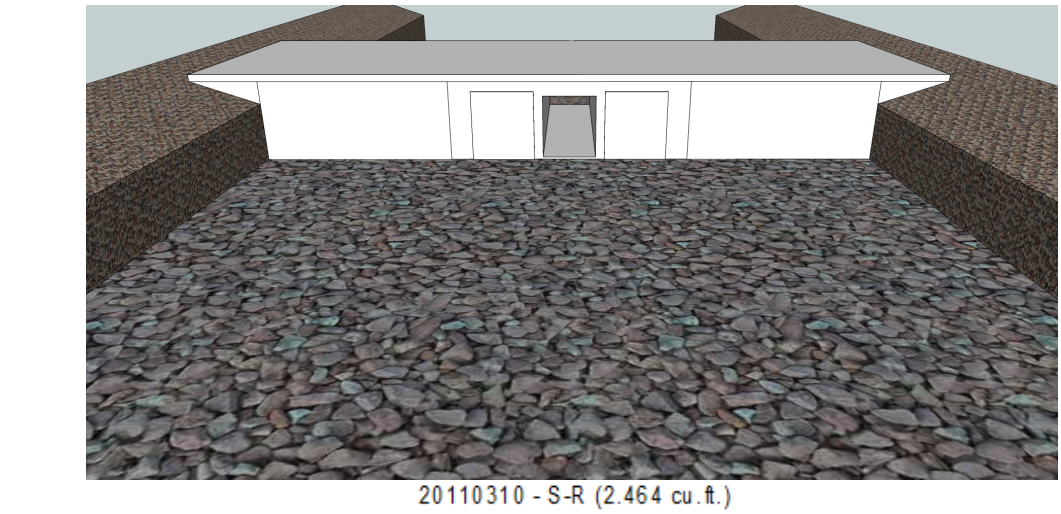

Figure 4.35. Typical Downstream Surface Model for Experimental Model S-R for 1.0 Percent Slope with Large Rocks

Figure 4.36 shows a U shaped gravel bar with a wing on the left bank side and some scour downstream of the culvert. Note the accumulation in the corners near the headwall.

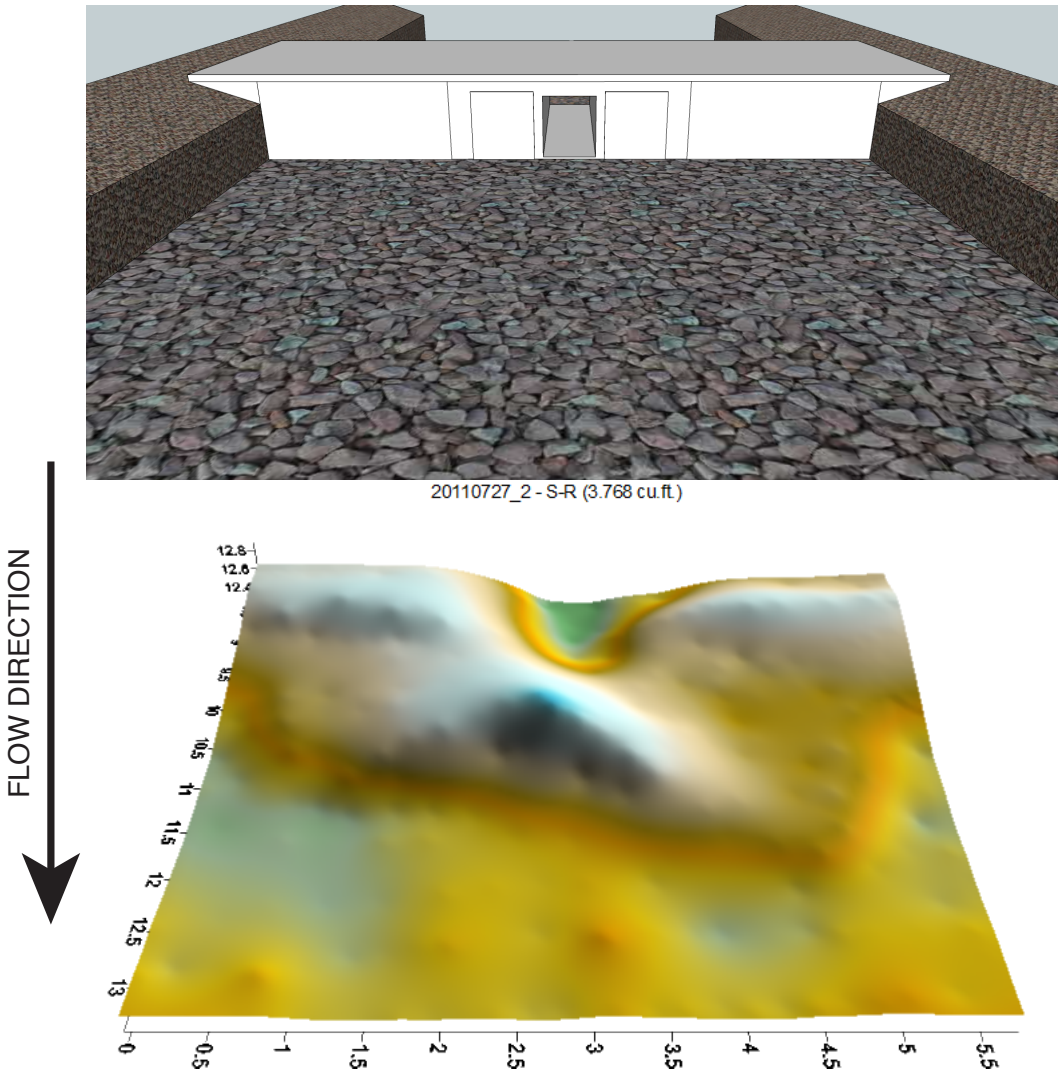

Figure 4.36. Typical Downstream Surface Model for Experimental Model S-R for 0.6 Percent Slope with Small Rocks

4.9 Comparison of Sediment Transport and Discharge

The survey volume and operational discharge for each experiment were averaged according to the slope, rock size, and culvert configuration to generate the V_s/Q numbers. A higher ratio indicates a tendency for solids to transport trough that configuration for a given flow rate. Table 4.1 and Figure 4.37 show the results of the experiments in regards to the larger rock size. Table 4.2 and Figure 4.38 show the results of the smaller rock size. In the figures, Low Slope is 0.3 percent, Medium Slope is 0.6 percent, and Steep Slope is 1.0 percent.

Table 4.1. Ratio of V_s/Q Values for Each Culvert Configuration with the Large Rock Size—Data are Shown in Figure 4.37

Large Rock Experiments								
	SB-I	0.059		SB-I	--		SB-I	0.246
	SB-C	--		SB-C	0.091		SB-C	.186
	M-4-C	.029		M-4-C	--		M-4-C	.210
Low	S-4-C	.071	**Medium**	S-4-C	--	**Steep**	S-4-C	.140
Slope	M-6-C	.051	**Slope**	M-6-C	.083	**Slope**	M-6-C	.294
	S-6-C	.063		S-6-C	.081		S-6-C	.196
	M-R	.059		M-R	.093		M-R	.390
	S-R	.103		S-R	.072		S-R	.207

The data listed in Table 4.1 and shown in Figure 4.37 tend to show that an increase in slope will increase the sediment transport volume for all else equal. The values were calculated for each slope, rock size, and culvert configuration tested in the experiments. There were typically 3 experiments on each configuration for a given slope and rock size with which to average the operational discharge and sediment transport volume. The average sediment transport volume is considered the average of the volume of sediment that passed through the culvert barrel for each experiment. The one case where the V_s/Q value does not increase with slope is that for the S-R configuration. The single rectangular barrel configuration was not clogged after any of the experiments involving it.

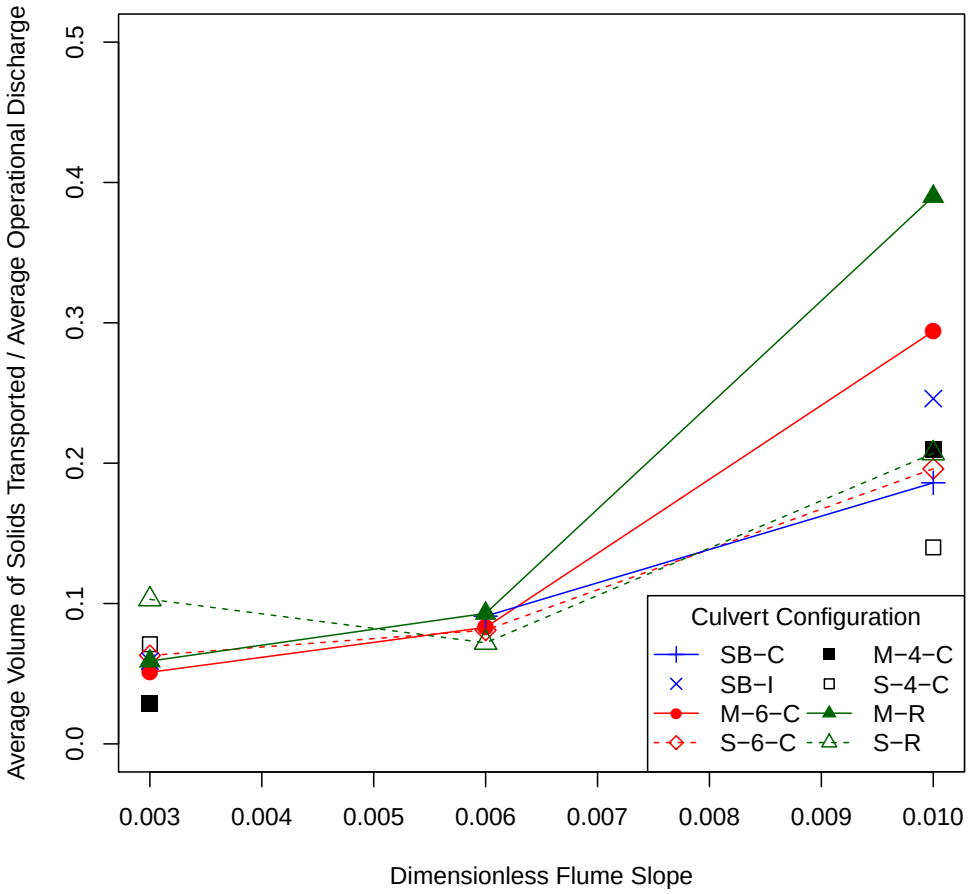

Figure 4.37. Plot of V_s/Q Ratios for Each Culvert Configuration for the Large Rocks—Data are Listed in Table 4.1

Table 4.2. Ratio of V_s/Q Values for Each Culvert Configuration with the Small Rock Size—Data are Shown in Figure 4.38

Small Rock Experiments					
	SB-I	0.235		SB-I	--
	SB-C	.228		SB-C	0.307
	M-4-C	.174		M-4-C	.253
Low	S-4-C	.105	**Medium**	S-4-C	.148
Slope	M-6-C	.239	**Slope**	M-6-C	.376
	S-6-C	.136		S-6-C	.240
	M-R	.142		M-R	.403
	S-R	.231		S-R	.299

The data listed in Table 4.2 and shown in Figure 4.38 tend to show that an increase in slope will increase the sediment transport volume for all else equal. The calculations were made in the same manner as those in Table 4.1 and Figure 4.37. The relation of sediment transport volume to operational discharge is useful in that it tends to show that an increase in slope leads to an increase in sediment transport volume for all else equal. This conceptually agrees with the existing equations given in the literature (Graf and Altinakar, 1988; Sturm, 2010; Yang, 1996).

In comparing V_s/Q for small rocks and large rocks, it is important to note that the values for the small rocks were larger than the values for the large rocks, given the same slope and configuration. Additionally, the values for the small rocks at medium slope were larger than the values for the large rocks at steep slope, and the values for the small rocks at low slope were larger than the values for the large rocks at medium slope. Reducing the size of the rocks increased the efficiency of the culvert in passing sediment.

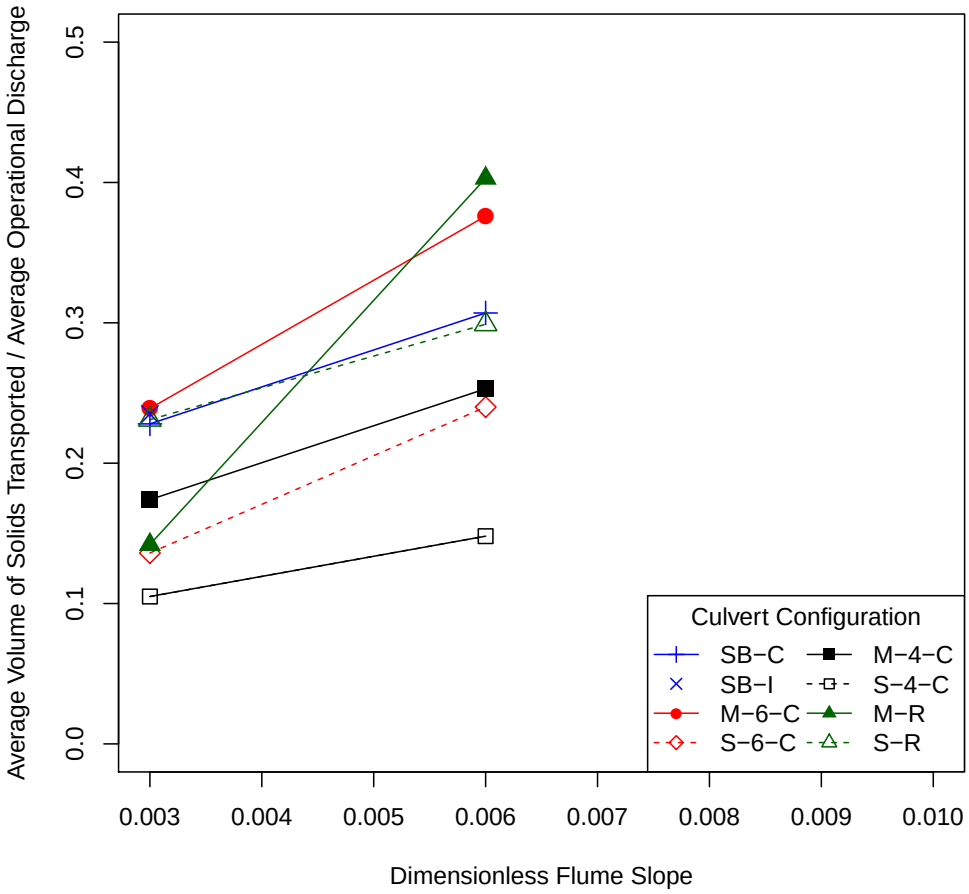

Figure 4.38. Plot of V_s/Q Ratios for Each Culvert Configuration for the Small Rocks—Data are Listed in Table 4.2

Dimensional analysis of the graphs shown in Figure 4.37 and Figure 4.38 returns units of seconds. The units of seconds to describe the effectiveness of a culvert passing solids seemed strange to the author, so another metric for comparison was devised.

The volume of solids transported was divided by the culvert flow area which was plotted against the operational discharge of the experiment divided by the square root of the dimensionless flume slope. These values were graphed according to rock size to simplify the visual interpretation. The graph for the large rocks is shown in Figure 4.39 and the graph for the small rocks is shown in Figure 4.40.

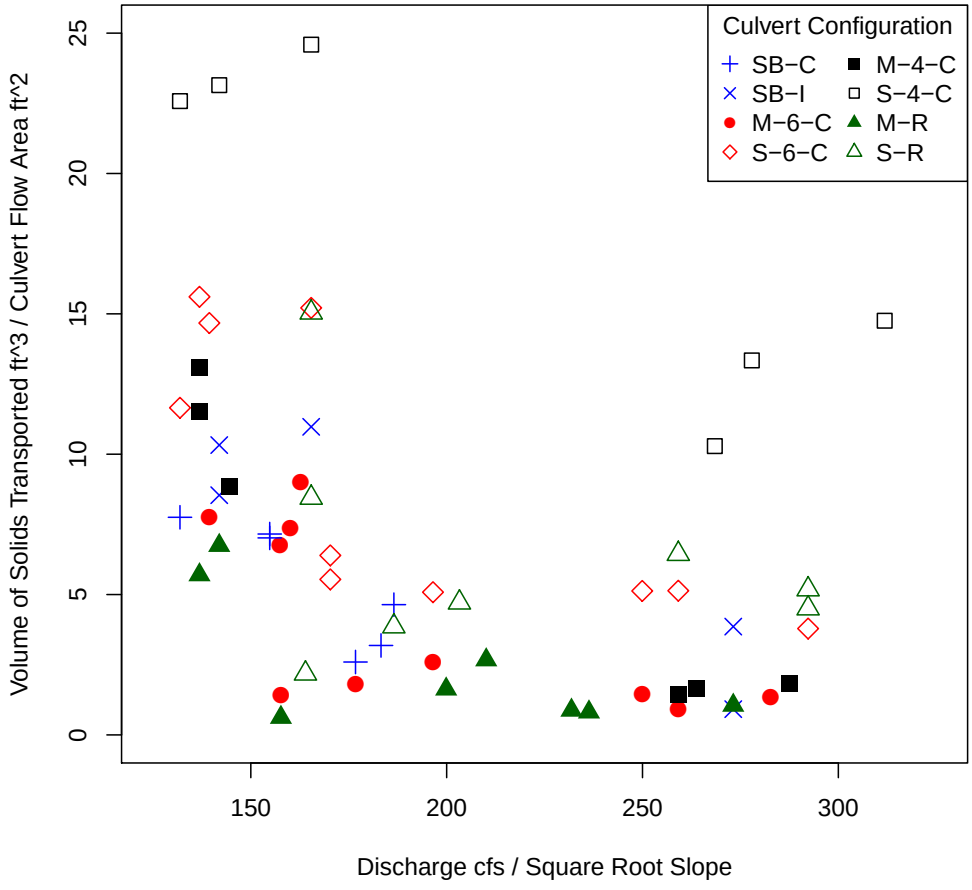

Figure 4.39. Plot of Volume of Solids Transported versus Peak Flow per Root Slope for Each Culvert Configuration for the Large Rocks

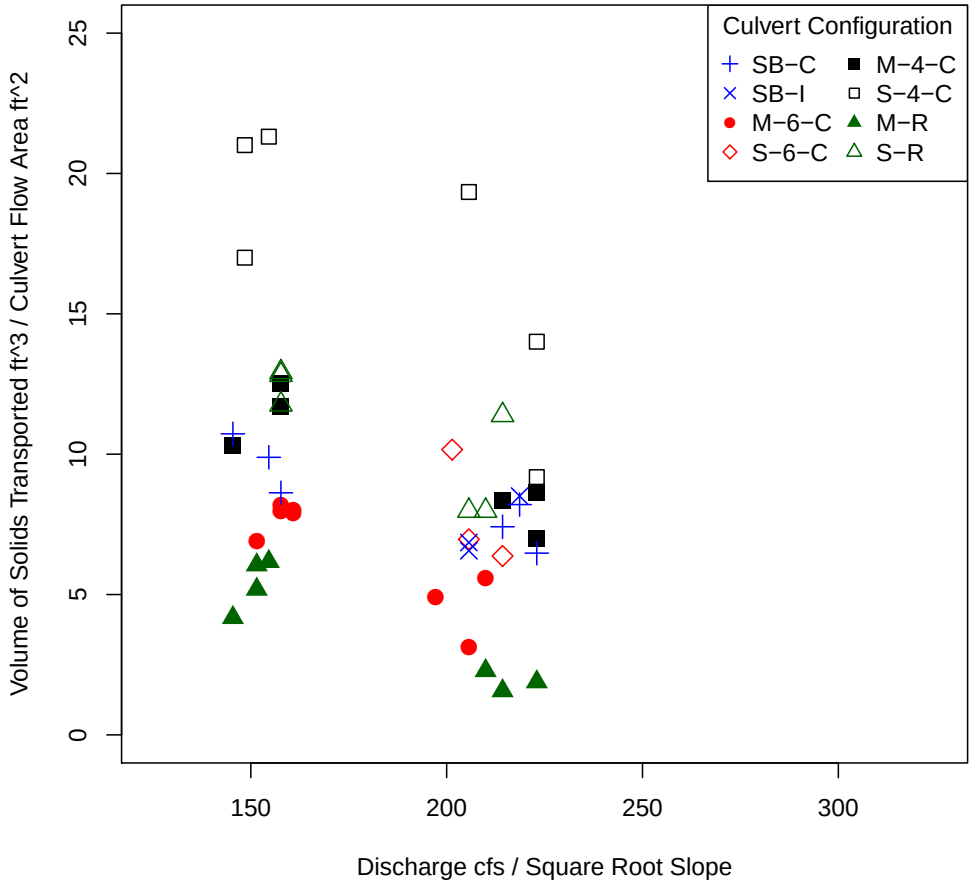

Figure 4.40. Plot of Volume of Solids Transported versus Peak Flow per Root Slope for Each Culvert Configuration for the Small Rocks

Note in Figure 4.39 that the experimental model S-4-C produced significantly different results from the rest of the experimental models with large rocks. There is evidence that the model performed similarly with the small rocks as shown in Figure 4.40. Also notable in these figures is that there appears to be a downward trend as the discharge increases within the "clusters" of experimental results for the same culvert configurations. The clustering of experimental results leads to the conclusion that the experimental trials were repeatable.

Chapter 5
Conclusions

5.1 Semi-Qualitative Performance Comparisons

The multiple rectangular barrel (M-R) configuration tended to clog the most out of all the configurations. This is attributable in part to the hydraulic inefficiency of rectangular prisms as pipes and presumably lower velocities within the barrels.

The next most likely configuration to clog was the multiple 4-inch barrel (M-4-C) configuration. This configuration had a very small cross-sectional area to pass the sediments.

The multiple 6-inch barrel (M-6-C) configuration clogged a few times, but for the most part, it stayed clear.

In comparing the 10 lowest sediment transport volumes from all of the experiments, 9 of the experiments resulted in a clog. There were 7 multiple barrel configurations, 2 single barrel configurations, and 1 staggered barrel configuration. Of the 10 highest sediment transport volumes, all 10 were multiple barrel configurations, with 4 of the experiments from the large rocks at steep slope and 6 of the experiments from the small rocks at medium slope. The full list of experiments is provided in the Appendix as a comma delimited file. The result that the multiple barrel configurations were present at the extremes of the data in terms of sediment transport volumes is particularly interesting. At low slopes, multiple barrel configurations tend to clog whereas at steeper slopes, multiple barrel configurations tend to not clog and actually transport substantial amounts of sediment. This relationship of slope and culvert flow area compared to the sediment transport volume should be studied so that more of an understanding of sediment transport processes in river-culvert systems can be reached.

5.2 Surveying as a Viable Alternative to Bucket Measurement

Using buckets to measure volume change is a very reliable measurement, but bucket counting is tedious manual labor that can be avoided by using surveying techniques. Surveying is used on jobsites all around the world for measuring cut and fill, therefore, using surveying as a tool for measuring cut and fill in open channels makes sense.

The comparison of bucket measurements to survey measurements led to a calculated conversion factor of 0.665 cubic feet per bucket, whereas converting 5 gallons to cubic feet has a conversion factor of 0.668. The difference in the two values is about 0.45 percent error.

5.3 Different Culvert Systems Convey Different Volumes of Solids

Comparing the V_s/Q values for each culvert configuration, with the same bed slope and rock size shows that there is a difference between the levels of performance of the different configurations. At lower slope, these differences are minor, and only lead to minor changes in bedforms. At higher slopes, the differences become much more apparent, and the V_s/Q ratio for one configuration can be more than twice the V_s/Q ratio for another configuration.

5.4 Bedforms Convey Some Sense of the Configuration

The bedforms might not look all that different from one another, but there are several notable differences between the types of bedforms observed in these experiments. The bedforms cannot be used as a predictor in terms of the specific geometry—the dimensions of each barrel—of the culvert that produced it, but the bedforms can be used to predict the general configuration (single barrel, multiple barrel, or staggered barrel.)

Multiple barrel configurations tended to generate the largest bedforms that spanned most of the channel and were nearly symmetric about the middle of the channel, whereas single barrel configurations tended to generate smaller bedforms that were typically asymmetrical. The staggered barrel configurations also tended to generate smaller bedforms that were connected by ridges.

5.5 Steeper Slopes Produce Relatively Larger Bedforms

On the steepest slope tested (1.0% for large rocks, 0.6% for small rocks) bedforms tended to have intricate patterns and particular shapes that look similar to, yet different from, a separate culvert configuration. Comparing Figure 5.1 to Figure 5.2 and Figure 5.3, it is evident that the bedforms are related.

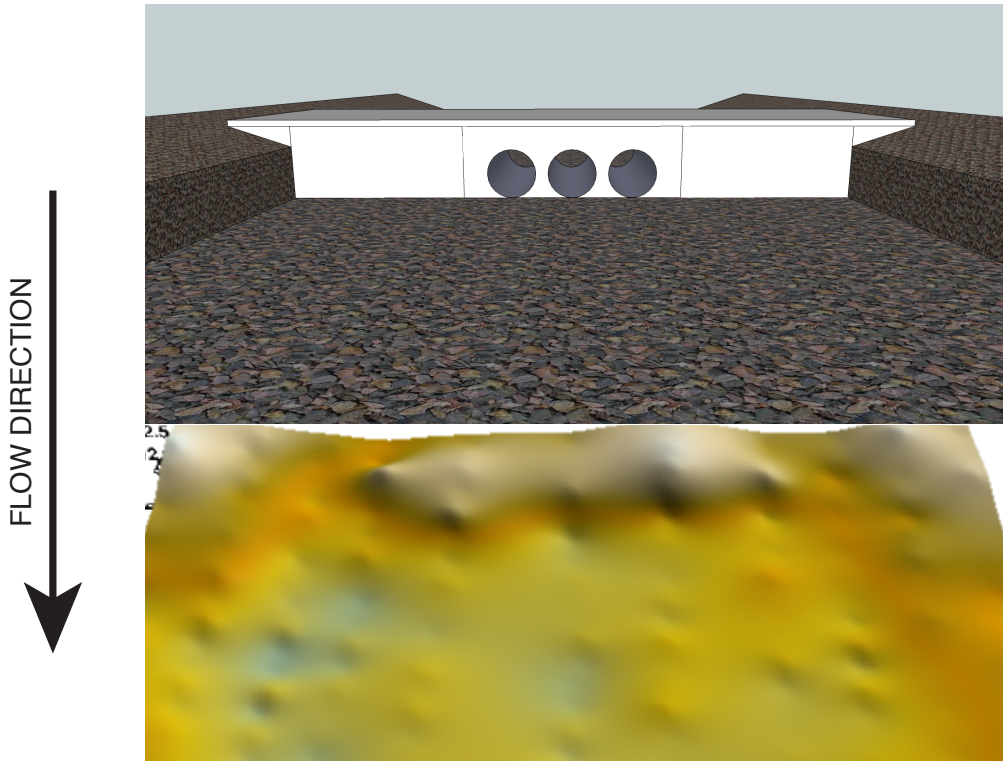

Figure 5.1. Small Bedform After Experiment on Experimental Model M-6-C at 0.3 Percent Slope with Large Rocks—Culvert Diagram Not to Scale, This figure is to be compared with Figure 5.2 and 5.3

The bedform caused by the low slope (0.3%) experiment (Figure 5.1) is a small flat bar, just downstream of the culvert outlet. There is barely detectable scour directly downstream of the outside edges of the flat bar. The medium slope (0.6%) experiment (Figure 5.2) resulted in a similar shaped bedform that is somewhat flat across the top, but there is slightly more visible scour directly downstream of the outside edges of the flat bar. The steep slope (1.0%) experiment (Figure 5.3) is considered a more developed bedform because it has the same basic shape as the others, but the material that was clogging the barrels or otherwise

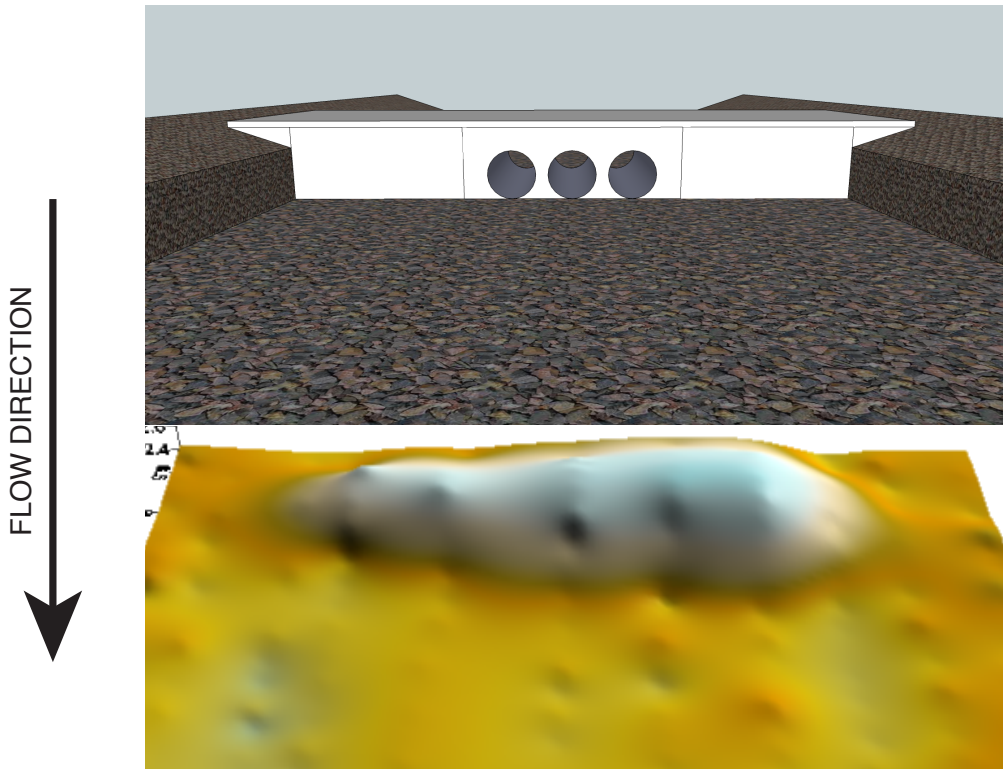

Figure 5.2. Medium Bedform After Experiment on Experimental Model M-6-C at 0.6 Percent Slope with Large Rocks—Culvert Diagram Not to Scale, This figure is to be compared with Figure 5.1 and 5.3

impeding the flow has been moved past the largest part of the bedform, into the area where the scour was in the less steep experiments. At steeper slopes, the bedforms showed a tendency to have wings. The blowout portions around the side of the bedform were oriented in the same direction—the direction of the flow going around the large part of the bedform.

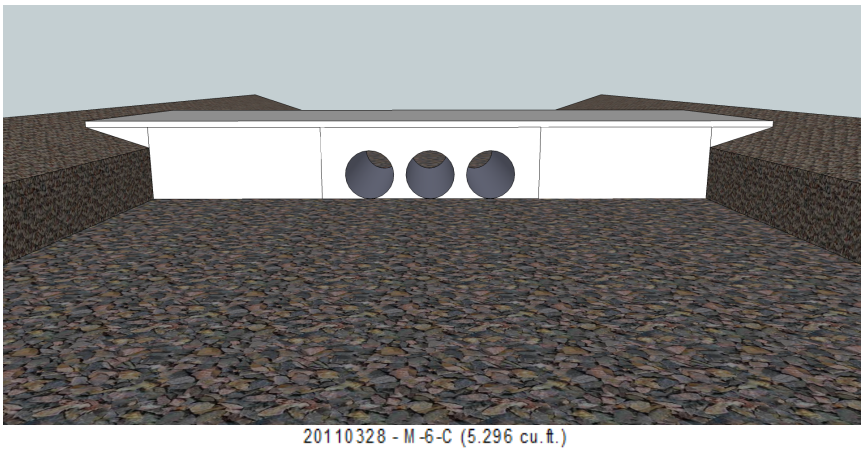

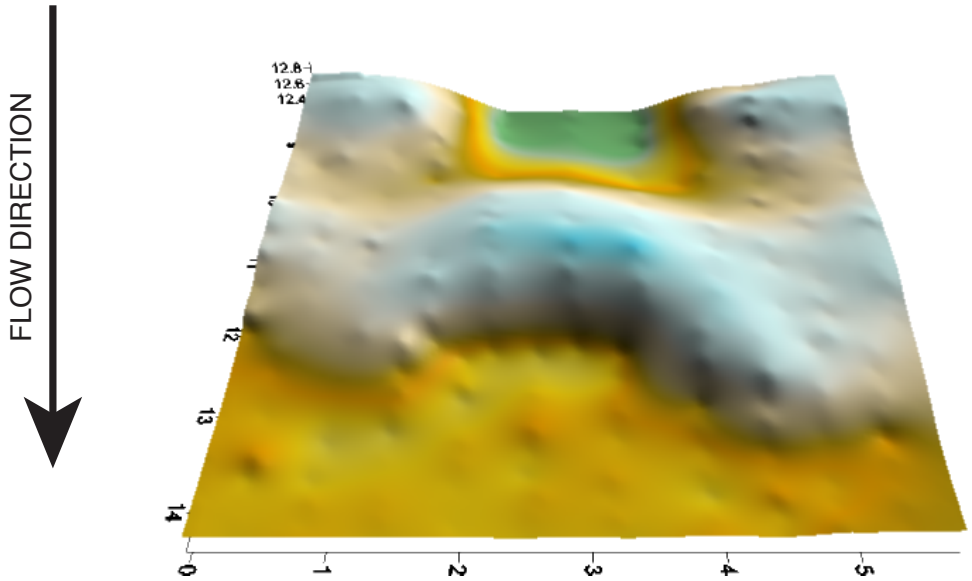

Figure 5.3. Large Bedform After Experiment on Experimental Model M-6-C at 1.0 Percent Slope with Large Rocks—Culvert Diagram Not to Scale, This figure is to be compared with Figure 5.1 and 5.2

5.6 Final Remarks

This thesis has shown that surveying is an effective means of representing and comparing topographic data for experiments in the lab. This is useful for researchers who wish to do similar studies on bedforms by remote sensing, especially by total station. Useful work in the future could be to do sensitivity analyses on surveying methods, and if there is a specific number of points in a survey that will optimize the representation of the surface.

Also, this thesis has documented the use of several methods to show that different culvert configurations transport sediments differently. The methods that provide evidence to this result are the V_s/Q ratio, the bedforms, and whether or not the configuration clogged. More research is needed to understand the local effects of culvert hydraulics on sediment transport processes.

References

Castro, J. (2003). Geomorphic impacts of culvert replacement and removal: Avoiding channel incision. Technical report, U.S. Fish and Wildlife Service.

Cleveland, T. G., Asquith, W. H., and Strom, K. (2009). Hydraulic Performance of Staggered-Barrel Culverts for Stream Crossings. Unpublished research report for Texas Department of Transportation Project 0-6549. Technical report, TxDOT.

Davis, R. E., Foote, F. S., Anderson, J. M., and Mikhail, E. M. (1981). *Surveying: Theory and Practice*. McGraw-Hill, sixth edition.

Dixon, J. (2011). MicroADV Operations Manual (unpublished). Developed for use by East Lab personnel.

Golden Software, I. (2002). *Surfer 8 User's Guide*. Golden, CO: Golden Software, Inc., first edition.

Graf, W. H. and Altinakar, M. (1988). *Fluvial Hydraulics*. New York: John Wiley & Sons, first edition.

Hotchkiss, R. H. and Frei, C. M. (2007). FHWA-HIF-07-033 Design for Fish Passage at Roadway-Stream Crossings: Synthesis Report. Technical report, FHWA.

House, M. R., Pyles, M. R., and White, D. (2005). Velocity distributions in streambed simulation culverts used for fish passage. *JAWRA*, 41(1):209–217.

Klingeman, P. C. (2003). Transport thresholds in gravel-bed rivers. *Sedimentation and Sediment Transport*, pages 229–236.

Schoklitsch, A. (1934). Der geschiebetrieb und die geschiebefracht. *Wasserkraft Wasserwirtschaft*, 4:1–7.

Sokkia Topcon (2009). *Series 50RX Operator's Manual*. Sokkia Topcon, third edition.

Sturm, T. W. (2010). *Open Channel Hydraulics*. New York: McGraw-Hill, second edition.

Tsihrintzis, V. A. (1995). Effects of sediment on drainage-culvert serviceability. *J. of Performance of Constructed Facilities*, 9(3):172–183.

Wargo, R. S. and Weisman, R. N. (2006). A comparison of single-cell and multicell culverts for stream crossings. *JAWRA*, 42(4):989–995.

Yang, C. T. (1996). *Sediment Transport: Theory and Practice*. New York: McGraw-Hill.

Appendix

Data for All Experimental Runs

The following listing of comma-delimited data are the results from each experimental run. Note that the clog value is only indicative of a measureable amount of rocks remaining in the culvert barrels.

```
# Date: Year/Month/Day of Experiment, starred (*)entries see Vs
# Config: Culvert Configuration
# Qop cfs: Operational Discharge for the experiment in cfs
# Vs ft^3: Volume of solids transported downstream of the
# culvert, from kriged surface of survey points, in cubic feet
# * indicates an issue with the survey points, bucket volume
# used instead
# Exp. hrs: Experiment duration in hours
# Rock Size: Nominal rock size (large or small)
# Flume Slope: Slope of flume for the experiment, dimensionless
# Clog: Binary indicator of a clog (0 or 1)
Date,Config,Qop cfs,Vs ft^3,Exp. hrs,Rock Size,Flume Slope,Clog
2011/01/04,SB-I,14.96,1.431,3.18,Large,0.003,0
2011/01/24,SB-I,14.96,0.340,1.83,Large,0.003,1
2011/01/25,M-4-C,14.45,0.436,2.00,Large,0.003,1
2011/01/27,M-4-C,14.19,-0.374,1.67,Large,0.003,1
2011/01/28,M-4-C,15.74,0.476,1.90,Large,0.003,1
2011/02/05,S-4-C,15.22,1.164,2.05,Large,0.003,1
2011/02/07,S-4-C,17.08,1.288,2.08,Large,0.003,1
2011/02/10,S-4-C,14.70,0.898,1.90,Large,0.003,1
2011/02/14,S-6-C,16.01,0.744,2.53,Large,0.003,1
2011/02/15,S-6-C,13.69,1.007,2.40,Large,0.003,1
2011/02/16,S-6-C,14.19,1.008,2.80,Large,0.003,1
2011/02/17,M-6-C,13.69,0.850,2.22,Large,0.003,1
2011/02/18,M-6-C,15.48,0.803,1.67,Large,0.003,1
2011/02/19,M-6-C,14.19,0.545,1.52,Large,0.003,1
```

```
2011/02/21,M-R,14.96,0.921,1.93,Large,0.003,1
2011/02/22,M-R,12.94,0.711,1.88,Large,0.003,1
2011/02/23,M-R,12.70,0.767,2.28,Large,0.003,1
2011/02/24,S-R,14.19,1.880,3.15,Large,0.003,0
2011/02/25,S-R,16.01,1.512,2.92,Large,0.003,0
2011/02/28,S-R,16.01,1.314,2.17,Large,0.003,0
2011/03/09,S-R,14.45,--,2.80,Large,0.003,0
2011/03/10,S-R,16.54,2.464,2.80,Large,0.010,0
2011/03/21,S-R,16.54,4.388,3.08,Large,0.010,0
2011/03/22,M-R,14.19,5.904,3.07,Large,0.010,0
2011/03/23,M-R,13.69,4.988,2.65,Large,0.010,0
2011/03/25,M-6-C,16.01,4.334,2.67,Large,0.010,0
2011/03/28,M-6-C,16.27,5.296,2.68,Large,0.010,0
2011/03/29,M-6-C,13.94,4.576,2.70,Large,0.010,0
2011/03/30,S-6-C,13.94,2.881,2.72,Large,0.010,0
2011/03/31,S-6-C,13.69,3.064,2.72,Large,0.010,0
2011/04/01,S-6-C,16.54,2.987,2.67,Large,0.010,0
2011/04/06,M-4-C,14.45,2.318,1.42,Large,0.010,0
2011/04/07,M-4-C,13.69,3.017,1.42,Large,0.010,0
2011/04/08,M-4-C,13.69,3.424,2.57,Large,0.010,0
2011/04/11,S-4-C,16.54,2.146,2.53,Large,0.010,0
2011/04/12,S-4-C,13.19,1.970,2.73,Large,0.010,0
2011/04/13,S-4-C,14.19,2.020,2.85,Large,0.010,0
2011/04/18,SB-I,16.54,4.071,2.68,Large,0.010,0
2011/04/19,SB-I,14.19,3.829,3.13,Large,0.010,0
2011/04/20,SB-I,14.19,3.167,2.98,Large,0.010,0
2011/04/25,SB-C,15.48,2.603,2.75,Large,0.010,0
2011/04/26,SB-C,13.19,2.875,2.85,Large,0.010,0
2011/04/29,SB-C,15.48,2.654,2.87,Large,0.010,0
2011/05/02,M-6-C,15.74,3.984,2.87,Large,0.010,0
2011/05/03,S-6-C,13.19,2.288,2.77,Large,0.010,0
2011/05/04,S-6-C,13.19,1.255,3.00,Large,0.006,0
2011/05/10,S-6-C,15.22,0.998,2.82,Large,0.006,0
2011/05/11,S-6-C,13.19,1.088,3.18,Large,0.006,0
2011/05/12,M-6-C,13.69,1.075,2.98,Large,0.006,1
2011/05/13,M-6-C,15.22,1.538,2.85,Large,0.006,1
2011/05/14,M-6-C,12.21,0.841,2.42,Large,0.006,1
2011/05/16,M-R,12.21,0.544,0.73,Large,0.006,1
2011/05/17,M-R,15.48,1.427,2.80,Large,0.006,1
2011/05/18,M-R,16.27,2.337,2.52,Large,0.006,1
2011/05/19,S-R,15.74,1.375,2.72,Large,0.006,0
2011/05/20,S-R,12.70,0.637,2.78,Large,0.006,0
2011/05/21,S-R,14.45,1.127,3.03,Large,0.006,0
2011/05/23,SB-C,13.69,0.963,2.90,Large,0.006,0
2011/05/24,SB-C,14.45,1.721,2.83,Large,0.006,0
2011/05/25,SB-C,14.19,1.182,2.87,Large,0.006,0
```

```
2011/07/22,M-R,11.26,3.655,2.92,Small,0.006,0
2011/07/23,M-R,11.74,4.538,3.15,Small,0.006,0
2011/07/25,M-R,11.74,5.297,3.48,Small,0.006,0
2011/07/25,M-R,11.97,5.402,3.67,Small,0.006,0
2011/07/26,S-R,12.21,--,3.72,Small,0.006,0
2011/07/27,S-R,12.21,3.740,3.45,Small,0.006,0
2011/07/27,S-R,12.21,3.768,3.57,Small,0.006,0
2011/07/28,S-R,12.21,3.432,3.62,Small,0.006,0
2011/07/29,SB-C,11.26,3.978,3.57,Small,0.006,0
2011/07/30,SB-C,11.97,3.667,3.52,Small,0.006,0
2011/07/31,SB-C,12.21,3.198,3.47,Small,0.006,0
2011/08/01,M-6-C,12.46,4.647,3.42,Small,0.006,0
2011/08/01,M-6-C,12.21,4.687,3.62,Small,0.006,0
2011/08/02,M-6-C,12.21,4.833,3.52,Small,0.006,0
2011/08/03,M-6-C,11.74,4.070,3.50,Small,0.006,0
2011/08/03,M-6-C,12.46,4.728,3.70,Small,0.006,0
2011/08/04,S-6-C,12.21,3.163,3.45,Small,0.006,0
2011/08/05,S-6-C,12.21,2.685,3.52,Small,0.006,0
2011/08/06,S-6-C,12.70,3.049,3.72,Small,0.006,0
2011/08/07,S-4-C,11.50,1.484,3.50,Small,0.006,0
2011/08/08,S-4-C,11.97,1.860,3.55,Small,0.006,0
2011/08/08,S-4-C,11.50,1.833,3.53,Small,0.006,0
2011/08/09,M-4-C,12.21,3.281,3.55,Small,0.006,0
2011/08/10,M-4-C,11.26,2.701,3.67,Small,0.006,0
2011/08/10,M-4-C,12.21,3.064,3.43,Small,0.006,0
2011/08/11,M-4-C,12.21,2.258,3.60,Small,0.003,1
2011/08/12,M-4-C,12.21,1.830,4.13,Small,0.003,1
2011/08/13,M-4-C,11.74,2.184,3.23,Small,0.003,1
2011/08/15,S-4-C,12.21,1.222,3.68,Small,0.003,0
2011/08/15,S-4-C,12.21,0.801,3.45,Small,0.003,0
2011/08/16,S-4-C,11.26,1.688,3.42,Small,0.003,0
2011/08/17,SB-I,11.26,2.542,3.43,Small,0.003,0
2011/08/17,SB-I,11.97,3.155,3.42,Small,0.003,1
2011/08/18,SB-I,11.26,2.433,3.45,Small,0.003,0
2011/08/19,M-6-C,11.50,3.287,3.47,Small,0.003,1
2011/08/20,M-6-C,11.26,1.841,3.02,Small,0.003,1
2011/08/21,M-6-C,10.80,2.886,3.15,Small,0.003,1
2011/08/22,S-6-C,11.26,1.368,3.47,Small,0.003,0
2011/08/22,S-6-C,11.74,1.251,3.50,Small,0.003,0
2011/08/23,S-6-C*,11.03,1.995,3.52,Small,0.003,0
2011/08/23,SB-C,11.74,2.750,3.67,Small,0.003,1
2011/08/24,SB-C,12.21,2.402,3.52,Small,0.003,0
2011/08/24,SB-C,11.97,3.043,3.27,Small,0.003,0
2011/08/25,M-R,11.50,2.001,2.62,Small,0.003,1
2011/08/25,M-R,11.74,1.373,2.48,Small,0.003,1
2011/08/26,M-R,12.21,1.652,2.47,Small,0.003,1
```

```
2011/08/26,S-R*,11.50,2.328,3.47,Small,0.003,0
2011/08/27,S-R*,11.26,2.328,3.45,Small,0.003,0
2011/08/29,S-R,11.74,3.322,3.50,Small,0.003,0
```

A Selected Example of Survey Points after Experimental Run

The following listing of comma-delimited data are from file name `20110722After.txt`.

```
# PID: Point IDentification number
# Northing in feet
# Easting in feet
# Elevation in feet
# X and Y are transformed and rotated in accordance
#   with Equations 3.1 and 3.2.
# X and Y in feet
PID,Northing,Easting,Elevation,Description,X,Y
600,97.3302,108.5362,12.395,0722EX,8.459,5.649
601,97.261,108.3491,12.369,0722EX,8.657,5.673
602,97.1956,108.2097,12.3339,0722EX,8.811,5.679
603,97.0897,108.0557,12.3154,0722EX,8.996,5.656
604,97.0119,107.8904,12.3413,0722EX,9.179,5.662
605,96.8904,107.6331,12.3945,0722EX,9.463,5.672
606,96.7971,107.4707,12.3615,0722EX,9.650,5.664
607,96.6314,107.2072,12.3962,0722EX,9.961,5.637
608,96.5762,107.0514,12.3821,0722EX,10.124,5.660
609,96.4926,106.874,12.3679,0722EX,10.320,5.667
610,96.4193,106.708,12.3632,0722EX,10.501,5.678
611,96.2744,106.4757,12.3908,0722EX,10.774,5.655
612,96.175,106.2995,12.3859,0722EX,10.977,5.648
613,96.0858,106.1344,12.3688,0722EX,11.164,5.644
614,95.9943,105.9929,12.361,0722EX,11.332,5.628
615,95.8635,105.7788,12.3768,0722EX,11.582,5.610
616,95.7977,105.5953,12.4094,0722EX,11.775,5.635
617,95.752,105.4447,12.3901,0722EX,11.930,5.664
618,95.617,105.1968,12.4257,0722EX,12.212,5.658
619,95.5247,105.048,12.4174,0722EX,12.387,5.644
620,95.0224,105.3419,12.3114,0722EX,12.356,5.063
621,95.1133,105.5561,12.3034,0722EX,12.124,5.045
622,95.2482,105.8186,12.2705,0722EX,11.829,5.045
623,95.3302,106.0263,12.2701,0722EX,11.607,5.022
624,95.43,106.2372,12.2763,0722EX,11.373,5.014
625,95.5106,106.3969,12.2958,0722EX,11.195,5.013
626,95.5525,106.5547,12.3529,0722EX,11.035,4.978
627,95.6627,106.6992,12.369,0722EX,10.856,5.009
628,95.7641,106.8901,12.4218,0722EX,10.640,5.012
629,95.8489,107.0837,12.4419,0722EX,10.429,4.999
630,95.9146,107.2465,12.4821,0722EX,10.254,4.982
631,95.9966,107.4384,12.5016,0722EX,10.046,4.967
632,96.1252,107.645,12.5369,0722EX,9.804,4.987
```

```
633,96.2108,107.7963,12.5463,0722EX,9.630,4.993
634,96.271,107.9479,12.5943,0722EX,9.468,4.977
635,96.3404,108.0879,12.5904,0722EX,9.311,4.975
636,96.666,108.5265,12.3653,0722EX,8.772,5.063
637,96.6687,108.6379,12.3692,0722EX,8.672,5.015
638,96.7235,108.7569,12.3597,0722EX,8.541,5.009
639,96.7639,108.9033,12.3556,0722EX,8.393,4.977
640,95.1801,105.1005,12.3822,0722EX,12.498,5.313
641,95.031,104.8036,12.4268,0722EX,12.830,5.317
642,94.9598,104.6484,12.4383,0722EX,13.001,5.325
643,94.8769,104.4662,12.4295,0722EX,13.201,5.335
644,94.782,104.3183,12.3942,0722EX,13.376,5.318
645,94.3045,104.619,12.3705,0722EX,13.328,4.756
646,94.4551,104.8571,12.3298,0722EX,13.047,4.781
647,94.5442,105.0216,12.3118,0722EX,12.860,4.784
648,94.6016,105.1586,12.3234,0722EX,12.712,4.773
649,94.6673,105.3219,12.285,0722EX,12.537,4.756
650,94.3086,105.6033,12.3013,0722EX,12.451,4.308
651,94.128,105.3175,12.3403,0722EX,12.788,4.279
652,94.0383,105.1048,12.3527,0722EX,13.018,4.297
653,93.9704,104.9403,12.3537,0722EX,13.195,4.312
654,93.8516,104.767,12.3557,0722EX,13.404,4.286
655,93.4506,105.1546,12.3453,0722EX,13.243,3.752
656,93.5375,105.2875,12.3762,0722EX,13.085,3.768
657,93.6168,105.4313,12.3986,0722EX,12.921,3.772
658,93.7011,105.6352,12.3943,0722EX,12.701,3.754
659,93.7795,105.8086,12.4038,0722EX,12.511,3.744
660,93.2931,106.0373,12.3865,0722EX,12.531,3.207
661,93.1413,105.7998,12.3837,0722EX,12.812,3.181
662,93.0636,105.6042,12.3842,0722EX,13.021,3.202
663,92.9695,105.4505,12.3915,0722EX,13.201,3.188
664,92.8719,105.2421,12.3686,0722EX,13.431,3.197
665,92.4242,105.6364,12.3688,0722EX,13.286,2.619
666,92.5244,105.8193,12.365,0722EX,13.077,2.624
667,92.6208,105.9498,12.3812,0722EX,12.917,2.650
668,92.7015,106.1169,12.4017,0722EX,12.731,2.645
669,92.7966,106.3086,12.3776,0722EX,12.517,2.641
670,92.3703,106.4786,12.3781,0722EX,12.562,2.185
671,92.2343,106.2323,12.3606,0722EX,12.843,2.177
672,92.1362,106.0276,12.3702,0722EX,13.070,2.183
673,92.0077,105.814,12.389,0722EX,13.319,2.167
674,91.8892,105.687,12.3889,0722EX,13.486,2.120
675,91.4792,106.0494,12.3835,0722EX,13.352,1.589
676,91.6208,106.2656,12.336,0722EX,13.095,1.616
677,91.6908,106.3903,12.3779,0722EX,12.952,1.621
678,91.8082,106.5728,12.348,0722EX,12.736,1.642
```

```
679,91.8921,106.746,12.3617,0722EX,12.543,1.637
680,91.3565,107.0224,12.3294,0722EX,12.543,1.034
681,91.1969,106.7636,12.345,0722EX,12.846,1.011
682,91.0839,106.5824,12.3498,0722EX,13.059,0.994
683,91.0078,106.3663,12.3578,0722EX,13.286,1.025
684,90.8943,106.2263,12.3712,0722EX,13.463,0.988
685,90.4667,106.6037,12.3914,0722EX,13.323,0.435
686,90.5807,106.7876,12.3831,0722EX,13.108,0.452
687,90.6655,106.9652,12.3779,0722EX,12.911,0.446
688,90.7493,107.1293,12.3726,0722EX,12.727,0.446
689,90.8546,107.3081,12.3619,0722EX,12.520,0.457
690,90.567,107.7126,12.428,0722EX,12.292,0.016
691,90.6895,107.9976,12.4033,0722EX,11.982,-0.006
692,90.7809,108.1863,12.429,0722EX,11.773,-0.011
693,90.8432,108.3594,12.4219,0722EX,11.590,-0.035
694,90.968,108.5696,12.4207,0722EX,11.346,-0.020
695,91.0288,108.6978,12.4201,0722EX,11.205,-0.025
696,91.1228,108.8606,12.4114,0722EX,11.017,-0.016
697,91.231,109.0728,12.4147,0722EX,10.779,-0.017
698,91.366,109.2975,12.3909,0722EX,10.517,0.000
699,91.4373,109.4364,12.3984,0722EX,10.361,-0.001
700,91.558,109.6762,12.4011,0722EX,10.092,-0.003
701,91.645,109.8868,12.4241,0722EX,9.865,-0.023
702,91.79,110.0958,12.4294,0722EX,9.613,0.010
703,91.873,110.2498,12.4571,0722EX,9.438,0.014
704,91.9763,110.4519,12.4557,0722EX,9.211,0.013
705,92.0769,110.683,12.3972,0722EX,8.960,-0.004
706,92.1437,110.7904,12.3955,0722EX,8.834,0.006
707,92.2266,110.9151,12.3919,0722EX,8.685,0.023
708,92.2498,111.006,12.4043,0722EX,8.593,0.002
709,92.3527,111.1759,12.3887,0722EX,8.395,0.015
710,92.8865,110.9467,12.3577,0722EX,8.354,0.595
711,92.8354,110.7666,12.3818,0722EX,8.538,0.632
712,92.5634,110.3505,12.5864,0722EX,9.032,0.581
713,92.6108,110.2147,12.6222,0722EX,9.131,0.685
714,92.5203,110.0365,12.626,0722EX,9.331,0.687
715,92.4361,109.9121,12.6264,0722EX,9.480,0.669
716,92.3294,109.7382,12.6086,0722EX,9.684,0.654
717,92.2534,109.6022,12.5713,0722EX,9.839,0.649
718,92.1489,109.3885,12.55,0722EX,10.077,0.654
719,92.0405,109.1888,12.512,0722EX,10.304,0.649
720,91.9628,109.0632,12.4356,0722EX,10.452,0.637
721,91.8651,108.8573,12.399,0722EX,10.679,0.645
722,91.7921,108.6909,12.3636,0722EX,10.861,0.656
723,91.6801,108.6094,12.2943,0722EX,10.985,0.594
724,91.5644,108.424,12.3124,0722EX,11.202,0.576
```

```
725,91.4878,108.2292,12.3145,0722EX,11.411,0.598
726,91.3586,107.9308,12.3435,0722EX,11.735,0.620
727,91.2929,107.7764,12.3415,0722EX,11.902,0.632
728,91.1739,107.5632,12.3611,0722EX,12.146,0.624
729,91.1243,107.3724,12.3691,0722EX,12.339,0.667
730,91.1696,107.2805,12.3594,0722EX,12.400,0.750
731,91.3481,107.2068,12.3759,0722EX,12.383,0.942
732,91.5391,107.1355,12.353,0722EX,12.359,1.145
733,91.7376,107.0643,12.3589,0722EX,12.331,1.354
734,91.8927,106.9211,12.3926,0722EX,12.387,1.557
735,92.0876,106.8409,12.3797,0722EX,12.369,1.767
736,92.3094,106.7703,12.3667,0722EX,12.330,1.997
737,92.445,106.6651,12.3717,0722EX,12.362,2.165
738,92.6176,106.5169,12.3817,0722EX,12.414,2.387
739,92.8141,106.4164,12.3893,0722EX,12.414,2.607
740,93.0114,106.374,12.375,0722EX,12.361,2.802
741,93.1895,106.2624,12.3702,0722EX,12.378,3.012
742,93.4017,106.243,12.3197,0722EX,12.298,3.209
743,93.5432,106.0283,12.4026,0722EX,12.424,3.433
744,93.7203,105.963,12.4056,0722EX,12.401,3.621
745,93.9279,105.9224,12.3984,0722EX,12.342,3.824
746,94.094,105.7939,12.3798,0722EX,12.380,4.030
747,94.3015,105.7389,12.3318,0722EX,12.334,4.240
748,94.517,105.7083,12.2547,0722EX,12.262,4.445
749,94.8107,105.4837,12.2482,0722EX,12.327,4.809
750,94.942,105.711,12.2233,0722EX,12.065,4.822
751,95.0007,106.0084,12.2338,0722EX,11.774,4.738
752,94.8907,106.1318,12.2237,0722EX,11.714,4.583
753,94.7855,106.1829,12.2432,0722EX,11.717,4.466
754,94.7022,106.2366,12.2888,0722EX,11.708,4.368
755,94.4465,106.2547,12.3749,0722EX,11.809,4.132
756,94.2659,106.349,12.3919,0722EX,11.808,3.929
757,94.1076,106.4591,12.3807,0722EX,11.783,3.737
758,93.9227,106.5266,12.3709,0722EX,11.807,3.542
759,93.7537,106.6568,12.3535,0722EX,11.769,3.332
760,93.5583,106.7623,12.345,0722EX,11.765,3.110
761,93.3744,106.8326,12.36,0722EX,11.787,2.915
762,93.1829,106.9208,12.3638,0722EX,11.796,2.704
763,93.0203,107.0627,12.3402,0722EX,11.745,2.494
764,92.82,107.1334,12.365,0722EX,11.774,2.284
765,92.6284,107.201,12.3793,0722EX,11.801,2.083
766,92.4605,107.3146,12.3696,0722EX,11.777,1.881
767,92.2562,107.4088,12.3736,0722EX,11.787,1.657
768,92.0805,107.5205,12.3707,0722EX,11.769,1.449
769,91.8938,107.5792,12.383,0722EX,11.802,1.256
770,92.1541,107.6674,12.3682,0722EX,11.604,1.447
```

```
771,91.9844,107.9803,12.2855,0722EX,11.404,1.153
772,91.9067,108.1772,12.2873,0722EX,11.265,0.994
773,91.6895,108.1605,12.2739,0722EX,11.379,0.808
774,91.799,108.4654,12.2701,0722EX,11.058,0.766
775,92.0021,108.4532,12.3104,0722EX,10.976,0.952
776,92.224,108.5236,12.3443,0722EX,10.811,1.117
777,92.414,108.4477,12.3861,0722EX,10.792,1.321
778,92.5639,108.337,12.3932,0722EX,10.821,1.505
779,92.6524,108.2227,12.361,0722EX,10.882,1.636
780,92.7902,108.0862,12.3679,0722EX,10.941,1.821
781,92.9414,107.9911,12.3752,0722EX,10.956,1.999
782,93.0857,107.9088,12.3831,0722EX,10.963,2.165
783,93.2531,107.782,12.4026,0722EX,10.999,2.371
784,93.3902,107.7366,12.3928,0722EX,10.976,2.514
785,93.4856,107.6418,12.3778,0722EX,11.017,2.642
786,93.7434,107.5003,12.3839,0722EX,11.024,2.936
787,93.9109,107.4006,12.3908,0722EX,11.036,3.131
788,94.1531,107.329,12.3713,0722EX,10.989,3.379
789,94.2722,107.1434,12.402,0722EX,11.099,3.570
790,94.4103,106.9493,12.405,0722EX,11.208,3.782
791,94.6302,106.8084,12.4114,0722EX,11.233,4.042
792,94.9228,106.7223,12.4394,0722EX,11.175,4.341
793,95.1447,106.797,12.4313,0722EX,11.007,4.504
794,95.437,106.812,12.4195,0722EX,10.859,4.757
795,95.1267,106.4957,12.3369,0722EX,11.283,4.626
796,95.892,109.3724,12.4773,0722EX,8.375,3.988
797,95.4933,109.5461,12.2523,0722EXR,8.404,3.554
798,95.1507,109.6805,12.3736,0722EX,8.441,3.187
799,94.8912,109.9032,12.248,0722EXC,8.363,2.855
800,95.6501,107.1332,12.4761,0722EX,10.476,4.799
801,95.2958,107.2149,12.5624,0722EX,10.566,4.447
802,95.1443,107.33,12.6379,0722EX,10.533,4.259
803,94.9644,107.39,12.6674,0722EX,10.562,4.072
804,94.813,107.5119,12.7024,0722EX,10.524,3.882
805,94.6214,107.5792,12.7441,0722EX,10.552,3.680
806,94.4503,107.682,12.7416,0722EX,10.539,3.481
807,94.2692,107.7681,12.7522,0722EX,10.545,3.281
808,94.0735,107.8585,12.7634,0722EX,10.555,3.065
809,93.9117,107.9651,12.754,0722EX,10.534,2.873
810,93.698,108.0098,12.7521,0722EX,10.592,2.662
811,93.4965,108.0979,12.7568,0722EX,10.606,2.443
812,93.3272,108.2056,12.7429,0722EX,10.588,2.243
813,93.1658,108.3535,12.705,0722EX,10.531,2.032
814,92.9814,108.4321,12.6648,0722EX,10.545,1.832
815,92.7972,108.5536,12.6006,0722EX,10.522,1.613
816,92.6288,108.6689,12.5863,0722EX,10.497,1.410
```

```
817,92.4815,108.7887,12.5359,0722EX,10.458,1.224
818,92.3004,108.8477,12.4903,0722EX,10.488,1.036
819,92.1262,108.9027,12.4476,0722EX,10.519,0.856
820,92.3827,109.4688,12.6161,0722EX,9.899,0.825
821,92.5912,109.3502,12.6316,0722EX,9.908,1.064
822,92.7837,109.2212,12.7163,0722EX,9.935,1.294
823,92.9595,109.1207,12.7617,0722EX,9.944,1.497
824,93.1556,109.0883,12.7769,0722EX,9.882,1.686
825,93.3145,108.9657,12.8271,0722EX,9.919,1.883
826,93.5148,108.7921,12.8679,0722EX,9.981,2.141
827,93.6706,108.7547,12.8613,0722EX,9.943,2.297
828,93.8593,108.6138,12.834,0722EX,9.982,2.529
829,94.0321,108.4755,12.8518,0722EX,10.025,2.746
830,94.1767,108.3023,12.9018,0722EX,10.113,2.954
831,94.3048,108.0942,12.9493,0722EX,10.239,3.163
832,94.5612,108.1823,12.9325,0722EX,10.043,3.350
833,94.7728,108.1728,12.8622,0722EX,9.955,3.543
834,94.9528,108.013,12.8216,0722EX,10.014,3.776
835,95.1289,107.8741,12.7777,0722EX,10.057,3.996
836,95.3133,107.8042,12.7319,0722EX,10.034,4.192
837,95.536,107.8203,12.6991,0722EX,9.918,4.383
838,95.6624,107.7217,12.6626,0722EX,9.948,4.540
839,95.8871,107.5929,12.5446,0722EX,9.959,4.799
840,96.326,108.1671,12.5881,0722EX,9.248,4.926
841,96.1204,108.2248,12.6836,0722EX,9.291,4.717
842,95.9719,108.4212,12.7455,0722EX,9.184,4.495
843,95.8305,108.6242,12.7427,0722EX,9.069,4.276
844,95.8577,109.0306,12.6019,0722EX,8.695,4.114
845,96.5895,108.9242,12.3587,0722EX,8.454,4.813
846,96.6145,108.7545,12.3575,0722EX,8.593,4.913
847,95.4167,109.1259,12.4127,0722EX,8.812,3.678
848,95.3106,108.6299,12.6185,0722EX,9.302,3.811
849,95.3279,108.2148,12.7414,0722EX,9.663,4.017
850,95.6229,107.9369,12.7001,0722EX,9.774,4.407
851,94.9571,108.5535,12.746,0722EX,9.532,3.532
852,94.5875,108.3568,12.9285,0722EX,9.876,3.294
853,94.6086,108.5164,12.8932,0722EX,9.725,3.239
854,94.4111,108.8675,12.7607,0722EX,9.503,2.903
855,94.3547,109.3042,12.639,0722EX,9.141,2.653
856,94.3989,109.8291,12.4607,0722EX,8.654,2.451
857,94.2668,109.8813,12.464,0722EX,8.668,2.310
858,94.0897,109.7126,12.5442,0722EX,8.899,2.230
859,93.9744,109.6406,12.5854,0722EX,9.016,2.160
860,93.778,109.4351,12.6975,0722EX,9.289,2.080
861,93.5031,109.2136,12.8083,0722EX,9.612,1.937
862,93.3492,109.1984,12.7936,0722EX,9.696,1.807
```

```
863,93.2483,109.4481,12.6892,0722EX,9.520,1.603
864,93.7534,110.4484,12.2656,0722EX,8.400,1.594
865,93.4869,110.1663,12.4624,0722EX,8.773,1.486
866,93.285,110.146,12.5511,0722EX,8.883,1.316
867,93.1217,110.1456,12.6192,0722EX,8.958,1.171
868,92.9605,110.1811,12.6471,0722EX,9.001,1.011
869,92.7588,110.1543,12.6674,0722EX,9.117,0.845
870,92.6385,110.1893,12.6356,0722EX,9.141,0.722
871,92.52,110.0702,12.6238,0722EX,9.301,0.671
872,94.9865,109.7307,12.2537,0722EX,8.472,3.019
873,94.6166,109.4755,12.4643,0722EXC,8.869,2.807
874,93.9857,109.8609,12.459,0722EXL,8.815,2.069
```

List of Benchmarks Available for Resection

These data are included to have an external archival copy of the data.

```
# PID: Point IDentification number
# Northing in feet
# Easting in feet
# Elevation in feet
# There is no transformation for these points because they
  are raw data read by the datalogger

PID,Northing,Easting,Elevation,Description
102,103.4201,111.6306,14.4175,PUMPBOLT2
103,109.3623,108.5875,14.4626,PUMPBOLT1
104,94.8702,94.4921,10.0115,PAINTTANK
105,92.5624,97.6957,20.8966,HANGBOLT1
106,78.7947,96.6560,16.8131,DOTDSLB
107,80.5045,98.4045,18.5457,HANGERLB3
108,86.6500,110.4988,18.5611,HANGERLB2
109,89.8248,108.6149,21.1916,EMTBOLT2
110,90.1738,117.4861,18.5353,HANGERLB1
111,95.6949,123.0105,18.4522,PIPEDOTLB
112,98.1695,121.6997,21.2599,EMTBOLT1
113,101.5455,119.2119,21.3495,BEAMDOT1
114,101.7574,119.8953,20.2925,PIPEDOTCLUS
115,120.4322,99.9989,10.0017,BRASSTABLET
116,106.3547,107.6183,21.1679,EMTBOLT3
117,130.5297,94.1064,13.6642,WESTWALLBOLT1
118,124.0275,81.2899,13.5986,WESTWALLBOLT2
119,110.0710,54.1257,10.5623,WESTWALLBOLT3
120,99.0864,71.0943,10.3642,FILTERNETOP
121,98.8302,70.8153,10.2145,FILTERNESIDEBOLT
122,94.8684,94.4928,10.0125,PAINTTANK
123,105.7274,116.0277,16.4585,PUMPBOLT3
124,106.1906,133.2318,15.2250,HEADTANKPORT
125,78.7997,96.6557,16.8125,DOTDSLB
130,90.4663,104.3052,21.0673,BOLTANGLE1
140,105.3182,115.5578,16.0049,PUMPBOLT4
141,107.8129,120.5442,16.2030,PUMPBOLT5
142,99.7552,128.6127,16.1103,CHUTELBBOLT
143,100.3675,128.9095,16.5041,HEADTANKLBWALKWAY50
144,78.6020,96.7898,15.4952,COLUMNDSLB
145,93.1769,125.0004,16.3130,COLUMNUSLB
146,86.6613,110.5025,18.5627,HANGERLB2
```